

論文 / 著書情報
Article / Book Information

題目(和文)	年代効果を受けた粘性土の力学的性質に対する堆積環境の影響
Title(English)	Effects of the depositional environment on the mechanical properties of aged clays
著者(和文)	齋藤禎二郎
Author(English)	
出典(和文)	学位:博士(工学), 学位授与機関:東京工業大学, 報告番号:甲第4894号, 授与年月日:2001年9月30日, 学位の種別:課程博士, 審査員:
Citation(English)	Degree:Doctor (Engineering), Conferring organization: Tokyo Institute of Technology, Report number:甲第4894号, Conferred date:2001/9/30, Degree Type:Course doctor, Examiner:
学位種別(和文)	博士論文
Type(English)	Doctoral Thesis

Effects of the Depositional Environment on the Mechanical Properties of Aged Clays

*A dissertation submitted to the department of Civil Engineering
in the partial fulfillment of the requirements for the Degree of*

Doctor of Engineering

by

Teijiro Saito

Academic Supervisor

Professor Hideki Ohta

Department of Civil Engineering
Toyko Institute of Technology, Japan
September, 2001

ACKNOWLEDGEMENTS

I wish to express my sincere gratitude to Prof. H. Ohta of Tokyo Institute of Technology for his warmhearted advice and valuable suggestions during the past three years. He suggested me to look for a theme in between civil engineering and geology.

I am deeply indebted to Associate Prof. A. Kitamura of Shizuoka University for his valuable suggestions. He reminds me of the pleasure of studying geology again. I am also indebted to Associate Prof. A. Iizuka of Kobe University for his kind advice and valuable suggestions throughout my period of attendance at Tokyo Institute of Technology. I had been really enjoyed his witty lecture.

I am grateful to Prof. O. Kusakabe, Prof. N. Ohtsuki, Prof. O. Murata, Associate Prof. J. Takemura and Associate Prof. J. Kuwano of Tokyo Institute of Technology for their valuable advice and suggestions during the past three years. Especially their kind advice helped me a lot throughout the last examination. I wish to express my sincere gratitude Mr. Y. Koyama and Mr. H. Seki of Japan Highway Public Corporation for their kind admission to use their soil investigation report in Niigata.

I am deeply indebted to honorary Prof. I. Hara of Hiroshima University, Prof. M. Oda of Saitama University and Associate Prof. R. Kitagawa of Hiroshima University for their kind advice and encouragement during the past three years.

Thanks are due to Dr. A. Takahashi, Dr. M. Koda and Dr. I. Kobayashi for their kind suggestions. They helped me a lot throughout the period of attendance at Tokyo Institute of Technology. Dr. Y. Hayasaka of Hiroshima University and Dr. J. Saiki of Tokyo Institute of Technology for their valuable suggestions on the chemical analysis.

Thanks are also due to all the member of 'TERAKOYA' for their valuable advice and suggestions. The discussion with the members in 'TERAKOYA' always gave me a lot of ideas to complete the thesis.

I would like to record my thank for the valuable help I have received from research student of the Shizuoka University and Tokyo Institute of Technology.

I wish to express my sincere gratitude to the President Y. Kanayama of Nishimatsu Construction Co., LTD. for giving me a chance to learn again for three years in Tokyo Institute of Technology. I am deeply indebted to Dr. T. Hosoi, Mr. T. Tannai, Dr. T. Fujii, Dr. T. Kitagawa, Mr. H. Goto, Mr. T. Hirano and Mr. S. Yamamoto of the Civil Design Dep. of Nishimatsu Construction Co., LTD. for their kind advice and encouragement during the past three years. I am also deeply indebted to Dr. T. Nomoto, Dr. T. Hagiwara, Mr. S. Imamura and Mr. O. Yoshino of the Research Center of the Nishimatsu Construction Co., LTD. for their kind advice and suggestions. Thanks are also due to Mr. T. Nagai, Mr. S. Sugawara, Mr. K. Kusano and Mr. D. P. Mundo of the Overseas Dep. of the Nishimatsu Construction Co., LTD. for his help and advice during the past three years.

Finally, I would like to record my thank for the encouragement I have received from my wife Misao, my children Seitaro & Tamaki and the other all my family throughout the period of attendance at Tokyo Institute of Technology.

ABSTRACT

The motivation of this study is making use of the geological information to a part of the civil engineering problems directly. Civil engineers have been interested in geology and understood that there should be deep relations between soil properties and the history of the ground. Geological information gives interesting story to the civil engineers, however, there is a few propose how we could make use of geology for practical use so far.

It has been recognized by civil engineers that the depositional environment is related to the physical and mechanical properties of soils (e.g. Kenney, 1964). Over the past few decades, a considerable number of studies have been conducted on the relation between the depositional environment and the properties of soils. Furthermore several studies have been made on the mechanism of compression of clays and its resulting void ratio, over-consolidation ratio *OCR*, aging and etc. (e.g. Bjerrum, 1967; Mesri, 1973; Sekiguchi, 1983; Tsuchida, 1999).

Prediction of the influences of excavation or embankment to the surrounding area is getting more and more important in these days together with the stability of the structures. In order to estimate such influences numerically, coupled elasto-plastic or elasto-viscoplastic Finite Element analysis (e.g. Sekiguchi and Ohta, 1977; Ohta and Sekiguchi, 1979; Iizuka and Ohta, 1987) is available. The elasto-plastic or elasto-viscoplastic F.E. deformation analysis requires initial conditions as additional information compare with the elastic analysis. Note that it is not necessary for elastic models. The studies on initial conditions are becoming more important because the initial condition is indispensable for elasto-plastic or elasto-viscoplastic finite element analysis.

The purpose of this investigation is to reason out the depthwise distribution of void ratio, unit weight and *OCR*. Age and plasticity index *PI* are set to be the parameters to describe the effect of aging and the difference of the properties of clays. The obtained theoretical equations enable engineers to check the effect of geological factors to the soil parameters or to estimate the initial condition for coupled elasto-plastic or elasto-viscoplastic F.E. analysis in case the enough laboratory tests are not available. Additionally geological method for the interpretation of boring logs based on the depositional environment analysis in order to make the most of the investigation data is also introduced in this study. Those geological techniques are useful to make a realistic soil profile which is also important for the accurate F.E. analysis.

This thesis is divided into 5 chapters including the introduction and the conclusions.

Chapter 1 is an introduction of this thesis.

Chapter 2 describes the theoretical soil parameters based on Bjerrum's hypothesis. Depositional age and plastic index (*PI*) are set to be the parameters which represent the geological information. All the parameters including the depth at present are obtained as the

function of the depositional age. Estimation chart for the soil parameters based on age and *PI* is proposed.

Chapter 3 shows a number of the results of the parametric studies for the theoretical soil parameters obtained in Chapter 2. The effect of *PI*, age, depositional rate and physical parameters are described. Five types of the depositional rate are used for the numerical simulations.

Chapter 4 shows the examples of the applications of the theory. Geological analysis and the interpretations of the depositional environment are also described. First example of the field data is the distribution of void ratio at San Joaquin Valley, California reported by Mead (1962). The tendency of the void ratio distribution is well explained by means of the geological analysis together with the theory derived from this study. Second example is Shiunji lagoon(Niigata, Japan) Calculated soil parameters based on *PI* and age is compared with measurements. Change of the depositional environment is analyzed by means of the results of the geological analysis of a series of boring core.

Chapter 5 is the conclusions derived from this study.

CONTENTS

Chapter 1	INTRODUCTION	
1.1	Objectives of this study	1
1.2	Organization of this thesis	3
	References	5
Chapter 2	ESTIMATION OF SOIL PARAMETERS	
2.1	Introduction	7
2.2	Bjerrum's hypothesis	7
2.3	Assumptions	9
2.4	Sedimentation and consolidation	9
2.5	Compression of aged clays	10
2.6	Settlement and age	12
2.7	Age and depth at present	12
2.8	Initial conditions	13
2.8.1	Thickness of the formation and depositional rate	13
2.8.2	Initial void ratio and submerged unit weight	14
2.9	Over-consolidation ratio	16
2.9.1	Theoretical over-consolidation ratio	16
2.9.2	Apparent pre-consolidation pressure and oedometer test	17
2.10	Chart for parameters estimation based on PI and age	18
2.11	Theory for various depositional rates	21
2.12	Conclusions	27
	References	28
	Appendix 1	30
	Appendix 2	31
	Appendix 3	33
Chapter 3	PARAMETRIC STUDY	
3.1	Introduction	35
3.2	Effect of age and PI	35
3.3	Effect of types of the depositional rate	37
3.4	Effect of material properties	47
3.5	Effect of the PI transition	79
3.6	Conclusions	82
	References	83

Chapter 4	APPLICATIONS OF THE THEORY& INTERPRETATIONS OF THE DEPOSITIONAL ENVIRONMENT	
4.1	Introduction	84
4.2	Meade's void ratio (San Joaquin valley, California)	87
4.3	Shiunji lagoon (Northeast of Niigata, Japan)	93
4.3.1	Location and Boring log	93
4.3.2	Smear slide	96
4.3.3	Soft X-ray photograph	99
4.3.4	Electric conductivity and pH	100
4.3.5	XRF analysis	102
4.3.6	Radiocarbon dating	105
4.3.7	Change of depositional environment and estimated properties	106
4.4	Conclusions	110
	References	111
	Appendix 1	113
	Appendix 2	117
	Appendix 3	123
Chapter 5	CONCLUSIONS	124

FIGURES

Fig.1.1	Organization chart of this thesis	4
Fig.2.1	Compressibility and shear strength of a clay exhibiting delayed consolidation	8
Fig.2.2	Definition of ‘instant’ and ‘delayed’ compression with ‘primary’ and ‘secondary’ compression	8
Fig.2.3	Coordinate system and the schematic drawing of the sedimentation	9
Fig.2.4	Bjerrum’s concept of delayed compression	10
Fig.2.5	Change of the relationship among soil phases caused by compression	11
Fig.2.6	Relationship of the age and the depth at present	12
Fig.2.7	PI- relation	16
Fig.2.8	The effect of condition of the oedometer test on the pre-consolidation pressure	18
Fig.2.9	Chart for soil parameter estimation based on PI and Age	19
Fig.2.10	Proposed determination procedure of input parameters(After Iizuka and Ohta, 1987)	20
Fig.2.11	An example of the age-depth relation(After Kraft et al., 1987)	21
Fig.2.12	Schematic diagram of age and depositional thickness h	22
Fig.2.13	Schematic diagram of age and depositional age	23
Fig.A.1	An example of the age-depth relation(After Finkelstein and Ferland, 1987)	31
Fig.A.2	An example of the age-depth relation(After Masuda, 2000)	31
Fig.A.3	An example of the age-depth relation(After Masuda, 2000)	32
Fig.A.4	An example of the age-depth relation(After Takemura, 2000)	32
Fig.3.1	Example of estimated distribution of soil properties	36
Fig.3.2	Effect of the depositional rate on the properties of clays (PI=60)	36
Fig.3.3	The effect of the depositional rate 1 of 5. Diagram of the t, e, ' and Po' (To=5000)	39
Fig.3.4	The effect of the depositional rate 2 of 5. Diagram of the t, e, ' and Po' (To=10000)	40
Fig.3.5	The effect of the depositional rate 3 of 5. Diagram of the t, e, ' and Po' (To=15000)	41
Fig.3.6	The effect of the depositional rate 4 of 5. Diagram of the Po', Pc' and OCR (To=5000,10000,15000 years)	42
Fig.3.7	The effect of the depositional rate 5 of 5. Enlarged diagram of the t, e, ' and Po' (PI=60, To=15000)	43
Fig.3.8	The relation between the C and C _C and consolidation pressure(After Mesri & Godlewski, 1977)	47
Fig.3.9	The relation between the C and C _C (After Mesri & Godlewski, 1977)	47
Fig.3.10	The effect of the amount of organic material in clay (After Matsuo et al., 1986)	49

Figs.3.11 The effect of the loading increment (After Matsuo et al., 1986)	49
Figs.3.12 The effect of the period of loading (After Matsuo et al., 1986)	50
Figs.3.13 The effect of the initial structures of clay (After Matsuo et al., 1986)	50
Fig.3.14 The diagram of the range of the C_u/C_L and the C_u (After Matsuo et al., 1986)	51
Figs3.15 The effect of σ'_v , σ'_h and σ'_v/σ'_h 1 of 5. Diagram of the t_e , σ'_v and Po' ($To=5000$)	54
Figs3.16 The effect of σ'_v , σ'_h and σ'_v/σ'_h 2 of 5. Diagram of the t_e , σ'_v and Po' ($To=10000$)	55
Figs3.17 The effect of σ'_v , σ'_h and σ'_v/σ'_h 3 of 5. Diagram of the t_e , σ'_v and Po' ($To=15000$)	56
Figs3.18 The effect of σ'_v , σ'_h and σ'_v/σ'_h 4 of 5. Diagram of the Po' , Pc' and OCR ($To=5000,10000,15000$ years)	57
Figs3.19 The effect of σ'_v , σ'_h and σ'_v/σ'_h 5 of 5. Enlarged diagram of the t_e , σ'_v and Po' ($PI=60, To=15000$)	58
Figs3.20 The effect of σ'_v/σ'_h 1 of 2. Diagram of the Po' , Pc' and OCR ($To=5000,10000,15000$ years)	64
Figs3.21 The effect of σ'_v/σ'_h 2 of 2. Enlarged diagram of the Po' , Pc' and OCR ($PI=60, To=15000$)	65
Figs3.22 The effect of σ'_v/σ'_h and σ'_v/σ'_h 1 of 5. Diagram of the t_e , σ'_v and Po' ($To=5000$)	71
Figs3.23 The effect of σ'_v/σ'_h and σ'_v/σ'_h 2 of 5. Diagram of the t_e , σ'_v and Po' ($To=10000$)	72
Figs3.24 The effect of σ'_v/σ'_h and σ'_v/σ'_h 3 of 5. Diagram of the t_e , σ'_v and Po' ($To=15000$)	73
Figs3.25 Diagram of the Po' , Pc' and OCR ($To=5000,10000,15000$ years) The effect of σ'_v/σ'_h 4 of 5	74
Figs3.26 The effect of σ'_v/σ'_h and σ'_v/σ'_h 5 of 5. Enlarged diagram of the t_e , σ'_v and Po' ($PI=60, To=15000$)	75
Figs.3.27 Effects of the transition of PI on the mechanical parameters	79
Fig.4.1 Examples of the importance of understanding depositional environment	85
Fig.4.2 Comparison with the field observation by Meade (1963) and Velde (1996)	87
Figs.4.3 Properties of sediments at San Joaquin valley, California (after Meade, R.H., 1963)	88
Fig.4.4 Clay mineral, adsorbed cation and PI (after Lambe and Whitman, 1969)	89
Fig.4.5 Flowchart of the geological analysis in section 4.3	93
Fig.4.6 The location of Shiunji lagoon (URBAN KUBOTA, No.17, p.51, 1979)	94
Fig.4.7 Boring data B1-71 (G.L.=T.P.+4.26m)	95
Fig.4.8 Burial depth distribution of the areal percentages of diatom in the smear slides	97
Fig.4.9 Relation of pH and E/C of the stirred water (after Yokoyama and Sato, 1987)	100
Figs.4.10 Distribution of pH and E/C of the stirred water of Shiunji lagoon, Niigata	101

Fig.4.11 Relation of pH and E/C of the stirred water of Shiunji lagoon, Niigata	102
Fig.4.12 Particle size, axial force vs. count of an element (Internal document of PHILLIPS, 2000)	103
Figs.4.13 The results of the quantitative XRF analysis of boring No.71 of Shiunji lagoon	104
Figs.4.14 Typical alluvial sea-level change (after Saito, 1995)	107
Figs.4.15 Estimated properties and test results of Shiunji lagoon	109
Figs.A.1 Calibration curves of major elements(1 of 2)	119
Figs.A.2 Calibration curves of major elements(2 of 2)	120
Figs.A.3 Calibration curves of minor elements	121

Photographs

Photos.4.1 Photographs of several kinds of Diatom in the smear slides of B1-69 & B1-71 under microscope (x2.0 of the photos. x400)	97
Photos.4.2 Soft X-ray photographs of Bor. B1-71	99

TABLES

Table 3.1 Arrangement of the graphs in Figs.3.3-3.5	38
Table 3.2 Arrangement of the graph in Figs.3.6	38
Table 3.3 Parameters lists of the calculations of Figs.3.3 and 3.6	44
Table 3.4 Parameters lists of the calculations of Figs.3.4 and 3.6	44
Table 3.5 Parameters lists of the calculations of Figs.3.5-3.7	45
Table 3.6 The list of the values of C / C_C for natural soil deposits (After Mesri & Godlewski,1977)	46
Table 3.7 Arrangement of the graphs in Figs.3.15-3.17	48
Table 3.8 Arrangement of the graphs in Figs.3.18	53
Table 3.9 Parameters lists of the calculations of Figs.3.15 and 3.18	53
Table 3.10 Parameters lists of the calculations of Figs.3.16 and 3.18	59
Table 3.11 Parameters lists of the calculations of Figs.3.17-3.19	60
Table 3.12 Arrangement of the graphs in Figs.3.18	61
Table 3.13 Parameters lists of the calculations of Figs.3.20 and 3.21	63
Table 3.14 Parameters lists of the calculations of Figs.3.20 and 3.21	66
Table 3.15 Parameters lists of the calculations of Figs.3.20 and 3.21	67
Table 3.16 Arrangement of the graphs in Figs.3.22-3.24	68
Table 3.17 Arrangement of the graphs in Figs.3.25	70
Table 3.18 Parameters lists of the calculations of Figs.3.22 and 3.25	76
Table 3.19 Parameters lists of the calculations of Figs.3.22 and 3.25	77
Table 3.20 Parameters lists of the calculations of Figs.3.24 and 3.25	78
Table 3.21 Parameters lists of the calculations of Figs.3.27	79
Table 3.22 Results of the calculations Case1 of Fig.3.24	80
Table 3.23 Results of the calculations Case2 of Fig.3.24	80
Table 3.24 Results of the calculations Case3 of Fig.3.24	80
Table 3.25 Results of the calculations Case4 of Fig.3.24	81
Table 3.26 Results of the calculations Case5 of Fig.3.24	81
Table 3.27 Summary of the parametric study	82
Table 4.1 Differences of marine and freshwater clays (after Kamon et al., 1995)	85
Table 4.2 List of geological analysis	86
Table 4.3 Fraction and PI (after Lambe and Whitman, 1969)	89
Table 4.4 Clay minerals (1/2), after Lambe & Whitman(1969)	90
Table 4.5 Clay minerals (2/2), after Lambe & Whitman(1969)	91
Table 4.6 Depositional environment with pH and E/C (after Yokoyama and Sato, 1987)	100
Table 4.7 Results of the radio carbon dating	105
Table A1 Results of the laboratory tests 1 of 4	113
Table A2 Results of the laboratory tests 2 of 4	114

Table A3 Results of the laboratory tests 3 of 4	115
Table A4 Results of the laboratory tests 4 of 4	116
Table A5 Chemical analysis of the standards proposed by JGS (1 of 2)	117
Table A6 Chemical analysis of the standards proposed by JGS (2 of 2)	118
Table A7 List of calibration curves	122
Table A8 Result of the estimation of B1-71 of Shiunji lagoon	123

NOTANTIONS

- λ : Compression index
- λ_s : Swelling index
- λ' : Coefficient of secondary compression
- γ_t : Unit weight of soil
- γ' : Submerged unit weight
- γ_w : Unit weight of water
- λ_r : Irreversibility ratio
- a : Ratio of w_n over w_L ($a = w_n / w_L$)
- C_c : Coefficient of consolidation
- C : Coefficient of secondary compression
- CI : Consistency index
- e : Void ratio at present
- e_{sd} : Void ratio just after the sedimentation
- G_s : Specific gravity
- H : In-situ thickness of a layer at present
- H_0 : Thickness of a layer before the compression
- K_0 : Coefficient of earth pressure at rest
- K_i : In-situ coefficient of earth pressure at rest
- LI : Liquid index
- OCR : Over-consolidation ratio
- PI : Plastic index
- p_0' : Over-burden pressure at rest
- p_c' : Over-consolidation pressure
- S : Settlement of soil after the sedimentation
- S_0 : Settlement of soil after the sedimentation at ground surface
- T_0 : Age of a soil at the bottom
- T_{10} : Age of a soil at the depth of 10m at present
- t_{age} : Age of a soil
- t_c : Reference time (= 24 hours in this study)
- V : Sedimentation rate
- V_a : Apparent sedimentation rate
- Z : Depth from the ground surface at present (Depth in the Z-coordinate, see Chapter 2)
- h : Depth of a soil before the compression (Depth in the h-coordinate, see Chapter 2)

Chapter 1

INTRODUCTION

1.1 Objectives of this study

The motivation of this study is to make use of the geological information to a part of the civil engineering problems in an explicit way. Civil engineers have been interested in geology and understood that there should be intrinsic relations between soil properties and the history of the ground formation. Geological information gives a interesting story to the civil engineers, however, there are little quantitative suggestions how we could make the best use of geology for practical engineering use so far in the field of foundation engineering.

Investigation of the history of the ground is a part of the fields of geology. Recent geological studies give us a lot of information how the soil formations near the ground surface were generated in the past 5,000 – 18,000 years. It should be noted that not only the latest soil formations but also all the sediments including soils and sedimentary rocks seem to be closely related to the sea-level changes in the geological history.

Sea-level changes have been brought to public attention by the deep connection with the sequences of sediments (Posamentier and Vail, 1988). The drastic development of this kind of geology began when the members of Exxon Research and Product Company organized new concept named “Sequential stratigraphy” based on seismic stratigraphy which is a kind of oil investigation techniques (Vail et al., 1977; Mitcham et al., 1977). Sequential stratigraphy combines sequences of the formations with the age of the sediments and the transition of the depositional environment based on seismic information. Various phases and sequences of the sediments in the field are due to the transition of the depositional environment. To quote Einsele, the modern geology proposed “the facies models demonstrating both the depositional environment and the resulting vertical sequences “(Einsele, 1992).

It has been recognized by civil engineers that the depositional environment is intrinsically related to the physical and mechanical properties of soils (e.g. Kenney, 1964). Over the past few decades, a considerable number of investigations have been conducted on the relation between the depositional environment and the mechanical properties of soils (e.g. Tohno,

1975, 1985, 1989; Shimizu, 1985; Kamei, 1997). Several studies have been made on the mechanism of compression of clays and its resulting void ratio, over-consolidation ratio *OCR*, aging and etc. (e.g. Bjerrum, 1967; Mesri, 1973; Sekiguchi, 1983; Tsuchida, 1999).

Many cities and industrial zones are located on the coastal regions, especially on the distributaries of major deltas. Consequently most of the populations are concentrated in these cities and people are utilizing the deltaic areas. In many deltas, a few tens meter thick marine clay sediments are deposited during the last ten thousand years and are laterally continuous (e.g., Suter, 1994). More and more construction projects are being intended on the thick marine clays for the sake of the social capital development and maintenance such as transportation system, disaster mitigation, energy supply and etc. Thus mechanical properties of clays are of primary importance for the coastal management of deltaic areas.

Prediction of the influences of excavation or embankment to the surrounding area is getting more and more important in these days together with the stability of the structures. In order to estimate such influences quantitatively, Finite Element analysis (F.E. analysis) is available. Elastic model has been the most popular mechanical model for F.E. analysis and stresses in the ground have usually been treated as total stresses. Higher accuracy in the prediction by F.E. analysis is required because not only of the social request to the construction industry but also of the optimization of the design itself. It had been widely accepted that the effective stress concept explains the behavior of the soil better than total stress concept (Terzaghi and Peck, 1948). A huge numbers of experiments demonstrated that the soil behaves at least elasto-plastic or sometimes elasto-viscoplastic way in a few decades (e.g. Schofield and Wroth, 1968; Ohta, 1971).

Latest studies developed the F.E. analysis as a tool to simulate soil behavior accompanied by the seepage flow of the ground water (e.g. Biot, 1941; Christian, 1968; Sandhu and Wilson, 1969). Coupled elasto-plastic or elasto-viscoplastic F. E. analysis is about to be applied to the actual projects in these days (e.g. Sekiguchi and Ohta, 1977; Ohta and Sekiguchi, 1979; Iizuka and Ohta, 1987). The elasto-plastic or elasto-viscoplastic F.E. analysis requires initial conditions as additional information. Note that the initial conditions are not necessary for elastic analysis. The investigations on initial conditions are becoming more important because the initial conditions are indispensable for elasto-plastic or elasto-viscoplastic finite element analysis.

The purpose of this investigation is to reason out the depthwise distribution of void ratio, unit weight and *OCR* in the alluvial deposits. Age and plasticity index *PI* are set to be the parameters to describe the effect of aging and the difference of the properties of clays. The obtained semi-theoretical equations enable engineers to check the effect of geological factors to the soil parameters or to estimate the initial condition for coupled elasto-plastic or elasto-viscoplastic F.E. analysis in cases the sufficient laboratory test results are not available. Additionally geological method for the interpretation of boring logs based on the depositional

environment analysis is also introduced in this study. Those geological techniques are useful to understand relationship between the distributions of the properties and the changes of depositional environment. Engineers need to understand the changes of the depositional environment in order to obtain proper soil profile for the reliable F.E. analysis.

1.2 Organization of this thesis

This thesis is divided into 6 chapters including the introduction and the conclusions. Fig.1.1 shows the flow chart of the organization of this thesis.

Chapter 1 is an introduction of this thesis.

Chapter 2 describes the estimation of soil parameters making use of Bjerrum's hypothesis. Depositional age and plastic index (PI) are set to be the parameters which represent the geological information. All the parameters including the depth at present are obtained as the function of the depositional age. Estimation chart for the soil parameters based on age and PI is proposed.

Chapter 3 shows a number of the results of the parametric studies for the theoretical soil parameters obtained in Chapter 2. The effect of PI , age, depositional rate mechanical soil parameters are demonstrated. Five types of the depositional rate are chosen in the numerical simulations.

Chapter 4 gives examples of the several applications of the proposed theory to the soil parameter estimation together with the interpretation of the depositional environment based on the geological information. First example of the field data is the distribution of void ratio at San Joaquin Valley, California reported by Meade (1962). The tendency of the void ratio distribution is well explained by means of the geological analysis together with the theory derived from this study. Another example is Shiunji lagoon (Niigata). Geological analysis is applied to the boring samples for this location in order to study the changes of the depositional environment. Mechanical parameters of the soil are estimated based on PI and age. The results of the estimation are compared with the results of the laboratory tests.

Chapter 5 is the conclusions derived from this study.

Engineering use of the geological information

**Initial condition for elasto-plastic or elasto-viscoplastic
F.E. analysis**

Chapter 2.

**Estimation of soil parameters of aged clays based on ‘PI’
and ‘Age’ which represents change of the depositional
environment**



Chapter 3.

Parametric studies on the estimated soil parameters



Chapter 4.

**(1)Application of the theory to the field data
(2)Application of the geological analysis to study change of
the depositional environment**



Chapter 5.

**Conclusions : A method to set mechanical properties of soil
considering the effect of the depositional environment is
proposed and applied to sites.**

Fig.1.1 Organization chart of this thesis

References

- Bjerrum, L. (1967): Engineering geology of Norwegian Normally-consolidated Marine Clays as related to Settlements of Buildings. *Geotechnique*, Vol.17, pp.83-118.
- Einsele, G. (1992): *Sedimentary Basin -Evolution, Facies and Sediment Budget*. Berlin: Springer-Verlag, 628p.
- Iizuka, A. and Ohta, H. (1987): A Determination Procedure of Input Parameters in Elasto-Viscoplastic Finite Element Analysis. *Soils and Foundations*, Vol.27, No. 3, pp.71-87.
- Kamei, T., Tokuoaka, T., Sanbe, Y. and Ishihara, H. (1997): Depositional environment and mechanical properties of Holocene deposits in Matsue, J., Japan Soc., Eng., Geol., Vol.38, No.5, pp.280-295, 1997.(in Japanese)
- Kenney, T.C. (1964): Sea-Level Movements and The Geologic Histories of the Post-Glacial Marine Soils at Boston, Nicolet, Ottawa and Oslo. *Geotechnique*, Vol.XIV., No.3, pp.203-230.
- Meade, R.H. (1962): Factors Influencing the Pore Volume of Fine-grained Sediments under Low-to-moderate Overburden Loads. *Sedimentology*, 2, pp.235-242.
- Mesri, G. (1973): Coefficient of Secondary Compression. *Proc. ASCE*, Vol.99, No.SM1,pp.123-137.
- Mitcham, R. M. Jr., Vail, P. R. and Sangree, J. B. (1977): Stratigraphic Interpretation of Seismic Reflection Patterns in Depositional Sequence. Amer. Assoc. Petrol. Geo. Mem., 26, 117-134.
- Ohta, H. (1971): Analysis of deformations of soils based on the theory of plasticity and its application to settlement of embankment, Kyoto Univ. Dr. Thesis.
- Ohta, H. and Sekiguchi, H. (1979): Constitutive Equations Considering Anisotropy and Stress Reorientation in Clay, Proc. 3rd Int. Conf. on Numerical Methods in Geomechanics, Vol. 1, pp.475-484.
- Posamentier, H.W., Jervey, M.T, and Vail P.R. (1988): Eustatic Control on Clastic Deposition I-Conceptual Framework. *Soc. Econ. Paleont. Miner. Spe. Publ.*, 42, pp.109-124.
- Posamentier, H.W. and Vail, P.R. (1988): Eustatic Control on Clastic Deposition II-Sequence and Systems Tract Models. *Soc. Econ. Paleont. Miner. Spe. Publ.*, 42, pp.125-154.
- Sekiguchi, H. (1983): Effects of Time on the Compressibility of Clay Skelton. *Proc. 18th Japan National Conference of Soil Mech. and Foundation Eng.*, pp.209-210. (in Japanese)
- Sekiguchi, H. and Ohta, H. (1977): Induced Anisotropy and Time Dependency of Clay, Proc. Specialty Session 9th Int. Conf. of Soil Mechanics and Foundation Engrg., pp.229-239.
- Schofield, A. and Roth, P. (1968): *Critical State Soil Mechanics*, London, McGRAW-HILL, 310p.
- Shimizu, K. (1985): Geological Engineering Study on natural and reclaimed soil in Tokyo Bay, Doctor Thesis of Tokyo Institute of Technology. (in Japanese)
- Suter, J.R. (1994): *Deltaic coasts. In: Carter R. W. G. and Woodroffe, C. D. (eds.) Coastal evolution: Late Quaternary shoreline morphodynamics*, Cambridge: Cambridge University Press.
- Tohno, I. (1975): Diagenesis and Mechanical Characteristics of Sediments –Relation Between Arrangement of Grain and Unconfined Compressive Strength of Quaternary Sands in Southern Kanto-, *Chishitu-gaku Zasshi*, Vol.81, No.9, pp. 547-558. (in Japanese)
- Tohno, I. (1980): GEOLOGICAL AGE AND PHYSICAL CHARACTERISTICS OF SEDIMENTS, *Tsuchi-to-Kiso*, Vol.28, No.7, pp. 21-28. (in Japanese)
- Tohno, I. (1989): Geological study on the physical and mechanical properties of sandy deposits in Japan, Doctor Thesis of Tokyo Institute of Technology, p.272.
- Terzaghi, K and Peck, R. B. (1948): *Soil Mechanics in Engineering Practice*, U.S.A., John Wiley & Sons, 707p.
- Tsuchida, T. (1999): Strength Mobilization due to Cementation of Clay, *Report of the Port and Harbour Research*

Institute, Vol.38, No.2, pp.99-129.

Vail, P.R., Todd, R. G. and Sangree, J. B. (1977a): Chronostratigraphic significance of seismic reflections. Amer. Assoc. Petrol. Geo. Mem., 26, 99-116.

ESTIMATION OF SOIL PARAMETERS

2.1 Introduction

Bjerrum is one of the pioneers who proposed a hypothesis introducing the effect of 'Age' into the compression of the soil. Bjerrum has demonstrated to estimate the settlement of old buildings based on his hypothesis.

The ground condition at present such as stress state, soil properties and soil profile are the result of the transition of the depositional environment and the passing geological time. This information is of primary importance for elasto-plastic or elasto-viscoplastic F.E. analysis.

An attempt obtaining the initial stress condition based on Bjerrum's hypothesis is made in this chapter. 'Age' and 'PI' (plastic index) are chosen as geological parameters in this study. 'Age' represents geological time and 'PI' represents the characteristics of soil, which reflect the transition of depositional environment.

The compression of aged clays is estimated based on Bjerrum's hypothesis. Void ratio, settlement, over-consolidation ratio are obtained as a function of age and PI. The relation between the depth at present and the age of the soil is derived by taking the initial condition and the present condition into account. Initial condition is obtained by interpreting the field data. Finally the estimation chart for soil parameters based on age and PI is proposed.

2.2 Bjerrum's hypothesis

Lauritts Bjerrum is one of the first engineers who estimated the effect of time on compressibility by introducing the concept of delayed compression. Bjerrum made a hypothesis based on the results of the consolidation test (Taylor, 1942; Crawford, 1965). Bjerrum's hypothesis is that the compressibility of aged clay cannot be described by a single curve in e - $\log p'$ diagram but required a system of parallel lines illustrated in Fig.2.1 (Bjerrum, 1967).

The compression of aged clay is divided into two parts. When there remains excess pore

pressure, the compression divided into instant and delayed compression. After the dissipation of the excess pore pressure, the compression divided into primary and secondary compression. The concept of delayed compression is shown Fig.2.1. The definition of ‘instant’ and ‘delayed’ compression compared with ‘primary’ and ‘secondary’ compression are shown in Fig.2.2.

Bjerrum was successful in explaining the settlement of old buildings without any contradiction by applying this hypothesis in his paper.

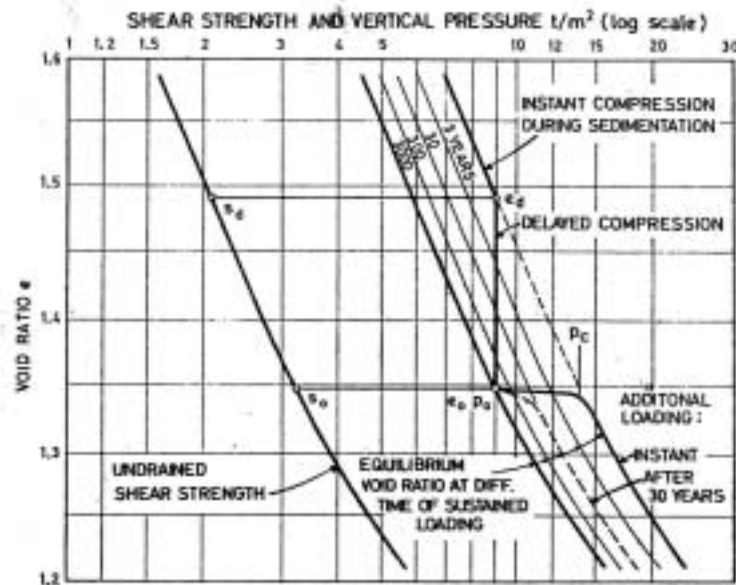


Fig.2.1 Compressibility and shear strength of a clay exhibiting delayed consolidation (After Bjerrum, L., 1967. Geotechnique, 17, p.95)

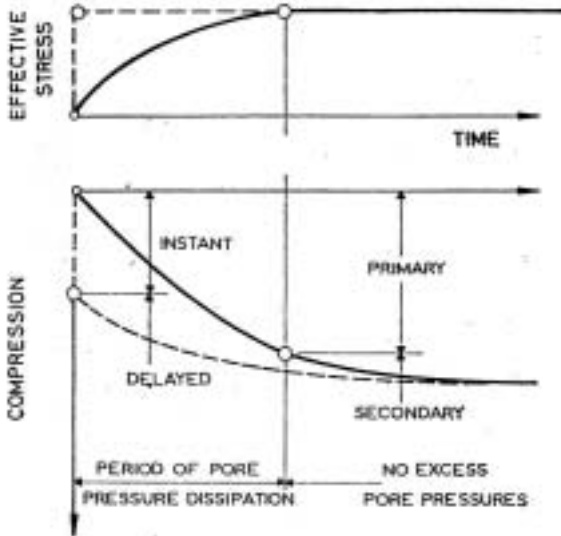


Fig.2.2 Definition of ‘instant’ and ‘delayed’ compression compared with ‘primary’ and ‘secondary’ compression (After Bjerrum, L., 1967. Geotechnique, 17, p.95)

2.3 Assumptions

In order to set the problem simple and obtain clear equations, assumptions are made in this study as follows:

- 1) The theory is based on Bjerrum's hypothesis.
Note that Bjerrum did not assume any constitutive equation in the paper.
- 2) Cementation, bonding and desiccation are not taken into account.
- 3) Primary and delayed compression may occur at the same time. Primary compression is completed in very short period compared with geological time scale.
- 4) Excess pore water pressure caused by sedimentation dissipates almost instantaneously.
- 5) The rate of the depositional rate is known. Constant rate is assumed in secs.2.4-2.10.
Several types of depositional rate are concerned in sec.2.11.
- 6) Depositional environment does not change over the period concerned.

2.4 Sedimentation and consolidation

Fig.2.3 shows two coordinate systems used in this study and the schematic drawing of sedimentation, in which "h" is the coordinate taking no account of settlement and "Z" is the depth at present after the completion of settlement. Let us assume the depositional rate $V = dh/dt$ to be constant in secs.2.4-2.10 for the simplicity. See sec.2.11 for another types of depositional rate.

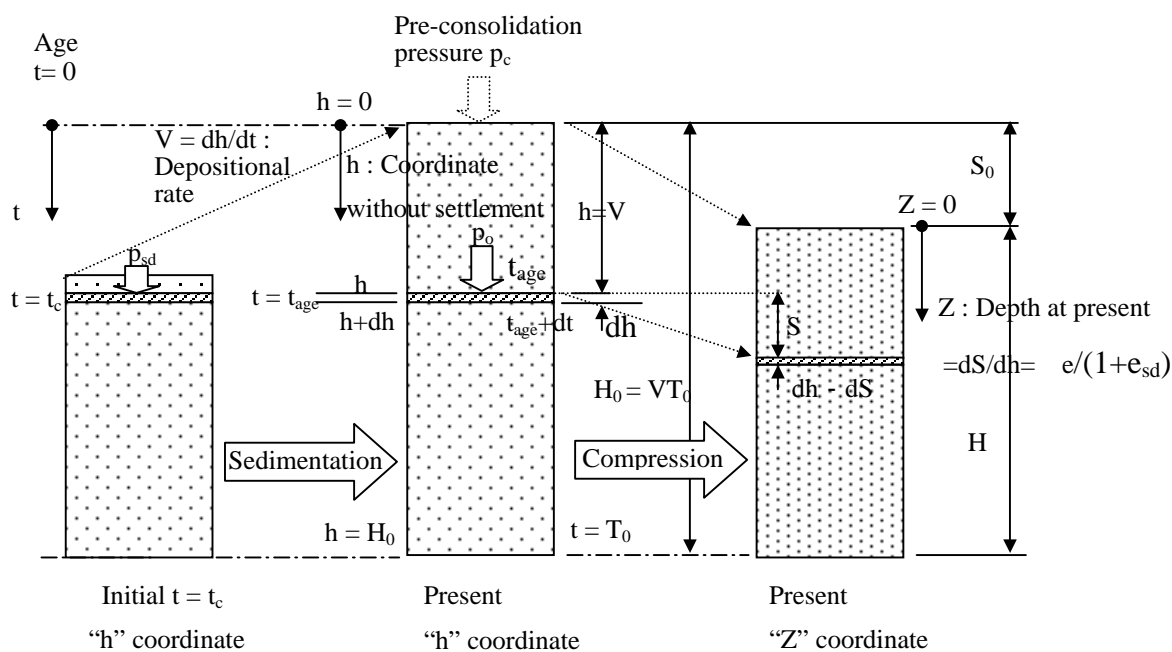


Fig.2.3 Coordinate systems and the schematic drawing of the sedimentation

2.5 Compression of aged clays

Through the concept of delayed compression, Bjerrum (1967) explained the settlement of clays after the sedimentation finished. Fig.2.4 shows that the sum of the primary compression during sedimentation and the delayed compression makes the total settlement. As demonstrated by Bjerrum (1967), the delayed compression results in the apparent pre-consolidation pressure p'_c greater than the geologically expected pre-consolidation pressure p'_o (i.e. the in-situ effective overburden pressure).

Initial overburden pressure p'_{sd} at the beginning of the sedimentation is assumed to be the pressure applied to the clay aged $t_c = 24$ hours for the sake of convenience in this study, where t_c is the incremental time of a loading step for the oedometer test in the laboratory. The t_c -line in Fig.2.4 is the reference for the delayed compression as demonstrated by Bjerrum. The t_{age} -line parallel to the t_c -line is obtained for the clay aged t_{age} after the sedimentation. The plot of the void ratio e vs. logarithm of the applied effective pressure $\ln p'$ returns back to the t_c -line during the oedometer test on an undisturbed specimen taken from the field. After the applied effective pressure reaches the apparent pre-consolidation pressure through the oedometer test, the plot moves on the t_c -line.

The change in the void ratio at rest $e_{in-situ}$ is the sum of the primary (elasto-plastic compression: $e_{e1} + e_p$) and delayed (visco-plastic compression: e_{vc}) compression. The sum of the compression elements is given by:

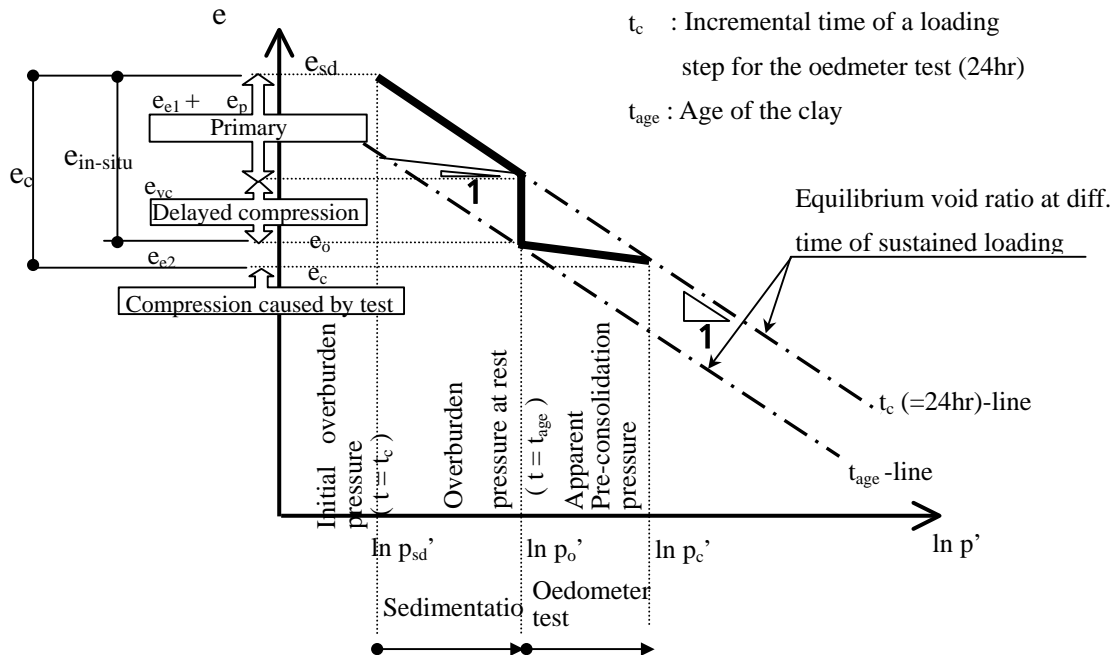


Fig.2.4 Bjerrum's concept of delayed compression

$$\begin{aligned}
\Delta e_{in-situ} &= \Delta e_p + \Delta e_{e1} + \Delta e_{vc} \\
&= (\lambda - \kappa) \ln\left(\frac{p'_0}{p'_{sd}}\right) + \kappa \ln\left(\frac{p'_0}{p'_{sd}}\right) + \alpha' \ln\left(\frac{t_{age}}{t_c}\right) \\
&= \lambda \ln\left(\frac{p'_0}{p'_{sd}}\right) + \alpha' \ln\left(\frac{t_{age}}{t_c}\right) \\
&= \lambda \ln\left(\frac{\gamma'_{sd} V t_{age}}{\gamma'_{sd} V t_c}\right) + \alpha' \ln\left(\frac{t_{age}}{t_c}\right) \\
&= \lambda \ln\left(\frac{t_{age}}{t_c}\right) + \alpha' \ln\left(\frac{t_{age}}{t_c}\right) \\
&= (\lambda + \alpha') \ln\left(\frac{t_{age}}{t_c}\right) ,
\end{aligned} \tag{2.1}$$

where α' is secondary compression index (Sekiguchi, 1977). Two constants λ , κ are related to compression index C_c and swelling index C_s as follow:

$$\alpha' = de/d(\ln t_{age}), \quad \lambda = 0.434C_c, \quad \kappa = 0.434C_s \tag{2.2}$$

Fig.2.5 describes the relationship among soil phases before and after the compression. The strain of the soil observed during a period from the initial state of the sedimentation to the present is given by:

$$\varepsilon = \frac{dS}{dh} = \frac{\Delta e_{in-situ}}{1 + e_{sd}} \tag{2.3}$$

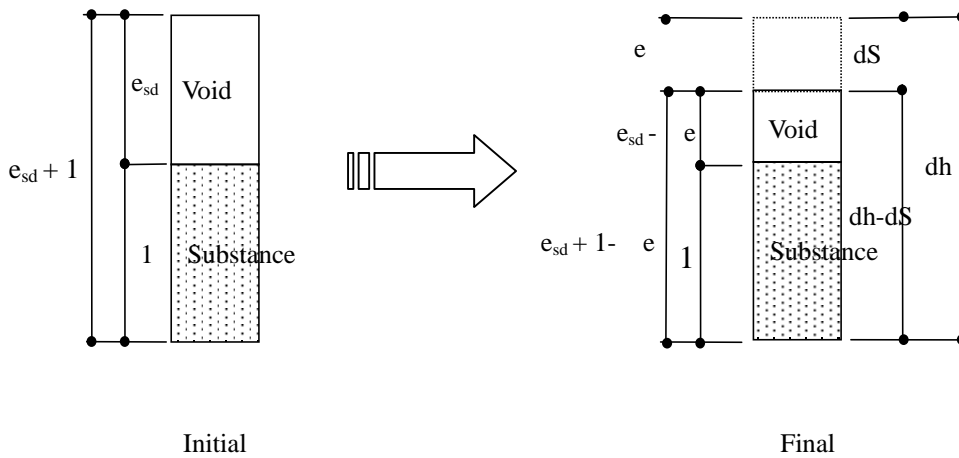


Fig.2.5 Change of the relationship among soil phases caused by compression

2.6 Settlement and age

From Fig.2.5 and Eq. (2.3) the settlement of a small clay element aged t with the height of dh is derived as follows:

$$dS = \varepsilon dh = \frac{\Delta e_{in-situ}}{1 + e_{sd}} dh = \frac{\lambda + \alpha'}{1 + e_{sd}} \ln \left(\frac{t}{t_c} \right) dh = \frac{\lambda + \alpha'}{1 + e_{sd}} \ln \left(\frac{t}{t_c} \right) V dt \quad (2.4)$$

The settlement of the surface of the ground aged t_{age} is derived by integrating Eq.(2.4) as follows, see Appendix 1:

$$\begin{aligned} S &= \int_{t_{age}}^{T_0} \frac{\lambda + \alpha'}{1 + e_{sd}} \ln \left(\frac{t}{t_c} \right) V dt \\ &= V \frac{\lambda + \alpha'}{1 + e_{sd}} \left\{ T_0 (\ln T_0 - \ln t_c - 1) - t_{age} (\ln t_{age} - \ln t_c - 1) \right\} \end{aligned} \quad (2.5)$$

The total settlement of a formation is obtained by taking the limitation of Eq. (2.5) with respect to t_{age} equal to zero, see Appendix 1.

$$\begin{aligned} S_0 &= \lim_{t_{age} \rightarrow 0} S(t_{age}) \\ &= \lim_{t_{age} \rightarrow 0} \left[V \frac{\lambda + \alpha'}{1 + e_{sd}} \left\{ T_0 (\ln T_0 - \ln t_c - 1) - t_{age} (\ln t_{age} - \ln t_c - 1) \right\} \right] \\ &= V \frac{\lambda + \alpha'}{1 + e_{sd}} \left\{ T_0 (\ln T_0 - \ln t_c - 1) \right\} \end{aligned} \quad (2.6)$$

2.7 Age and depth at present

Fig.2.6 describes the depositional thickness and the depth at present.

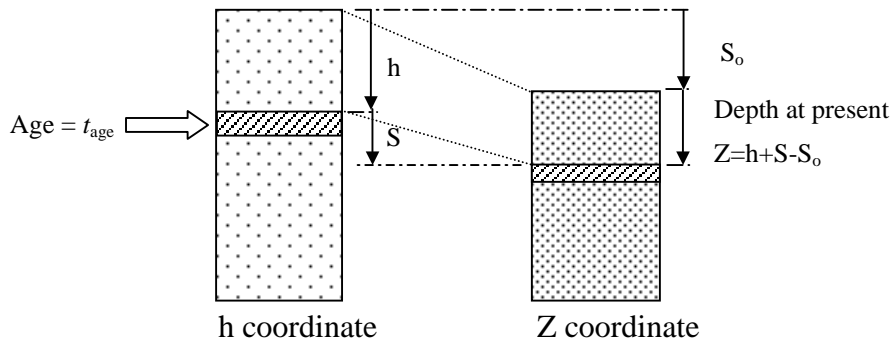


Fig.2.6 Relationship of the age and the depth at present

Present depth of a clay element in the formation is related to its age as follows:

$$\begin{aligned}
 Z &= h + S - S_0 \\
 &= Vt_{age} \left\{ 1 - \frac{\lambda + \alpha'}{1 + e_{sd}} (\ln t_{age} - \ln t_c - 1) \right\}
 \end{aligned} \tag{2.7}$$

2.8 Initial conditions

Initial conditions have to be specified in such a way that they are logically in accordance with the present soil conditions such as 1) thickness of the layer, 2) unit weight, 3) age. For example the total thickness H_0 of the sediment turns to be a formation with the present thickness H after the consolidation which consists of primary and delayed compression. In order to achieve no contradiction between initial and present soil conditions, required are the reasonable setting of the depositional rate, the initial void ratio and the unit weight as shown in 2.8.1 and 2.8.2.

2.8.1 Thickness of the formation and depositional rate

The initial thickness of the formation H_0 turned to be the present thickness H due to the total settlement S_0 . The present thickness of the formation H is given by:

$$\begin{aligned}
 H &= H_0 - S_0 \\
 &= H_0 - V \frac{\lambda + \alpha'}{1 + e_{sd}} \{ T_0 (\ln T_0 - \ln t_c - 1) \}
 \end{aligned} \tag{2.8}$$

The relationship of apparent and true depositional rate (V_a and V respectively) is obtained by dividing both side of Eq. (2.8) by T_0 as follows:

$$\frac{H}{T_0} = \frac{H_0}{T_0} \left\{ 1 - \frac{\lambda + \alpha'}{1 + e_{sd}} (\ln T_0 - \ln t_c - 1) \right\} \tag{2.9}$$

$$V_a = V \left\{ 1 - \frac{\lambda + \alpha'}{1 + e_{sd}} (\ln T_0 - \ln t_c - 1) \right\} \tag{2.10}$$

2.8.2 Initial void ratio and submerged unit weight

The unit weights of the clay at the stage of the initial and the present are given:

$$\gamma'_{sd} = \frac{G_s - 1}{1 + e_{sd}} \gamma_w \quad (2.11)$$

$$\gamma' = \frac{G_s - 1}{1 + e_{sd} - \Delta e_{in-situ}} \gamma_w = \frac{G_s - 1}{1 + e_{sd} - (\lambda + \alpha') \ln \left(\frac{t_{age}}{t_c} \right)} \gamma_w, \quad (2.12)$$

where G_s is the specific gravity of the soil substance.

Though it is difficult for us to measure initial unit weight γ'_{sd} and void ratio e_{sd} directly, the information from the boring data is available to estimate initial unit weight and void ratio in the following procedure. Suppose the average unit weight of the soil ranging from the ground surface down to a certain depth (H) aged $t_{age}=T$ can be obtained by the boring data. Those averaged void ratio and unit weight are derived by averaging theoretical distributions as follows:

$$\overline{\Delta e} = \frac{1}{H} \int_0^H \Delta e_{in-situ} dh = (\lambda + \alpha') (\ln T - \ln t_c - 1) \quad (2.13)$$

$$\overline{\gamma'} = \frac{G_s - 1}{1 + e_{sd} - \overline{\Delta e}} \gamma_w = \frac{G_s - 1}{1 + e_{sd} - (\lambda + \alpha') (\ln T - \ln t_c - 1)} \gamma_w \quad (2.14)$$

Thus initial void ratio is given by substituting averaged unit weight and averaged void ratio into Eq. (2.14):

$$e_{sd} = \frac{(G_s - 1) \gamma_w}{\overline{\gamma'}} + \overline{\Delta e} - 1 \quad (2.15)$$

Finally initial unit weight γ'_{sd} is estimated by substituting initial void ratio e_{sd} into Eq. (2.11). Let us present an example how to make use of the boring data in order to calculate initial unit weight γ'_{sd} and void ratio e_{sd} which are given by Eqs. (2.11) - (2.15).

Tsuji (2000) presented the distribution of the unit weight and plasticity index PI of shallow marine clays at many places in the world. As shown in Fig.2.7 the tendency of the relation between unit weight and PI indicates that the lower the PI , the heavier the unit weight

and vice versa. Consequently the effect of the plasticity index to the initial condition is taken into account in this investigation by obtaining the relation between unit weight and PI . The effect of PI to the unit weight of clays is due to the effect of PI to the water content. Let us then try to relate PI with water content.

Terzaghi and Peck (1967) correlated C_c and w_L as shown in Eq.(2.16), where C_c is the compression index and w_L is the liquid limit.

$$C_c = 0.009(w_L - 10), \text{Terzaghi and Peck(1967)} \quad (2.16)$$

Eq. (2.17) is the C_c and PI relation proposed by Iizuka and Ohta(1987).

$$\lambda = 0.434C_c = 0.015 + 0.007PI, \text{Iizuka and Ohta(1987)} \quad (2.17)$$

The relationship between PI and w_L is given by substituting Eq.(2.16) into Eq.(2.17).

$$w_L = 1.79PI + 13.8 \quad (2.18)$$

The natural water content w_n is related to the liquid limit w_L and PI as shown in Eq. (2.19) by introducing the ratio $a = w_n / w_L$:

$$w_n = aw_L = a(1.79PI + 13.8) \quad (2.19)$$

where,

$$a = \frac{w_n}{w_L} = (w_L - PI \times CI) / w_L = 1 - PI \times CI / w_L = 1 - PI(1 - LI) / w_L$$

Thus the unit weight related to PI is given by:

$$\bar{\gamma}' = \frac{G_s - 1}{1 + G_s \frac{w_n}{100}} \gamma_w = \frac{G_s - 1}{1 + G_s \frac{a(1.79PI + 13.8)}{100}} \gamma_w \quad (2.20)$$

Fig.2.7 shows the comparison of Eq. (2.20) and the distribution of unit weight of natural marine clay at the depths shallower than 10m. All the data in Fig.2.7 are given by Tsuji (2000). Eq. (2.20) is in agreement with the data of the natural clay if we assume that $G_s=2.7$ and the ratio “a” is in the range of 0.6 - 1.0.

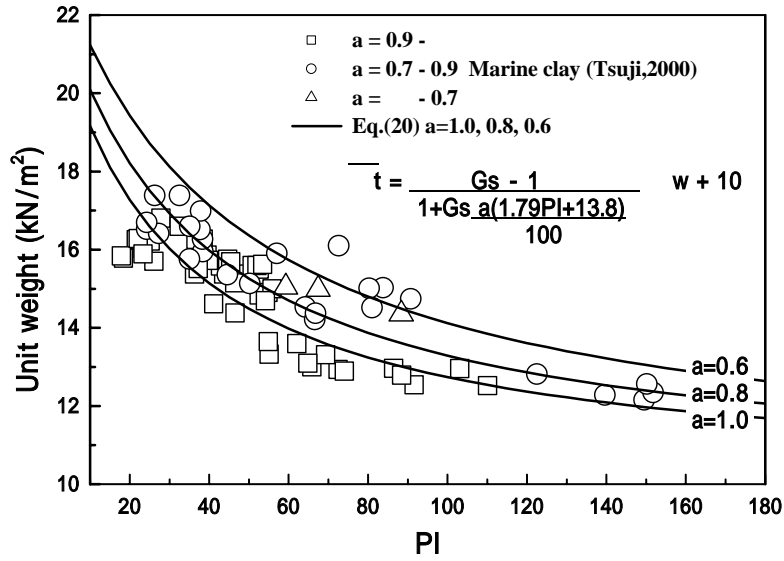


Fig.2.7 PI- relation

Eq.(2.20) and Fig.2.7 enable us to estimate average unit weight of the formation at the depths shallower than 10m. Average compression can be obtain by substituting the age of soil T at 10m, $t_c = 24$ hours, λ and κ into Eq.(2.13). σ'_{sd} and e_{sd} can be calculated by means of Eqs.(2.11), (2.15). This example shows that the initial conditions can be estimated by taking the plasticity of clays into account.

2.9 Over-consolidation ratio

2.9.1 Theoretical over-consolidation ratio

Fig.2.4 indicates that the total compression of clay e_c from the beginning of the sedimentation through the oedometer test is obtained as follows:

$$\begin{aligned} \Delta e_c &= \Delta e_p + \Delta e_{e1} + \Delta e_{vc} + \Delta e_{e2} \\ &= (\lambda - \kappa) \ln\left(\frac{p'_0}{p'_{sd}}\right) + \kappa \ln\left(\frac{p'_0}{p'_{sd}}\right) + \alpha' \ln\left(\frac{t_{age}}{t_c}\right) + \kappa \ln\left(\frac{p'_c}{p'_0}\right) \end{aligned} \quad (2.21)$$

At the same time, e_c is directly given as:

$$\Delta e_c = \lambda \ln\left(\frac{p'_c}{p'_{sd}}\right) \quad (2.22)$$

Theoretical *OCR* is given by comparing Eqs. (2.21) and (2.22) as follows:

$$\lambda \ln \left(\frac{p'_0}{p'_{sd}} \right) + \alpha' \ln \left(\frac{t_{age}}{t_c} \right) + \kappa \ln \left(\frac{p'_c}{p'_0} \right) = \lambda \ln \left(\frac{p'_c}{p'_{sd}} \right) \quad (2.23)$$

$$p_0' \left(\frac{t_{age}}{t_c} \right)^{\frac{\alpha'}{\lambda - \kappa}} = p_c' \quad (2.24)$$

$$OCR = \frac{p_c'}{p_0'} = \left(\frac{t_{age}}{t_c} \right)^{\frac{\alpha'}{\lambda - \kappa}} = \left(\frac{t_{age}}{t_c} \right)^{\frac{\alpha'}{\lambda(1 - \kappa/\lambda)}} = \left(\frac{t_{age}}{t_c} \right)^{\frac{\alpha'}{\lambda\Lambda}}, \quad (2.25)$$

where $\Lambda = 1 - \kappa/\lambda$ is the irreversibility ratio, Iizuka(1997).

Several types of approach to the physical meaning of *OCR* are proposed (e.g. Mesri & Choi,1979; Murakami, 1979/1980; Mesri & Castro, 1987; Iizuka, 1997) based on several sets of assumptions. In deriving Eq.(2.25), it is assumed that primary and delayed compression may occur at the same time. Eq.(2.25) results in the same equation proposed by Iizuka(1997).

2.9.2 Apparent pre-consolidation pressure and oedometer test

Bjerrum (1967) mentioned that the apparent pre-consolidation pressure p_c' obtained by oedometer test is greater than the in-situ overburden pressure because of the delayed compression (cf. Fig.2.4). Crawford (1964) reported that the longer the incremental time of a loading step in the oedometer test, the smaller the pre-consolidation pressure. The effect of the incremental time of a loading step in the oedometer test to the pre-consolidation pressure is derived from Eq. (2.25) as follows:

$$p_c' = p_0' \left(\frac{t_{age}}{t_c} \right)^{\frac{\alpha'}{\lambda - \kappa}} \Rightarrow \frac{p_c'}{p_{c[STD]}'}, = \left(\frac{t_{c[STD]}}{t_c} \right)^{\frac{\alpha'}{\lambda - \kappa}}, \quad (2.26)$$

where $p_{c[STD]}$ and $t_{c[STD]}$ are the pre-consolidation pressure and the incremental time of a loading step for the standard oedometer test. In the case where $t_{c[STD]}$ is 24 hours, Equation (2.26) is in agreement with Crawford (1964).

Vaid et al.(1979) noted the effect of the strain rate on the pre-consolidation pressure. They pointed out that the smaller the strain rate, the smaller the pre-consolidation pressure. The effect of the strain rate on the pre-consolidation pressure is also derived from Equation (2.26) as follows:

$$p_c' = p_0' \left(\frac{t_{age}}{t_c} \right)^{\frac{\alpha'}{\lambda - \kappa}} = p_0' \left(\frac{\dot{\epsilon}_c}{\dot{\epsilon}} \right)^{\frac{\alpha'}{\lambda - \kappa}} \Rightarrow \frac{p_c'}{p_{c[STD]}'}, = \left(\frac{\dot{\epsilon}_c}{\dot{\epsilon}_{c[STD]}} \right)^{\frac{\alpha'}{\lambda - \kappa}} \quad (2.27)$$

$$\text{where } \dot{\epsilon} = \frac{1}{1+e_{sd}} \frac{de}{dt_{age}} = \frac{1}{1+e_{sd}} \frac{\alpha'}{t_{age}} \Rightarrow t_{age} = \frac{\alpha'}{1+e_{sd}} \frac{1}{\dot{\epsilon}} \quad (2.28)$$

$$\therefore de = d(\alpha' \ln t_{age}) = \alpha' \frac{d \ln t_{age}}{dt_{age}} dt_{age} = \alpha' \frac{dt_{age}}{t_{age}} \quad (2.29)$$

Eq. (2.27) corresponds to Vaid et al.(1979). Fig.2.8 shows the effect of the oedometer test condition to the pre-consolidation pressure. The parameters used in the calculation are as follows:

$$\alpha' = 9.45 \times 10^{-3} \quad , \quad \lambda = 0.435 \quad , \quad \kappa = 0.208$$

The calculation simulating the loading time effect and the strain rate effect show the same tendency as Crawford (1964) and Vaid et al. (1979).

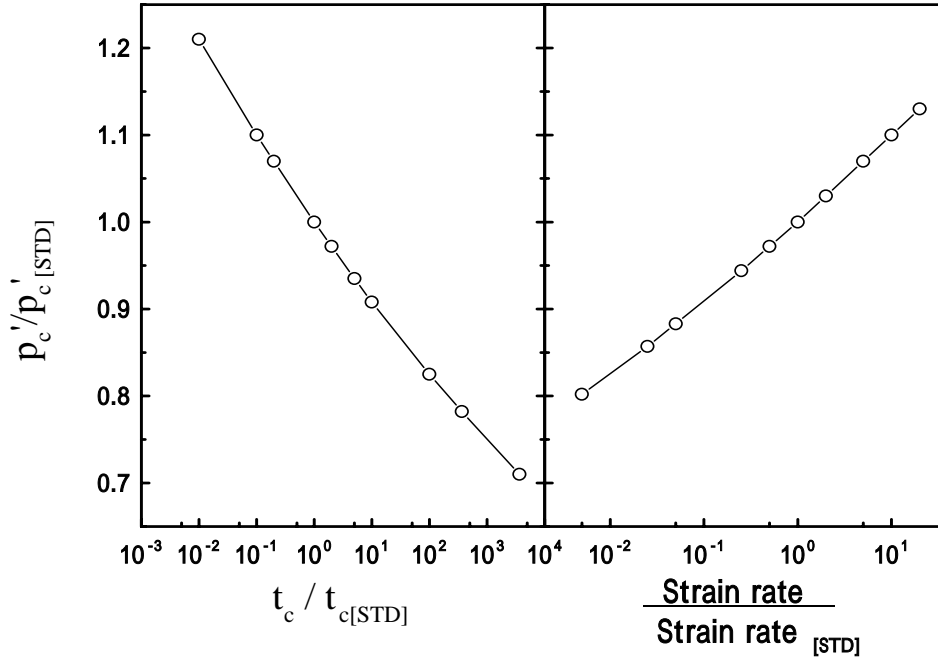
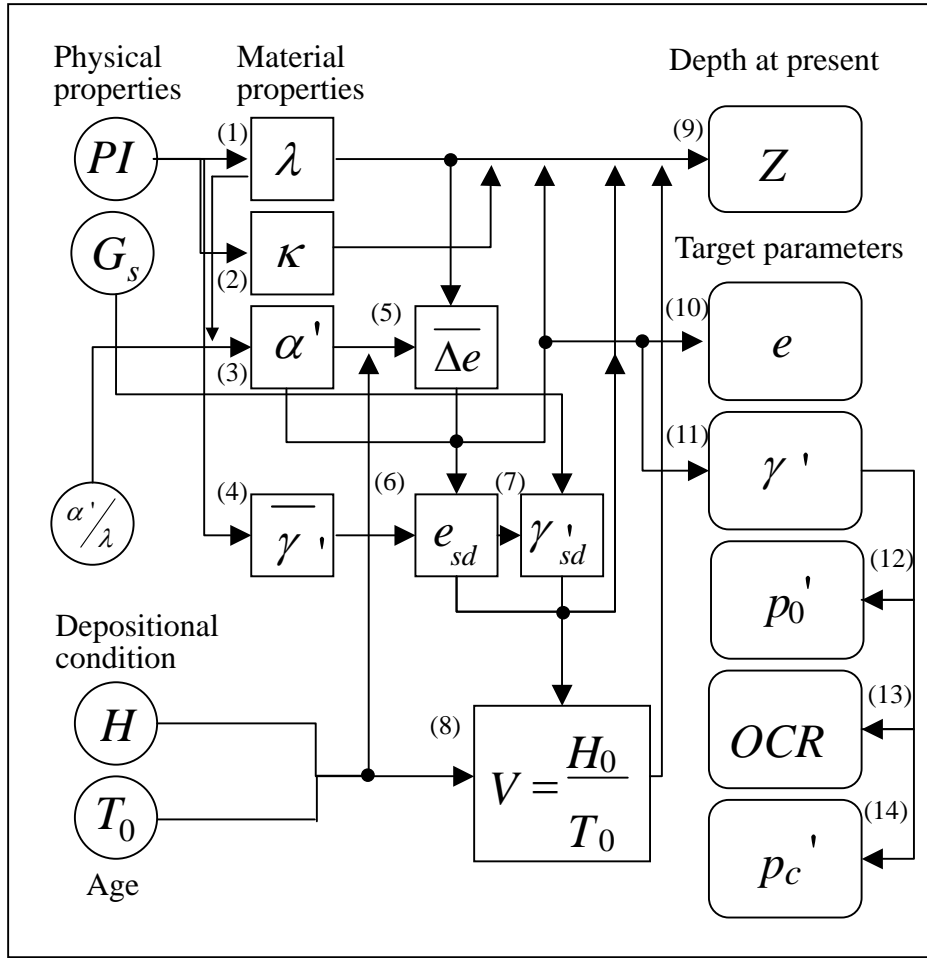


Fig.2.8 The effect of condition of the oedometer test on the pre-consolidation pressure

2.10 Chart for parameters estimation based on PI and age

Fig.2.9 is the chart for soil parameters estimation based on the age and the plasticity of soils. It is possible for engineers to estimate all the parameters required for the elasto-viscoplastic finite element analysis by using the determination diagram (Fig.2.10) proposed by Iizuka and Ohta (1987) together with the chart in Fig.2.9.



$$(1) \lambda = 0.015 + 0.007PI \quad \text{Iizuka \& Ohta(1987)}$$

$$(7) \gamma'_{sd} = \frac{G_s - 1}{1 + e_{sd}} \gamma_w$$

$$\kappa = \lambda(1 - \Lambda)$$

$$\text{where } \Lambda = M/1.75 \quad \text{Karube(1975)}$$

$$(2) M = 6 \sin \phi' / (3 - \sin \phi')$$

$$\sin \phi' = 0.81 - 0.233 \log PI \quad \text{Kenny(1959)}$$

$$(8) V = \frac{H}{T_0} \left/ \left\{ 1 - \frac{\lambda + \alpha'}{1 + e_{sd}} (\ln T_0 - \ln t_c - 1) \right\} \right.$$

$$(9) Z = V t_{age} \left\{ 1 - \frac{\lambda + \alpha'}{1 + e_{sd}} (\ln t_{age} - \ln t_c - 1) \right\}$$

$$(10) e = e_{sd} - (\lambda + \alpha') \ln (t_{age} / t_c)$$

$$(3) \frac{\alpha'}{\lambda} = 0.05 \pm 0.02 (\text{clay}) \quad \text{Mesri \&}$$

$$0.07 \pm 0.02 (\text{peat}) \quad \text{Godlewski(1977)}$$

$$(11) \gamma' = \frac{G_s - 1}{1 + e_{sd} - (\lambda + \alpha') \ln (t_{age} / t_c)} \gamma_w$$

$$(4) \bar{\gamma}' = \frac{(G_s - 1) \gamma_w}{1 + G_s a (1.79 PI + 13.8) / 100}, \quad a = w_n / w_L$$

$$(12) OCR = \left(t_{age} / t_c \right)^{\frac{\alpha'}{\lambda - \kappa}} \quad \text{Iizuka(1997)}$$

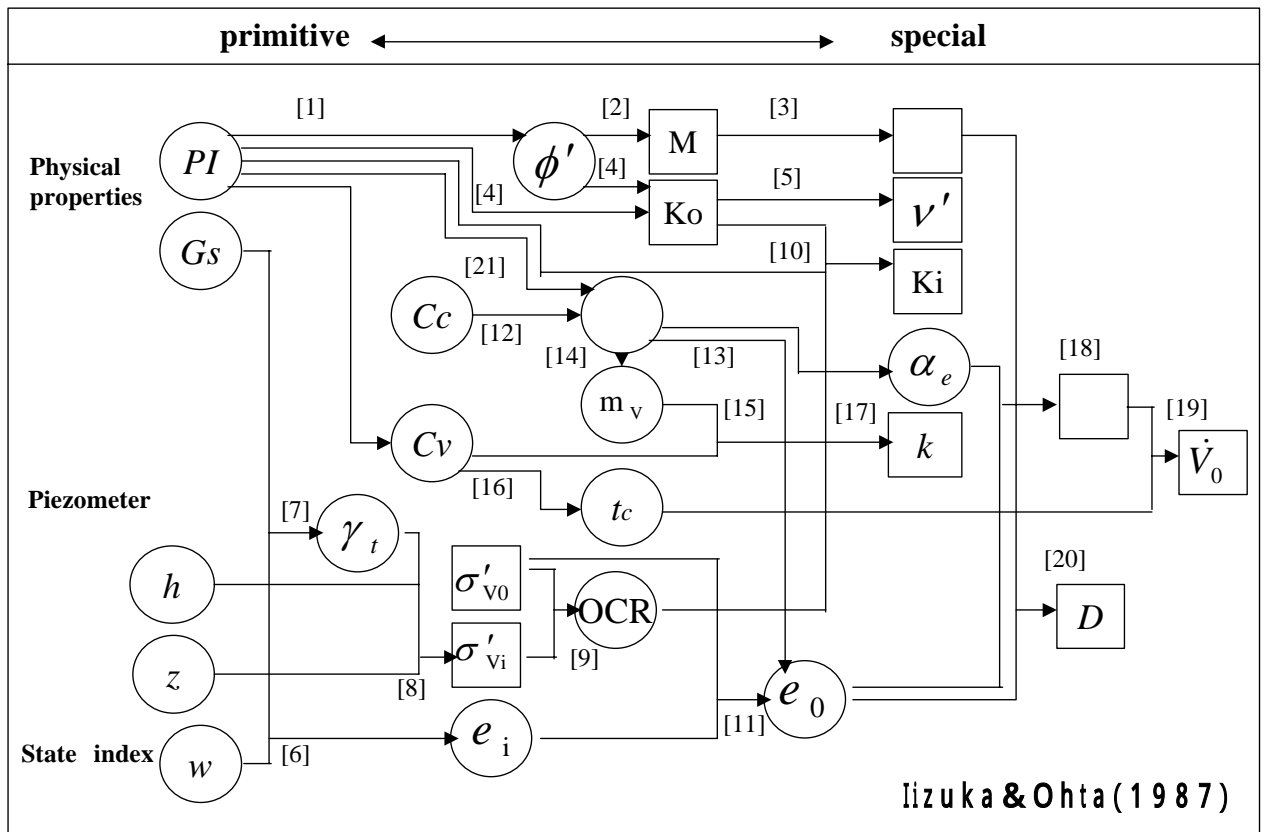
$$(5) \bar{\Delta e} = (\lambda + \alpha') (\ln T - \ln t_c - 1)$$

$$(13) p'_0 = \gamma'_{sd} V t_{age}$$

$$(6) e_{sd} = \frac{(G_s - 1) \gamma_w}{\bar{\gamma}'} + \bar{\Delta e} - 1$$

$$(14) p'_c = p'_0 \left(t_{age} / t_c \right)^{\frac{\alpha'}{\lambda - \kappa}}$$

Fig.2.9 Chart for soil parameter estimation based on PI and Age



$$[1] \sin \phi' = 0.81 - 0.233 \log PI \quad \text{Kenny(1959)}$$

$$[2] M = 6 \sin \phi' / (3 - \sin \phi')$$

$$[3] \Lambda = M / 1.75 \quad \text{Karube (1975)}$$

$$[4] K_0 = 0.44 + 0.42 \times 10^{-2} PI \quad \text{Massarsch(1979)}$$

$$K_0 = 1 - \sin \phi' \quad \text{Jakey(1944)}$$

$$[5] \nu' = K_0 / (1 + K_0)$$

$$[6] e_i = w G_s$$

$$[7] \gamma_t = G_s \gamma_w (1 + w) / (1 + G_s w)$$

$$[8] \sigma'_{vi} = \gamma_t z - p_w$$

$$[9] OCR = \sigma'_{v0} / \sigma'_{vi}$$

$$[10] K_i = K_0 (OCR)^{0.54 \exp(-P/122)} \quad \text{Alpan(1967)}$$

$$[11] e_0 = e_i - \lambda(1 - \Lambda) \ln(\overline{OCR}) \quad \overline{OCR} = \frac{1 + 2K_0}{1 + 2K_i} OCR$$

$$[12] \lambda = 0.434 Cc$$

$$[13] e_0 = 3.78 + 0.156$$

$$[14] m_v = 3 / [(1 + e_0)(1 + 2K_0) \nu'_{v0}]$$

$$[15] k = m_v c_v \gamma_w$$

$$[16] t_c \approx t_{90} = H^2 T_v (U = 90\%) / c_v$$

$$[17] \alpha_e / \lambda = 0.05 \pm 0.02 \quad (\text{clay})$$

$$\text{Mesri \& Godlewski(1977)}$$

$$= 0.07 \pm 0.02 \quad (\text{peat})$$

$$\text{Sekiguchi(1977)}$$

$$[18] \alpha = \alpha_e / (1 + e_0) \quad \text{Sekiguchi(1977)}$$

$$[19] \dot{V}_0 = \alpha / t_c \quad \text{Sekiguchi(1977)}$$

$$[20] D = \lambda \Lambda / [M(1 + e_0)] \quad \text{Ohta(1971)}$$

$$[21] \lambda = 0.015 + 0.007 PI$$

$$[22] \log c_v (\text{cm}^2 / \text{min}) = -0.025 PI - 0.25 \pm 1$$

Fig.2.10 Proposed determination procedure of input parameters

(After Iizuka and Ohta, 1987, Soils and Foundations, Vol.27, No.3, p.77)

2.11 Theory of the soil parameters for various depositional rates

Depositional rate is assumed to be constant in secs.2.4-2.10 for the simplicity. The field observation and the dating of the formations indicate that actual depositional rates are not always constant during the geological time according to. Fig.2.11 and Figures in the appendix 2 show the examples of the transition of the depositional rate in the sedimentation as Age-Depth diagram. The transition of the depositional rate is supposed to be results of the sea-level changes which are also periodic (e.g. Haq et.al., 1988, Posamentier and Vail, 1988). Though we are not concerned with this topic deeper in this chapter, examples of the sea-level changes are introduced in chapter 5.

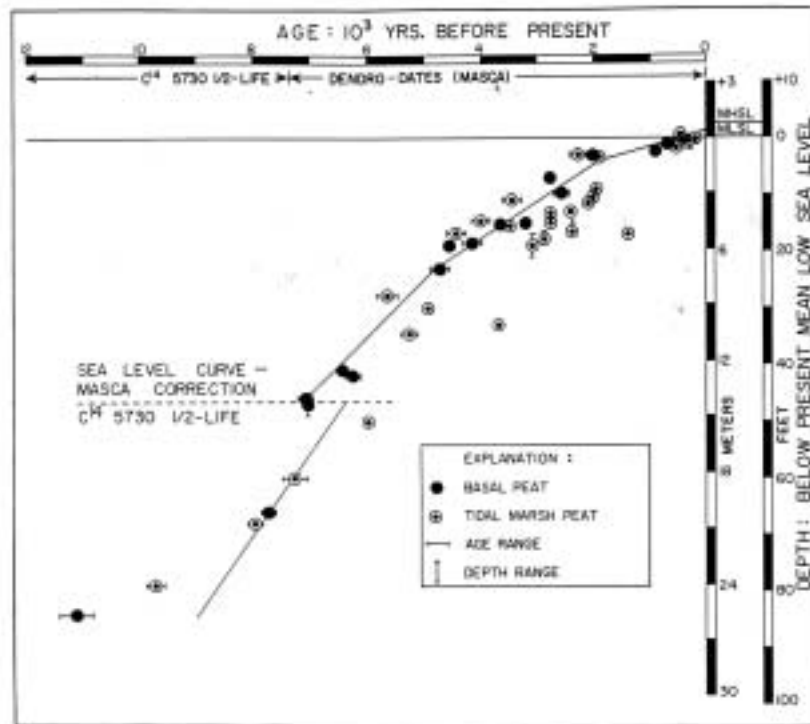


Fig. 2.—A local relative sea-level rise curve for the Delaware coastal zone based on basal peat. The sea-level curve shown is a smooth line average and is not mathematically derived. Other data from tidal marsh peats have been used for paleogeographic reconstructions but have not been used in drawing an irregular curve based on the basal peat data shown. Densidade (MASCA) corrections after Ralph and others (1977); from Kraft, 1976.

Fig.2.11 An example of the age-depth relation (After Kraft et.al., 1987)

(1) Age and depositional thickness h

Additional four models of depositional rate are chosen in order to investigate the effect of depositional rate in Chapter 3. First the age-depth relations are set for each model as follows:

$$\text{(Type1)} \quad h = C_1 t \quad (2.30)$$

$$\text{(Type2)} \quad h = C_1 t - C_2 \sin\left(\frac{2\pi t}{T_0}\right) \quad (2.31)$$

$$\text{(Type3)} \quad h = C_1 t + C_2 \sin\left(\frac{2\pi t}{T_0}\right) \quad (2.32)$$

$$\text{(Type4)} \quad h = C_1 t - C_2 \sin\left(\frac{\pi t}{T_0}\right) \quad (2.33)$$

$$\text{(Type5)} \quad h = C_1 t + C_2 \sin\left(\frac{\pi t}{T_0}\right) \quad (2.34)$$

where C_1 and C_2 are constant. Note that Type 1 is constant depositional rate which has been studied in the previous sections. The diagram of age-h relation is illustrated in Fig.2.12.

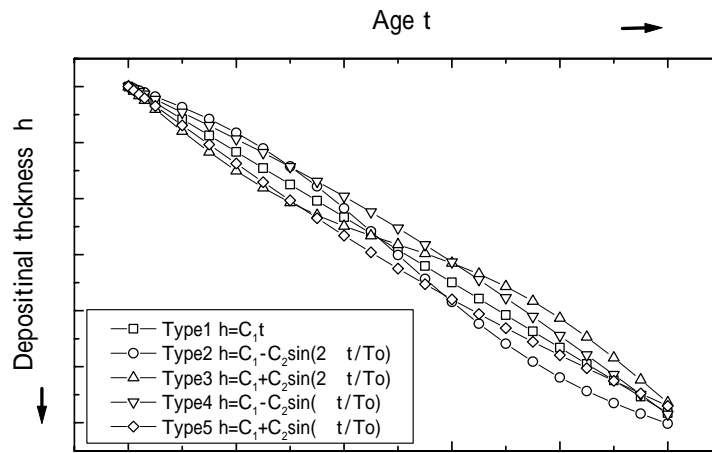


Fig.2.12 Schematic diagram of age and depositional thickness h

(2) Depositional rate

Each type of depositional rate is given by:

$$\text{(Type1)} \quad V = \frac{dh}{dt} = C_1 \quad (2.35)$$

$$\text{(Type2)} \quad V = \frac{dh}{dt} = C_1 - C_2 \frac{2\pi}{T_0} \cos\left(\frac{2\pi t}{T_0}\right) \quad (2.36)$$

$$\text{(Type3)} \quad V = \frac{dh}{dt} = C_1 + C_2 \frac{2\pi}{T_0} \cos\left(\frac{2\pi t}{T_0}\right) \quad (2.37)$$

$$\text{(Type4)} \quad V = \frac{dh}{dt} = C_1 - C_2 \frac{\pi}{T_0} \cos\left(\frac{\pi t}{T_0}\right) \quad (2.38)$$

$$(Type5) \quad V = \frac{dh}{dt} = C_1 + C_2 \frac{\pi}{T_0} \cos\left(\frac{\pi t}{T_0}\right) \quad (2.39)$$

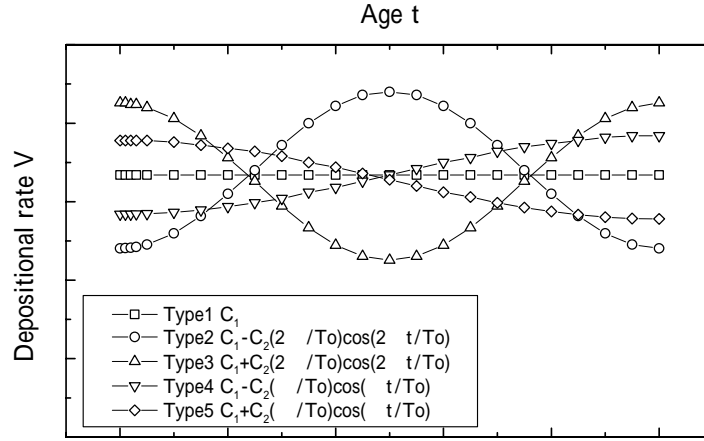


Fig.2.13 Schematic diagram of age and depositional age

(3) Compression of soil

Compression is as follows, see Fig.2.1 :

$$\begin{aligned} \Delta e &= \lambda \ln\left(\frac{p_0'}{p_{sd}'}\right) + \alpha' \ln\left(\frac{t}{t_c}\right) \\ &= \lambda \ln\left(\frac{\gamma_{sd}' h(t)}{\gamma_{sd}' h(t_c)}\right) + \alpha' \ln\left(\frac{t}{t_c}\right) \\ &= \lambda \ln\left(\frac{h(t)}{h(t_c)}\right) + \alpha' \ln\left(\frac{t}{t_c}\right) \end{aligned} \quad (2.40)$$

Each type of compression is given by substituting Eqs.(2.30)-(2.34) into Eq.(2.40).

$$(Type1) \quad \Delta e = \lambda \ln\left(\frac{t}{t_c}\right) + \alpha' \ln\left(\frac{t}{t_c}\right) = (\lambda + \alpha') \ln\left(\frac{t}{t_c}\right) \quad (2.41)$$

$$(Type2) \quad \Delta e = \lambda \ln\left\{ \frac{C_1 t - C_2 \sin\left(\frac{2\pi t}{T_0}\right)}{C_1 t_c - C_2 \sin\left(\frac{2\pi t_c}{T_0}\right)} \right\} + \alpha' \ln\left(\frac{t}{t_c}\right) \quad (2.42)$$

$$(Type3) \quad \Delta e = \lambda \ln \left\{ \frac{C_1 t + C_2 \sin\left(\frac{2\pi t}{T_0}\right)}{C_1 t_c + C_2 \sin\left(\frac{2\pi t_c}{T_0}\right)} \right\} + \alpha' \ln\left(\frac{t}{t_c}\right) \quad (2.43)$$

$$(Type4) \quad \Delta e = \lambda \ln \left\{ \frac{C_1 t - C_2 \sin\left(\frac{\pi t}{T_0}\right)}{C_1 t_c - C_2 \sin\left(\frac{\pi t_c}{T_0}\right)} \right\} + \alpha' \ln\left(\frac{t}{t_c}\right) \quad (2.45)$$

$$(Type5) \quad \Delta e = \lambda \ln \left\{ \frac{C_1 t + C_2 \sin\left(\frac{\pi t}{T_0}\right)}{C_1 t_c + C_2 \sin\left(\frac{\pi t_c}{T_0}\right)} \right\} + \alpha' \ln\left(\frac{t}{t_c}\right) \quad (2.46)$$

(4) Settlement

Settlement is derived as follow:

$$S = \int_{t_{age}}^{T_0} \frac{\Delta e V}{1 + e_{sd}} dt \quad (2.47)$$

Each type of the settlement is given by substituting Eqs. (2.35)-(2.39) and Eqs. (2.41)-(2.46) into Eq.(2.47)

$$(Type1) \quad S = \int_{t_{age}}^{T_0} \frac{C_1}{1 + e_{sd}} (\lambda + \alpha') \ln\left(\frac{t}{t_c}\right) dt \quad (2.48)$$

$$(Type2) \quad S = \int_{t_{age}}^{T_0} \frac{1}{1 + e_{sd}} \left[\lambda \ln \left\{ \frac{C_1 t - C_2 \sin\left(\frac{2\pi t}{T_0}\right)}{C_1 t_c - C_2 \sin\left(\frac{2\pi t_c}{T_0}\right)} \right\} + \alpha' \ln\left(\frac{t}{t_c}\right) \right] \left\{ C_1 - C_2 \frac{2\pi}{T_0} \cos\left(\frac{2\pi t}{T_0}\right) \right\} dt \quad (2.49)$$

$$\text{(Type3)} S = \int_{t_{age}}^{T_0} \frac{1}{1 + e_{sd}} \left[\lambda \ln \left\{ \frac{C_1 t + C_2 \sin\left(\frac{2\pi t}{T_0}\right)}{C_1 t_c + C_2 \sin\left(\frac{2\pi t_c}{T_0}\right)} \right\} + \alpha' \ln\left(\frac{t}{t_c}\right) \right] \left\{ C_1 + C_2 \frac{2\pi}{T_0} \cos\left(\frac{2\pi t}{T_0}\right) \right\} dt \quad (2.50)$$

$$\text{(Type4)} S = \int_{t_{age}}^{T_0} \frac{1}{1 + e_{sd}} \left[\lambda \ln \left\{ \frac{C_1 t - C_2 \sin\left(\frac{\pi t}{T_0}\right)}{C_1 t_c - C_2 \sin\left(\frac{\pi t_c}{T_0}\right)} \right\} + \alpha' \ln\left(\frac{t}{t_c}\right) \right] \left\{ C_1 - C_2 \frac{\pi}{T_0} \cos\left(\frac{\pi t}{T_0}\right) \right\} dt \quad (2.51)$$

$$\text{(Type5)} S = \int_{t_{age}}^{T_0} \frac{1}{1 + e_{sd}} \left[\lambda \ln \left\{ \frac{C_1 t + C_2 \sin\left(\frac{\pi t}{T_0}\right)}{C_1 t_c + C_2 \sin\left(\frac{\pi t_c}{T_0}\right)} \right\} + \alpha' \ln\left(\frac{t}{t_c}\right) \right] \left\{ C_1 + C_2 \frac{\pi}{T_0} \cos\left(\frac{\pi t}{T_0}\right) \right\} dt \quad (2.52)$$

(5) Age and depth at present

The relation between depth at present and age of soil is given as follows:

$$\begin{aligned} Z &= h + S - S_0 \\ &= h + \int_{t_{age}}^{T_0} \frac{\Delta e V}{1 + e_{sd}} dt - \int_0^{T_0} \frac{\Delta e V}{1 + e_{sd}} dt \\ &= h - \int_0^{t_{age}} \frac{\Delta e V}{1 + e_{sd}} dt \end{aligned} \quad (2.53)$$

$$\text{(Type1)} \quad Z = C_1 t_{age} \left\{ 1 - \frac{\lambda + \alpha'}{1 + e_{sd}} (\ln t_{age} - \ln t_c - 1) \right\} \quad (2.54)$$

(Type2)

$$Z = \left\{ C_1 t_{age} - C_2 \sin\left(\frac{2\pi t_{age}}{T_0}\right) \right\} - \int_{t_c}^{t_{age}} \frac{1}{1 + e_{sd}} \left[\lambda \ln \left\{ \frac{C_1 t - C_2 \sin\left(\frac{2\pi t}{T_0}\right)}{C_1 t_c - C_2 \sin\left(\frac{2\pi t_c}{T_0}\right)} \right\} + \alpha' \ln\left(\frac{t}{t_c}\right) \right] \left\{ C_1 - C_2 \frac{2\pi}{T_0} \cos\left(\frac{2\pi t}{T_0}\right) \right\} dt$$

(2.55)

(Type3)

$$Z = \left\{ C_1 t_{age} + C_2 \sin\left(\frac{2\pi t_{age}}{T_0}\right) \right\} - \int_{t_c}^{t_{age}} \frac{1}{1+e_{sd}} \left[\lambda \ln \left\{ \frac{C_1 t + C_2 \sin\left(\frac{2\pi t}{T_0}\right)}{C_1 t_c + C_2 \sin\left(\frac{2\pi t_c}{T_0}\right)} \right\} + \alpha' \ln\left(\frac{t}{t_c}\right) \right] \left\{ C_1 + C_2 \frac{2\pi}{T_0} \cos\left(\frac{2\pi t}{T_0}\right) \right\} dt$$

(2.56)
(Type4)

$$Z = \left\{ C_1 t_{age} - C_2 \sin\left(\frac{\pi t_{age}}{T_0}\right) \right\} - \int_{t_c}^{t_{age}} \frac{1}{1+e_{sd}} \left[\lambda \ln \left\{ \frac{C_1 t - C_2 \sin\left(\frac{\pi t}{T_0}\right)}{C_1 t_c - C_2 \sin\left(\frac{\pi t_c}{T_0}\right)} \right\} + \alpha' \ln\left(\frac{t}{t_c}\right) \right] \left\{ C_1 - C_2 \frac{\pi}{T_0} \cos\left(\frac{\pi t}{T_0}\right) \right\} dt$$

(2.57)
(Type5)

$$Z = \left\{ C_1 t_{age} + C_2 \sin\left(\frac{\pi t_{age}}{T_0}\right) \right\} - \int_{t_c}^{t_{age}} \frac{1}{1+e_{sd}} \left[\lambda \ln \left\{ \frac{C_1 t + C_2 \sin\left(\frac{\pi t}{T_0}\right)}{C_1 t_c + C_2 \sin\left(\frac{\pi t_c}{T_0}\right)} \right\} + \alpha' \ln\left(\frac{t}{t_c}\right) \right] \left\{ C_1 + C_2 \frac{\pi}{T_0} \cos\left(\frac{\pi t}{T_0}\right) \right\} dt$$

(2.58)

(6) Initial unit weight and void ratio

The initial unit weight and void ratio is derived by the same method for constant depositional rate (i.e. Type 1) as follows:

- i) Estimate $\bar{\gamma}'$ which represents the average unit weight down to a depth of 10m the by substituting PI into Eq.(2.20).
- ii) Set the age of the soil at the depth of 10m. at the concerned site
- iii) Estimate average compression Δe by means of Eqs.(2.41)-(2.46).
- iv) Substitute Δe into Eq.(2.15) in order to obtain e_{sd} .
- v) γ_{sd}' is given by substituting e_{sd} into Eq.(2.11).
- vi) Check the thickness at present H and the age of the soil at the depth of 10m are correct or not after the calculations of all the soil parameters.
- vii) Repeat the procedure ii)-vi) until all the parameters, the thickness at present H and the age of the soil at the depth of 10m show no contradiction.

Note that integration of equations can be carried out Gauss-Legendre's numerical integration without any difficulty.

2.12 CONCLUSIONS

Physical properties and in situ stress history of clays are becoming more and more important to specify the initial conditions of the elasto-(visco)plastic finite element analysis. An attempt is made to derive the theoretical distribution of the soil properties and stress condition based on Bjerrum's hypothesis in this chapter. The conclusions of this chapter are as follows:

- (1) Theoretical depthwise distributions of the soil parameters and stress history are reasoned out based on Bjerrum's hypothesis. Assumptions are made in this study as follows. 1) The theory is based on Bjerrum's hypothesis. 2) Cementation, bonding and desiccation are not taken into account. 3) Primary and delayed compression may occur at the same time. Primary compression is completed in very short period compared with geological time scale. 4) Excess pore water pressure caused by sedimentation dissipates almost instantaneously. 5) The rate of the sedimentation is constant. 6) Depositional environment does not change over the period concerned.
- (2) Theoretical depthwise distribution of soil parameters such as age, void ratio, unit weight, initial overburden soil pressure, *OCR* and pre-consolidation pressure are derived in this chapter. Required information for the soil parameter estimation are plastic limit *PI* and Age of the lowermost of the formation.
- (3) Estimation chart is proposed for the soil parameters based on Age and *PI* of the soil.
- (4) Theoretical distributions of soil parameters are obtained for several types of depositional rate.

References

- Aboshi, H. (1973): An experimental investigation on the similitude in the consolidation of a soft clay, including the secondary creep settlement, Proc. 8th ICSMFE., Vol.4, No.3, pp.88-89.
- Aboshi, H. and Matsuda, H. (1981): Secondary consolidation and settlement analysis of clays, Tsuchi-to-Kiso, Vol.29, No. 3, pp. 19-24.
- Alpan, I. (1967): The Empirical Evaluation of the Coefficient K_0 , K_{OR} , Soils and Foundations, Vol.7, No.1, pp.31-40.
- Bjerrum, L. (1967): Engineering Geology of Norwegian Normally-consolidated Marine Clays as related to Settlements of Buildings. *Geotechnique*, Vol.17, pp.83-118.
- Crawford, C.B. (1964): Interpretation of Consolidation Test, *J. Soil Mech. Found. Div., ASCE*, 90 SM5), p.87-102.
- Finkelstein, K. and Ferland, M.A. (1987): Back-barrier to Sea-level Rise, Eastern Shore of Virginia. *Soc. Econ. Paleont. Miner. Spe. Publ.*, 41, pp.129-143.
- Imai, G. (1985): *Easy to Understand Principles of Soil Mechanics*, pp.45-91, The Japanese Geotechnical Society, p.243. (in Japanese)
- Iizuka, A. (1997): Significance of Reference and Initial Conditions in Elasto-Viscoplastic Settlement Prediction. *Tsuchi-To-Kiso JGS*, Vol.45, No.2, pp.11-14. (in Japanese)
- Iizuka, A and Ohta, H. (1987): A Determination Procedure of Input Parameters in Elasto-Viscoplastic Finite Element Analysis. *Soils and Foundations*, Vol.27, No. 3, pp.71-87.
- Jakey, J. (1944): Tarajmechanika, J. Hungarian Arch. and Eng., Budapest, pp355-358.
- Karube, D. (1975): Unstandarized Triaxial Testing Procedures and Related Subjects for Inquiry. *Proc. 20th Symp. on Geotech. Eng.* pp.45-60.
- Kraft, J.C., Chrzastowski, M.J., Belknap, D.F., Toscano, M.A., F(1987): The Transgressive Barrier-Lagoon Coast of Delaware: Morphostratigraphy, Sedimentary Sequences and Responses to Relative Rise in Sea Level. *Soc. Econ. Paleont. Miner. Spe. Publ.*, 41, pp.129-143.
- Kenney, T.C. (1959): Discussion on Proc. Paper 1732(Wu,1958). *Proc. ASCE*, Vol.85, SM3, pp.67-79.
- Lambe, T.W. and Whitman, R. V. (1969): *Soil Mechanics*. New York: John Wiley & Sons.
- Massarsh, K. R. (1979): Lateral Earth Pressure in Normally consolidated Clay, Design Parameters in Geotechnical Engineering, Vol. 2, pp. 245-249.
- Masuda, F. (2000): Age of the sediments and depositional rate based on sedimentation curve, Chikyu Monthly, Vol.22, No.3, pp. 191-196.(in Japanese)
- Mesri, G (1973): Coefficient of Secondary Compression. *Proc. ASCE*, Vol.99, No.SM1,pp.123-137.
- Mesri, G and Choi, Y.K. (1979): Discussion on "Strain Rate Behaviour of Saint-Jean-Vianney Clay" by VAID, Y.P. et.al.. *Can. Geotech. J.*, 16, pp.831-834.
- Mesri, G and Godlewski, P.M. (1977): Time-and Stress-compressibility Interrelationship, *J. Geotech.Eng.Div.,ASCE*, 103(GT5), pp.417-430.
- Mesri, G and Castro, A. (1987): C / C_c Concept and K_0 during Secondary Compression. *J. Geotech. Div.,ASCE*, Vol.113(GT3), pp.230-247.
- Murakami, Y. (1979): Excess Pore-Water Pressure and Preconsolidation Effect Developed in Normally Consolidated Clays of Some Age. *Soils and Foundations*, Vol.19, No.4, pp.17-29.
- Murakami, Y. (1980): A Method for Estimating the Consolidation of A Normally Consolidated Clay of Some Age. *Soils and Foundations*, Vol.20, No.4, pp.83-93.

- Ohta, H. (1971): Analysis of Deformations of Soils based on the Theory of Plasticity and its Application to Settlement of Embankments, Doctor Thesis, Kyoto University.
- Ohta, H. (1992): Chapter 4 Deformation of Soft Ground (71-142) in *Soft Ground -Theory and Practice-*. Tokyo: ed. by the Japanese Society of Soil Mechanics and Foundation Engineering.(in Japanese)
- Posamentier, H.W., Jervey, M.T, and Vail P.R. (1988): Eustatic Control on Clastic Deposition I-Conceptual Framework. *Soc. Econ. Paleont. Miner. Spe. Publ.*, 42, pp.109-124.
- Posamentier, H.W. and Vail, P.R. (1988): Eustatic Control on Clastic Deposition II-Sequence and Systems Tract Models. *Soc. Econ. Paleont. Miner. Spe. Publ.*, 42, pp.125-154.
- Sekiguchi, H. (1983): Effects of Time on the Compressibility of Clay Skelton. *Proc. 18th Japan National Conference of Soil Mech. and Foundation Eng.*, pp.209-210. (in Japanese)
- Skempton, A.W. (1953): The Colloidal Activity of Clays. *Proc. 3rd. ICSM*, Vol.1.
- Takemura, K. (2000): Subjects surrounding the study on the Biwako Lake Sediments, *Chikyu Monthly*, Vol.22, No.3, pp. 149-155. (in Japanese)
- Tavenas, F. and Leroueil, S. (1987): State-of-art on laboratory and in situ stress-strain-time behavior of soft clays, *Proc. Int. Symp. Geotech. Eng. of Soft Soils*, Mexico City, pp.1-46.
- Terzaghi, K and Peck, R. B. (1948): *Soil Mechanics in Engineering Practice*, U.S.A., John Wiley & Sons, 707p.
- Tsuchida, T. (1999): Strength Mobilization due to Cementation of Clay, *Report of the Port and Harbour Research Institute*, Vol.38, No.2, pp.99-129.
- Tsuji,K. (2000): The Mechanical Meaning of the Constant Volume Shear Box Test and its Engineering Application to the Deformation and the Failure Problems of Marine Clay. *Dr. Thesis of Tokyo Institute of Technology*, 212p. (in Japanese)
- Vaid, Y.P., Robertson, P.K. and Campanella, R.G. (1979): Strain Rate Behaviour of Saint-Jean-Vianney Clay. *Can. Geotech. J.*,16, pp.34-42.
- Vail, B.U., Hardenbol, J., and Vail P.R. (1988): Eustatic Control on Clastic Deposition I-Conceptual Framework. *Soc. Econ. Paleont. Miner. Spe. Publ.*, 42, pp.109-124.

Appendix.1

1 The integration in Eq.(2.5) is as follow:

$$\int \ln x dx = x(\ln x - 1) + C .$$

2. The limitation in Eq.(2.6) is given by means of L'Hospital's rule.

$$\begin{aligned} \lim_{x \rightarrow 0} x \ln x &= \lim_{x \rightarrow 0} \frac{\ln x}{\frac{1}{x}} \\ &= \lim_{x \rightarrow 0} \frac{\frac{1}{x}}{-\frac{1}{x^2}} \\ &= \lim_{x \rightarrow 0} -x \\ &= -0 \end{aligned}$$

Appendix.2

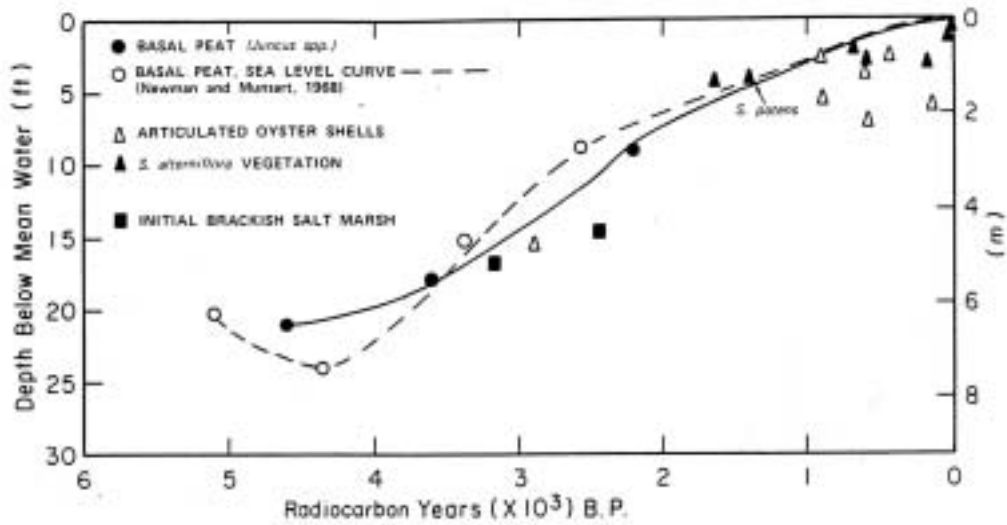


Fig. 4.—A sea-level curve for the study area (solid line) for approximately the last 4.6 ka. Newman and Mattart's (1968) sea-level curve is also shown (dashed line), although their two oldest dates, from small humic acid samples, may be inaccurate. An envelope encompassing the dates from both studies is possibly a better estimate of the local sea-level history.

Fig.A.1 An example of the age-depth relation (After Finkelstein and Ferland, 1987)

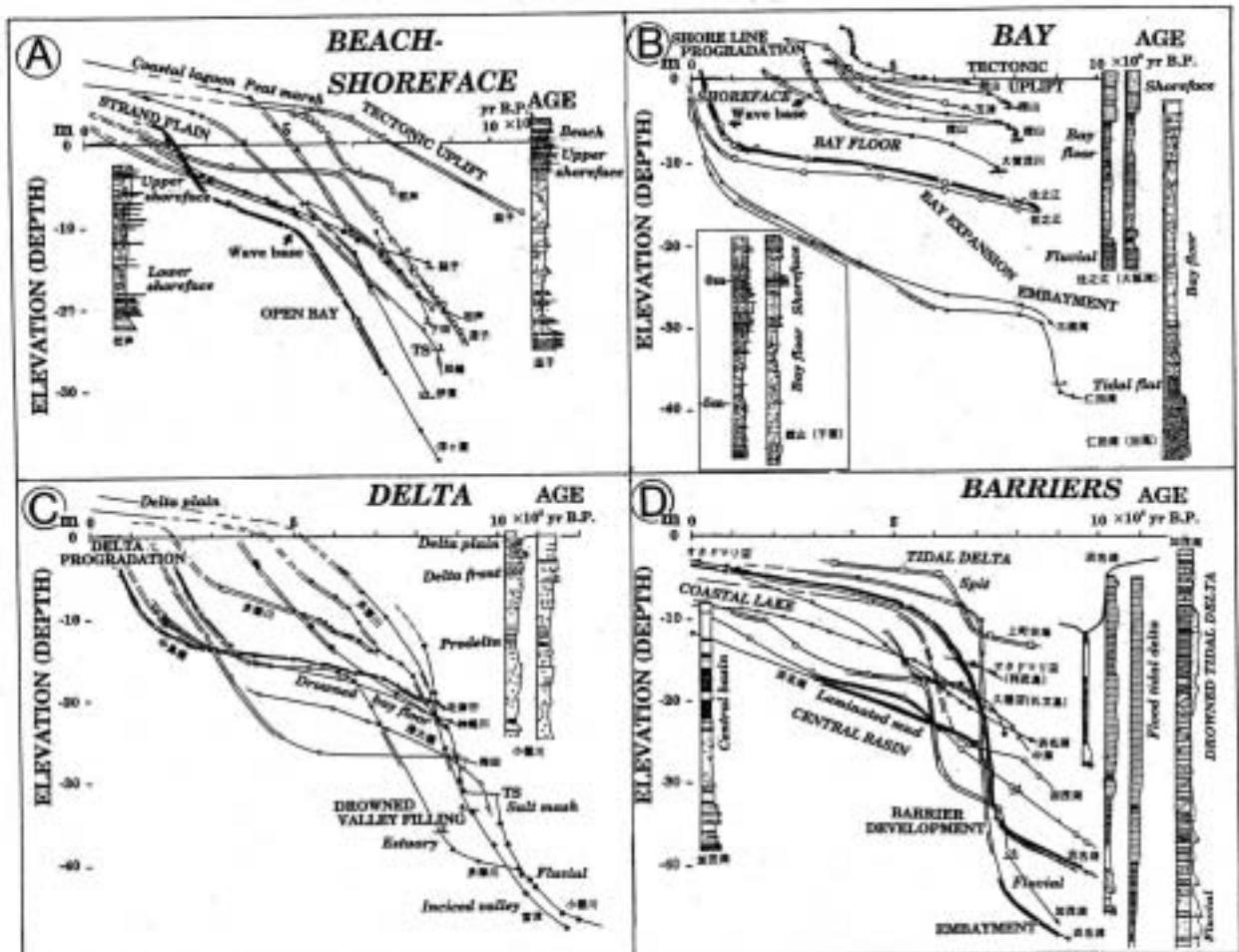


図3 各種システム (A: 海浜-外浜, B: 内湾, C: 三角洲, D: バリヤー) の堆積曲線。各種システムに固有の変化パターンが認められる。

Fig.A.2 An example of the age-depth relation (After Masuda, 2000)

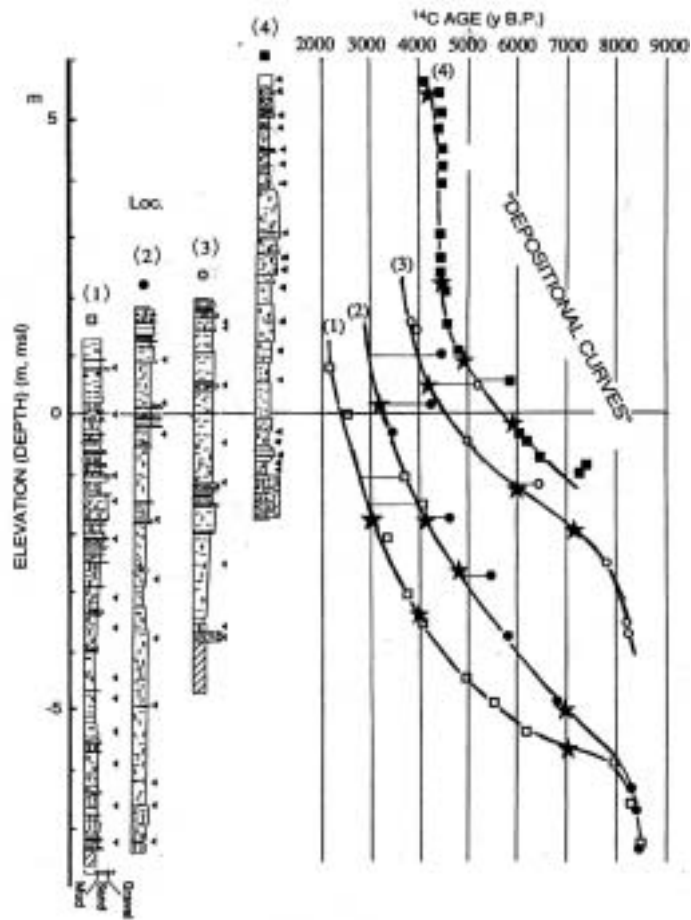


Fig.A.3 An example of the age-depth relation (After Masuda, 2000)

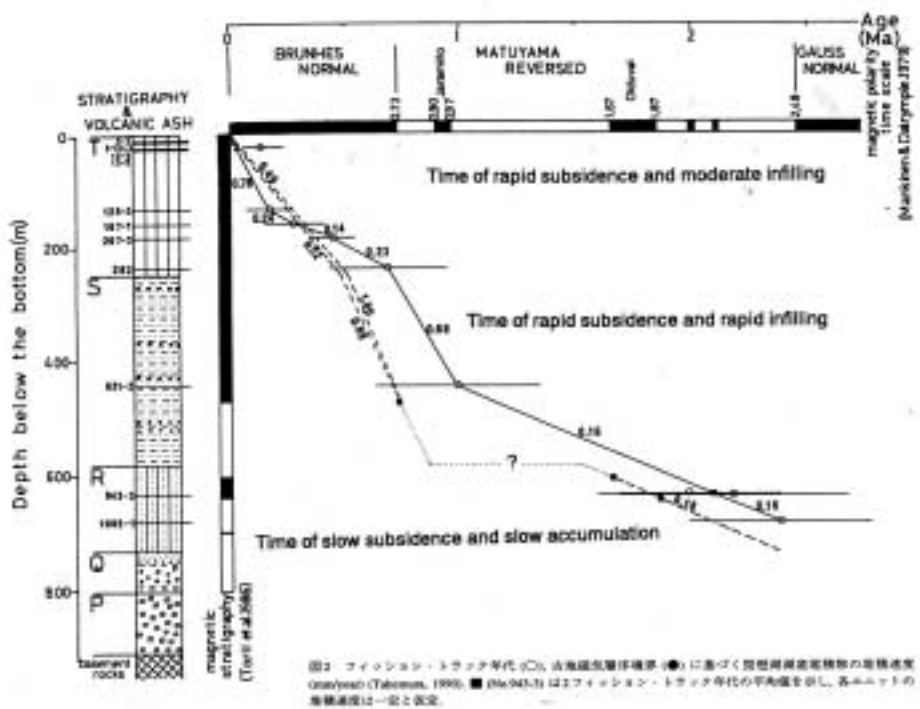


Fig.A.4 An example of the age-depth relation (After Takemura, 2000)

Appendix.3

Comments on the assumptions in 2.3 are as follows:

(1) Assumption of linear e - $\ln p'$ relation. Although some experimental data show that e - $\ln p'$ might not be linear at the beginning of the self-weight consolidation. However geological age of the formation studied in this thesis are several thousands years old which are old enough to neglect the non-linearity of e - $\ln p'$ relationship.

(2) Cementation and bonding are also very important factors when aging of soils is studied. There are still a lot of difficulties to deal with bonding and cementation because there is no method to distinguish or separate these effect on the mechanical properties. Even though only the phenomena assumed in 2.3 is dealt with in this study, the results obtained in this study must be a help to separate the effect of cementation and bonding and etc. from the total effect of aging on the mechanical properties of aged clays.

(3) Primary and delayed compression may occur at the same time. This assumption is made because there is no experimental evidence that shows no creep compression occurs during primary compression. On the other hand some experimental data shows that primary and secondary compression may occur at the same time (e.g. Imai, 1988; Aboshi, 1973, 1981).

(4) Reference time t_c is required as long as linear e - $\ln p'$ relation is assumed in the theory because $t=0$ is not in the definite range. According to the results in this study Void ratio, unit weight, overburden pressure and depth at present are independent of the reference time t_c as shown in the following Eqs. On the other hand pre-consolidation pressure and OCR are dependent on the reference time t_c as observed in experiments.

(Void ratio)

$$\begin{aligned}
 e &= e_{sd} - \Delta e \\
 &= \left\{ \frac{(G_s - 1)\gamma_w}{\gamma'} - 1 + (\lambda + \alpha')(\ln T_{10} - \ln t_c - 1) \right\} - (\lambda + \alpha') \ln \left(\frac{t}{t_c} \right) \\
 &= \frac{(G_s - 1)\gamma_w}{\gamma'} - 1 + (\lambda + \alpha')(\ln T_{10} - \ln t_c - 1) - (\lambda + \alpha')(\ln t - \ln t_c) \\
 &= \frac{(G_s - 1)\gamma_w}{\gamma'} - 1 + (\lambda + \alpha')(\ln T_{10} - \ln t - 1)
 \end{aligned}$$

(Depth at present)

$$\begin{aligned}
Z &= V \times t \times \left\{ 1 - \frac{(\lambda + \alpha')}{(1 + e_{sd})} (\ln t - \ln t_c - 1) \right\} \\
&= \frac{H(1 + e_{sd})}{T_0 \left\{ (1 + e_{sd}) - (\lambda + \alpha')(\ln T_0 - \ln t_c - 1) \right\}} \times t \times \left\{ 1 - \frac{(\lambda + \alpha')}{(1 + e_{sd})} (\ln t - \ln t_c - 1) \right\} \\
&= H \times \frac{t}{T_0} \times \frac{\left\{ (1 + e_{sd}) - (\lambda + \alpha')(\ln t - \ln t_c - 1) \right\}}{\left\{ (1 + e_{sd}) - (\lambda + \alpha')(\ln T_0 - \ln t_c - 1) \right\}} \\
&= H \times \frac{t}{T_0} \times \frac{\left\{ \frac{(G_s - 1)\gamma_w}{\gamma'} + (\lambda + \alpha')(\ln T_{10} - \ln t_c - 1) - (\lambda + \alpha')(\ln t - \ln t_c - 1) \right\}}{\left\{ \frac{(G_s - 1)\gamma_w}{\gamma'} + (\lambda + \alpha')(\ln T_{10} - \ln t_c - 1) - (\lambda + \alpha')(\ln T_0 - \ln t_c - 1) \right\}} \\
&= H \times \frac{t}{T_0} \times \frac{\left\{ \frac{(G_s - 1)\gamma_w}{\gamma'} + (\lambda + \alpha')(\ln T_{10} - \ln t) \right\}}{\left\{ \frac{(G_s - 1)\gamma_w}{\gamma'} + (\lambda + \alpha')(\ln T_{10} - \ln T_0) \right\}}
\end{aligned}$$

(Submerged unit weight and overburden pressure)

$$\gamma' = \frac{(G_s - 1)\gamma_w}{1 + e} \quad , \quad p_0' = \gamma' \times Z$$

Chapter 3

PARAMETRIC STUDIES

3.1 Introduction

Theoretical soil parameters derived in Chapter 2 are examined in this chapter. Age, PI , depositional rate and several physical properties are needed in the estimation proposed in this paper. The purpose of this chapter is to examine how the age, depositional rate and several physical properties influence the estimated soil properties. Another purpose is to study what the distributions of the soil properties look like depending on the transition of PI (i.e. transition of the depositional environment).

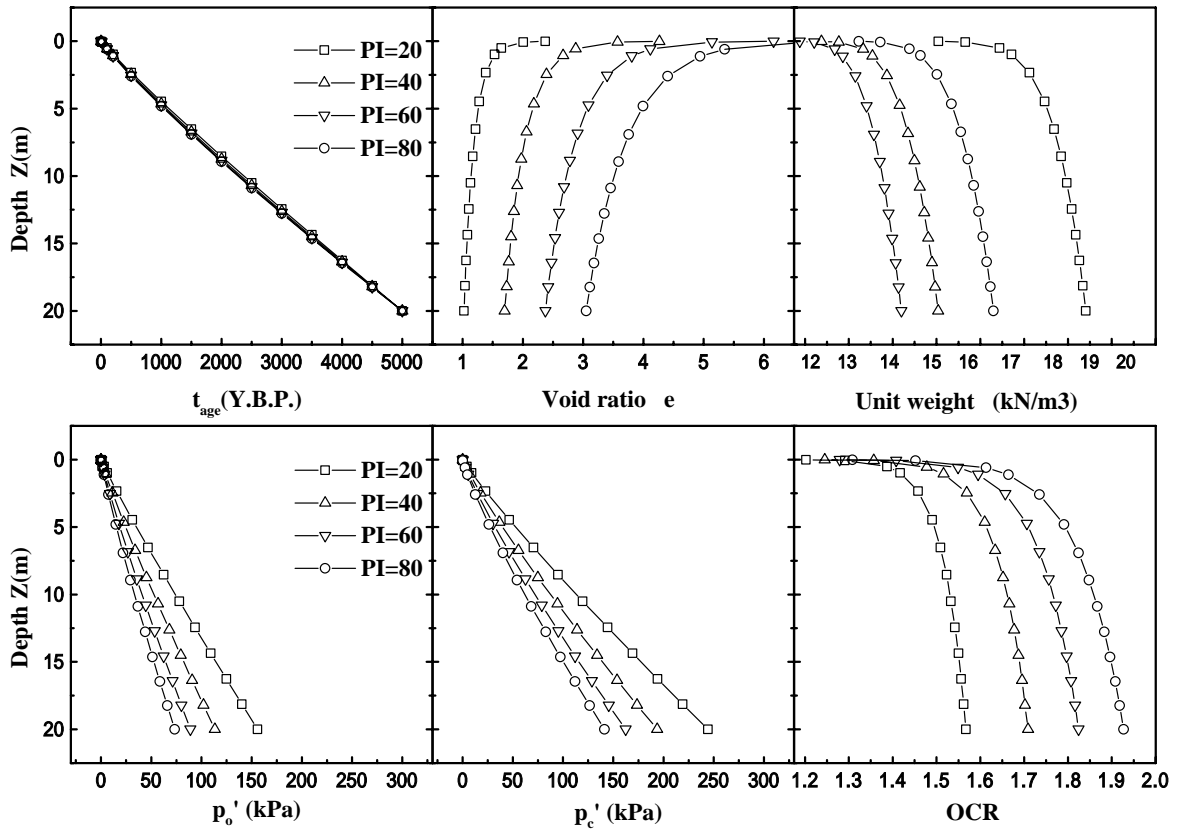
3.2 Effect of age and PI

Figs.3.1 shows examples of estimated curves. It is clear that the difference of the plasticity unexpectedly appears in the calculated distribution of e , p_o' , p_c' and OCR . Those theoretical distributions of soil properties are calculated under the condition as follows: (1) Present thickness is 20m. (2) The lowermost of the formation is 5000 years old. (3) Four cases of PI of 20,40,60 80 are chosen. (4) The initial conditions are estimated by assuming w_n equal to w_L ($a = 1.0$) in Eq.(2.20).

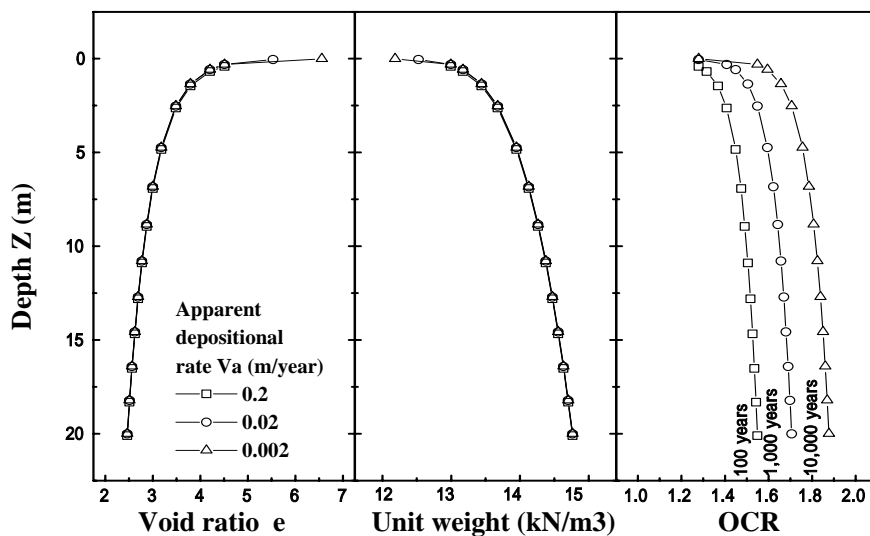
Figs.3.2 show the effect of the depositional rate on the soil properties. Depositional rate influences OCR considerably. On the other hand there are almost no effects of the depositional rate on the void ratio and unit weight. Calculation is carried out by assuming: (1) PI equals to 60, (2) apparent depositional rates are 0.2, 0.02, 0.002 m/year which correspond to 100, 1000, 10000 years respectively for 20m sedimentation.

According to those two kinds of simulations (Figs.3.1 and 3.2), the distributions of void ratio, unit weight, and overburden pressure reflect the difference of the plasticity and depositional rate. The effects both of plasticity and depositional rate appear in OCR and apparent pre-consolidation pressure. Each distribution in Figs.3.1 and 3.2 is smooth and simple because it is assumed that the depositional environment does not change through the sedimentation period

in order to set the problem simpler. In the actual clay deposits in the field, sequences of in situ clays reflect the transition of depositional environment. Thus the distribution of the natural soil properties are expected more complex and could be irregular depending on the transition of the depositional environment.



Figs. 3.1 Example of estimated distribution of soil properties



Figs.3.2 Effect of the depositional rate on the properties of clays (PI=60)

3.3 Effect of types of the depositional rate

The effects of the type of the depositional rate are investigated in this section. The conditions of the calculation are given:

1) PI : 10, 20, 40, 60, 80 and 100

2) Age : 5000,10000 and15000 years for the present thickness of 25m of soil

3) Types of the depositional rate are as follows (c.f. Chapter 2):

$$\text{(Type1)} \quad V = \frac{dh}{dt} = C_1 \quad (3.1)$$

$$\text{(Type2)} \quad V = \frac{dh}{dt} = C_1 - C_2 \frac{2\pi}{T_0} \cos\left(\frac{2\pi t}{T_0}\right) \quad (3.2)$$

$$\text{(Type3)} \quad V = \frac{dh}{dt} = C_1 + C_2 \frac{2\pi}{T_0} \cos\left(\frac{2\pi t}{T_0}\right) \quad (3.3)$$

$$\text{(Type4)} \quad V = \frac{dh}{dt} = C_1 - C_2 \frac{\pi}{T_0} \cos\left(\frac{\pi t}{T_0}\right) \quad (3.4)$$

$$\text{(Type5)} \quad V = \frac{dh}{dt} = C_1 + C_2 \frac{\pi}{T_0} \cos\left(\frac{\pi t}{T_0}\right) \quad (3.5)$$

, where T_0 equals to 5000, 10000 and 15000 years respectively.

4) The parameters for depositional rate are set so that total present thickness becomes 25m at the ages of 5000, 10000, 15000 respectively.

Calculations are carried out by means of Gauss-Legendre's numerical integration. Figs.3.1-3.4 are the results the calculation. The parameters used for the calculation are listed in the Tables 3.3-3.5.

The diagram shown in Figs.3.3-3.6 are arranged as follows (each box corresponding a graph in the figures) :

[Figs.3.3-3-5]

The corresponding depositional ages are $T_o=5,000$ years for Figs.3.3, $T_o=10,000$ for Figs.3.4 and $T_o=15,000$ for Figs.3.5.

Table 3.1 Arrangement of the graphs in Figs3.3-3.5

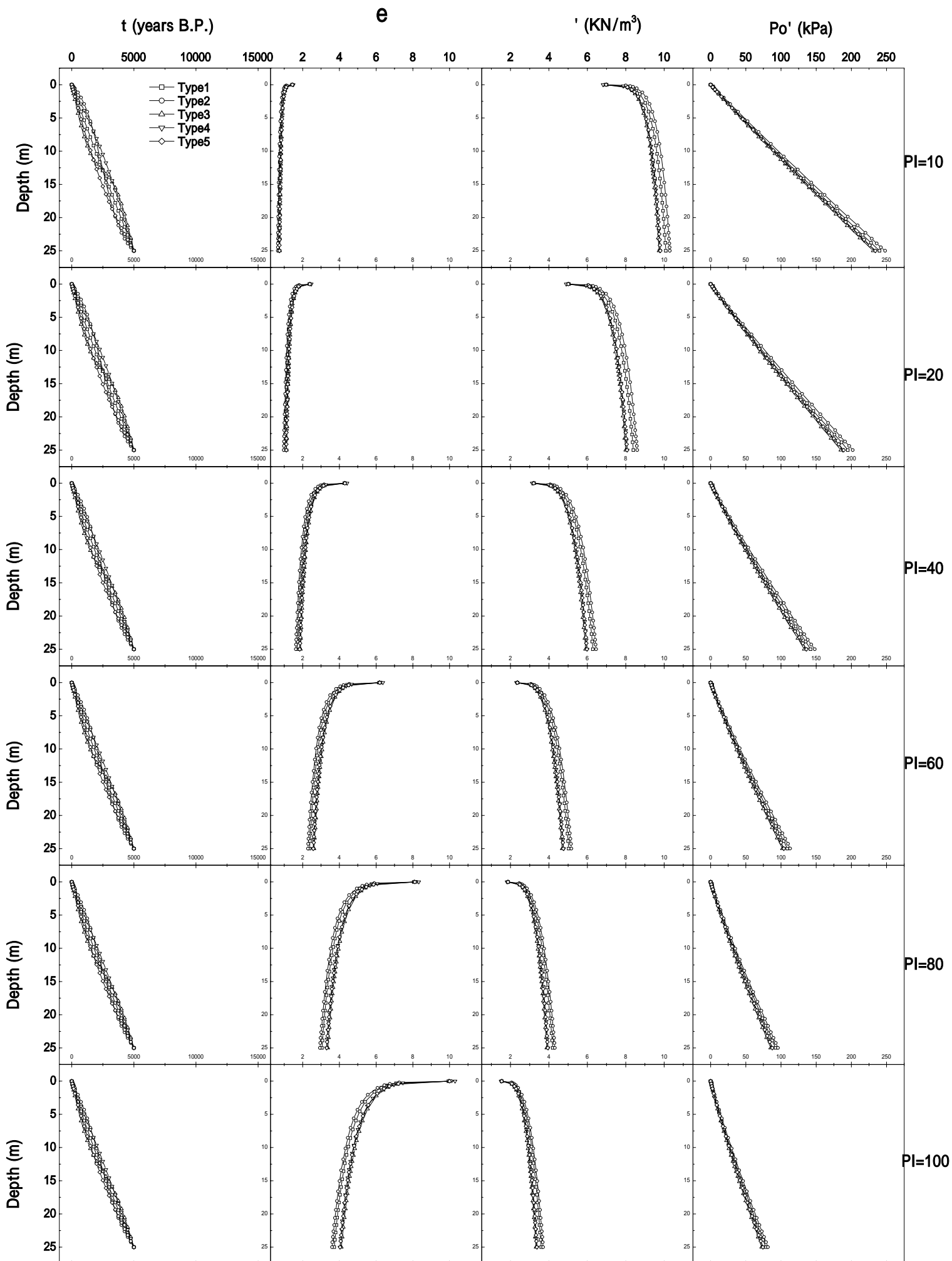
t-Depth PI=10 V=Type1-Type5	e-Depth PI=10 V=Type1-Type5	'-Depth PI=10 V=Type1-Type5	Po'-Depth PI=10 V=Type1-Type5
t-Depth PI=20 V=Type1-Type5	e-Depth PI=20 V=Type1-Type5	'-Depth PI=20 V=Type1-Type5	Po'-Depth PI=20 V=Type1-Type5
t-Depth PI=40 V=Type1-Type5	e-Depth PI=40 V=Type1-Type5	'-Depth PI=40 V=Type1-Type5	Po'-Depth PI=40 V=Type1-Type5
t-Depth PI=60 V=Type1-Type5	e-Depth PI=60 V=Type1-Type5	'-Depth PI=60 V=Type1-Type5	Po'-Depth PI=60 V=Type1-Type5
t-Depth PI=80 V=Type1-Type5	e-Depth PI=80 V=Type1-Type5	'-Depth PI=80 V=Type1-Type5	Po'-Depth PI=80 V=Type1-Type5
t-Depth PI=100 V=Type1-Type5	e-Depth PI=100 V=Type1-Type5	'-Depth PI=100 V=Type1-Type5	Po'-Depth PI=100 V=Type1-Type5

[Figs.3.6]

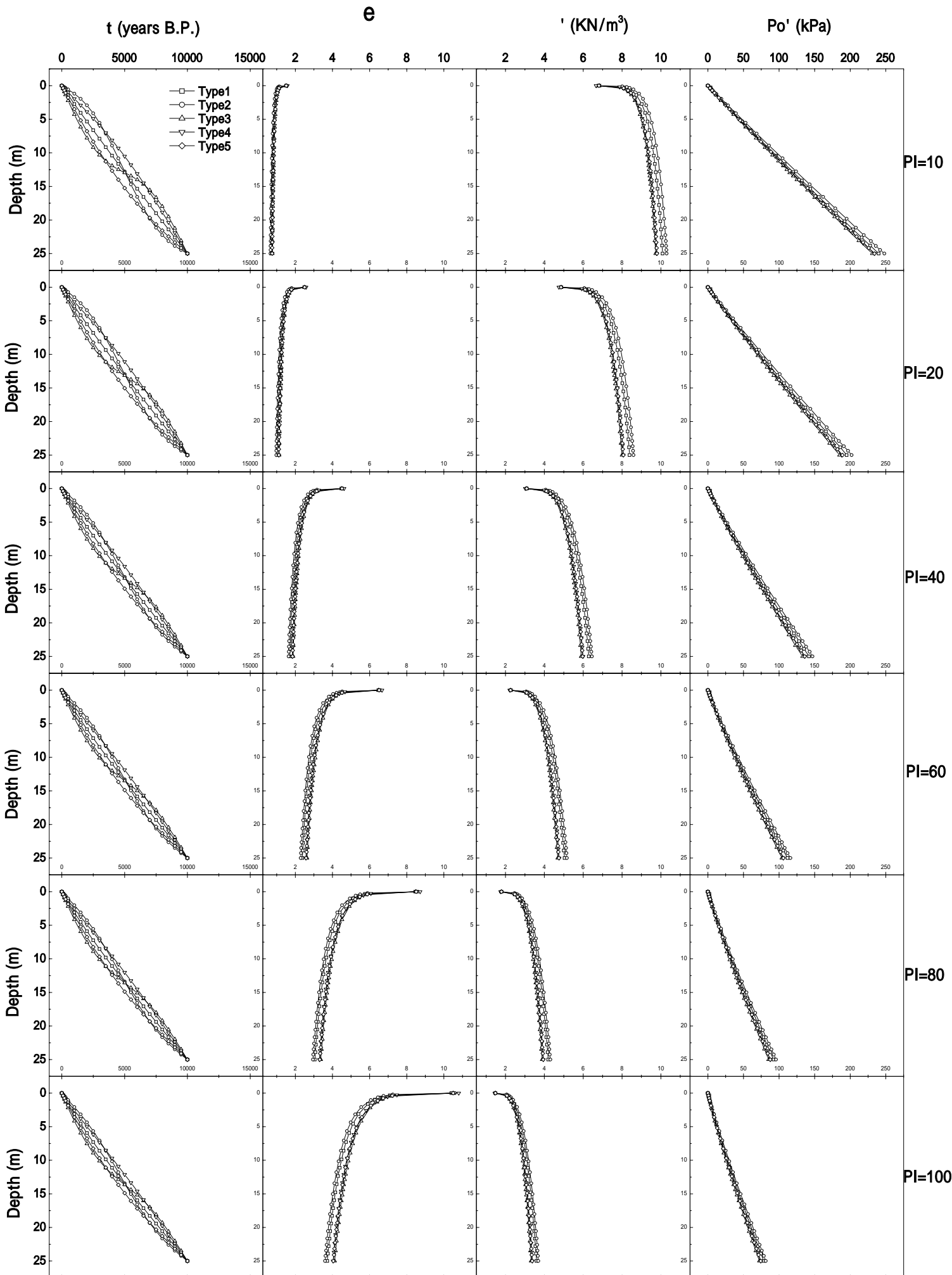
Table 3.2 Arrangement of the graphs in Figs3.6

To=5,000 Po' & Pc'-Depth PI=10 V=Type1-Type5	To=5,000 OCR-Depth PI=10 V=Type1-Type5	To=10,000 Po' & Pc'-Depth PI=10 V=Type1-Type5	To=10,000 OCR-Depth PI=10 V=Type1-Type5	To=15,000 Po' & Pc'-Depth PI=10 V=Type1-Type5	To=15,000 OCR-Depth PI=10 V=Type1-Type5
To=5,000 Po' & Pc'-Depth PI=20 V=Type1-Type5	To=5,000 OCR-Depth PI=20 V=Type1-Type5	To=10,000 Po' & Pc'-Depth PI=20 V=Type1-Type5	To=10,000 OCR-Depth PI=20 V=Type1-Type5	To=15,000 Po' & Pc'-Depth PI=20 V=Type1-Type5	To=15,000 OCR-Depth PI=20 V=Type1-Type5
To=5,000 Po' & Pc'-Depth PI=40 V=Type1-Type5	To=5,000 OCR-Depth PI=40 V=Type1-Type5	To=10,000 Po' & Pc'-Depth PI=40 V=Type1-Type5	To=10,000 OCR-Depth PI=40 V=Type1-Type5	To=15,000 Po' & Pc'-Depth PI=40 V=Type1-Type5	To=15,000 OCR-Depth PI=40 V=Type1-Type5
To=5,000 Po' & Pc'-Depth PI=60 V=Type1-Type5	To=5,000 OCR-Depth PI=60 V=Type1-Type5	To=10,000 Po' & Pc'-Depth PI=60 V=Type1-Type5	To=10,000 OCR-Depth PI=60 V=Type1-Type5	To=15,000 Po' & Pc'-Depth PI=60 V=Type1-Type5	To=15,000 OCR-Depth PI=60 V=Type1-Type5
To=5,000 Po' & Pc'-Depth PI=80 V=Type1-Type5	To=5,000 OCR-Depth PI=80 V=Type1-Type5	To=10,000 Po' & Pc'-Depth PI=80 V=Type1-Type5	To=10,000 OCR-Depth PI=80 V=Type1-Type5	To=15,000 Po' & Pc'-Depth PI=80 V=Type1-Type5	To=15,000 OCR-Depth PI=80 V=Type1-Type5
To=5,000 Po' & Pc'-Depth PI=100 V=Type1-Type5	To=5,000 OCR-Depth PI=100 V=Type1-Type5	To=10,000 Po' & Pc'-Depth PI=100 V=Type1-Type5	To=10,000 OCR-Depth PI=100 V=Type1-Type5	To=15,000 Po' & Pc'-Depth PI=100 V=Type1-Type5	To=15,000 OCR-Depth PI=100 V=Type1-Type5

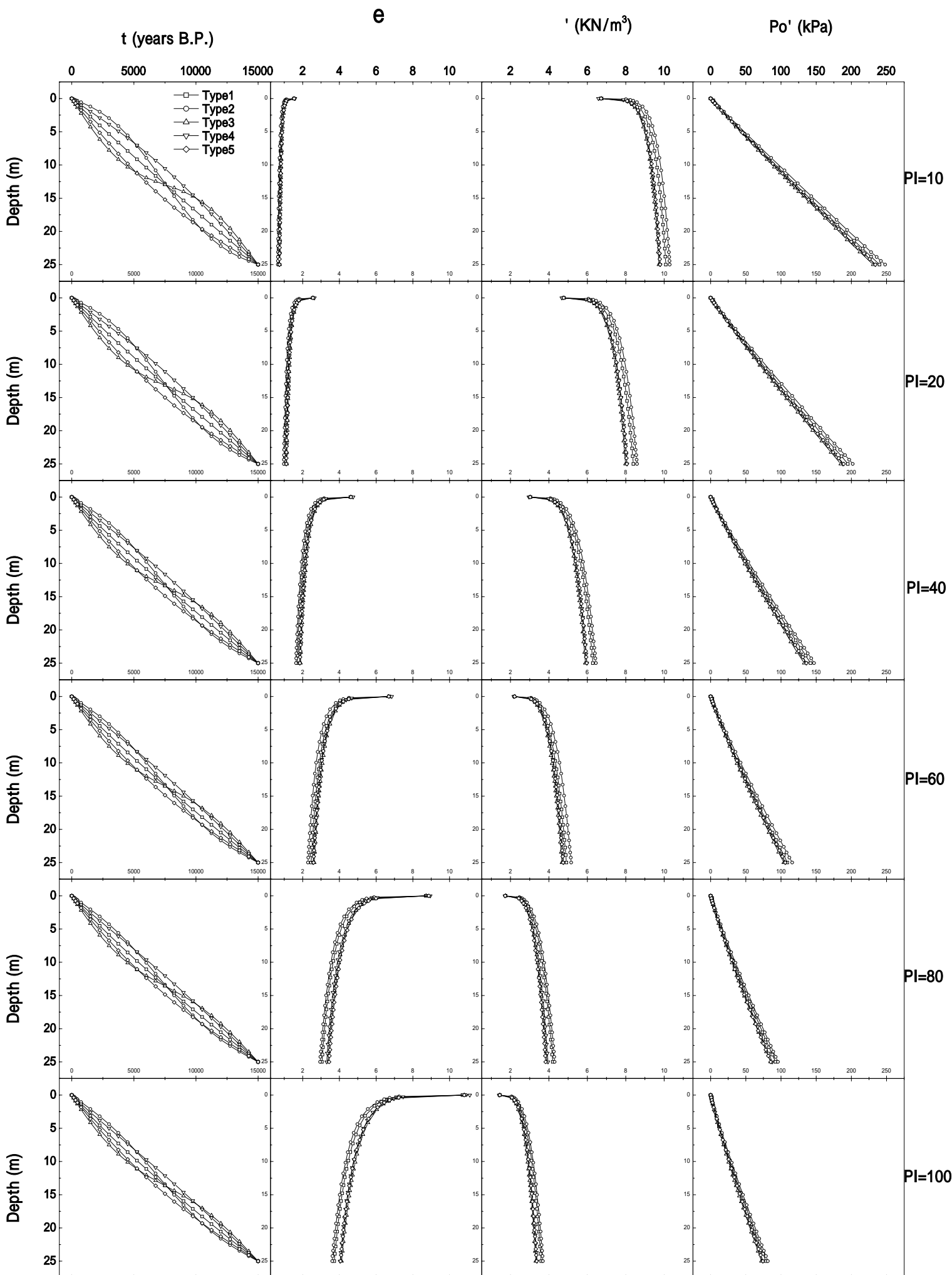
All the parameters for the calculations are listed in Tables 3.3-3.5.



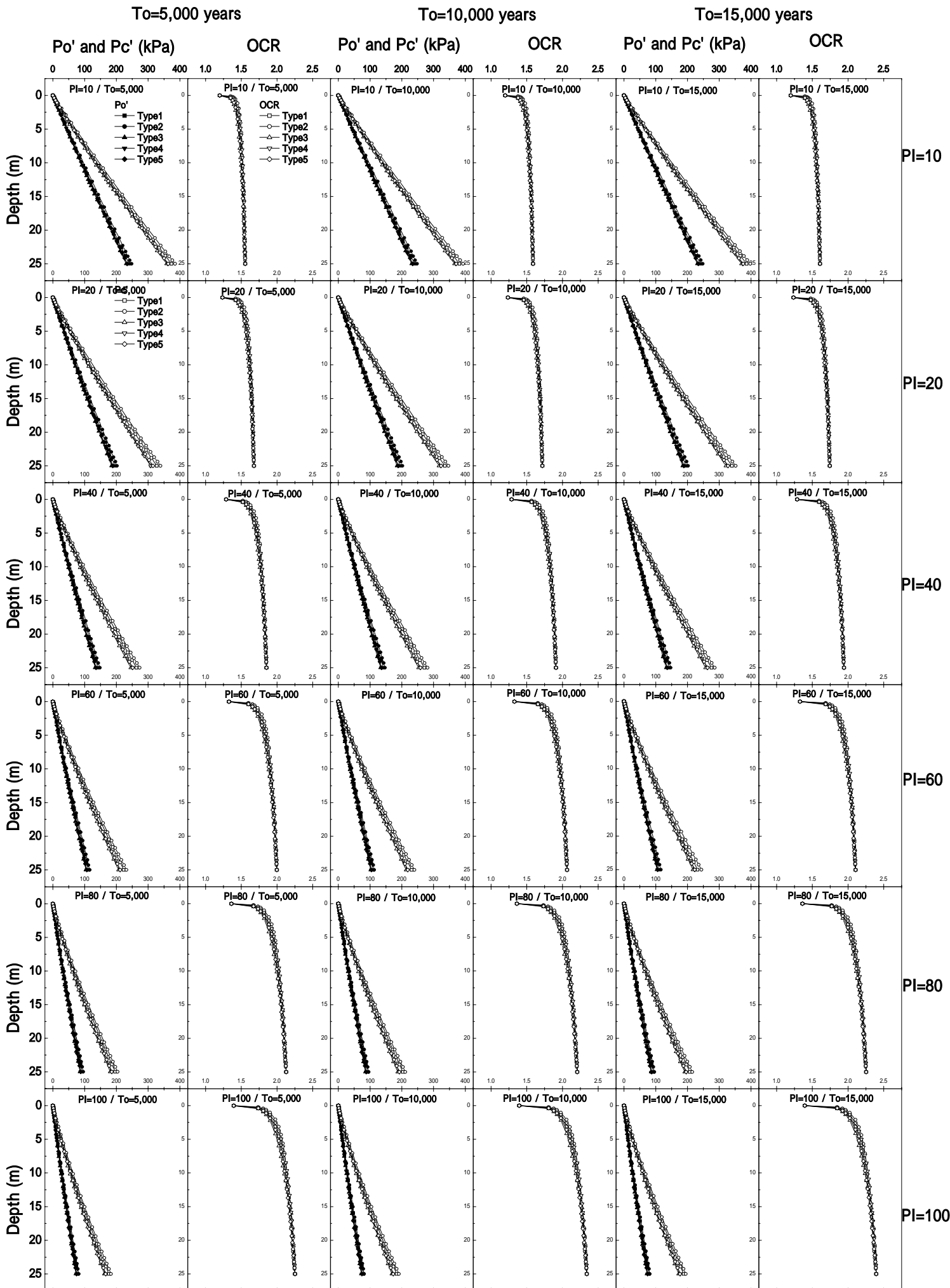
Figs.3.3 The effect of the depositional rate 1 of 5. $t, e, ' \text{ and } Po'$ ($To=5,000$)



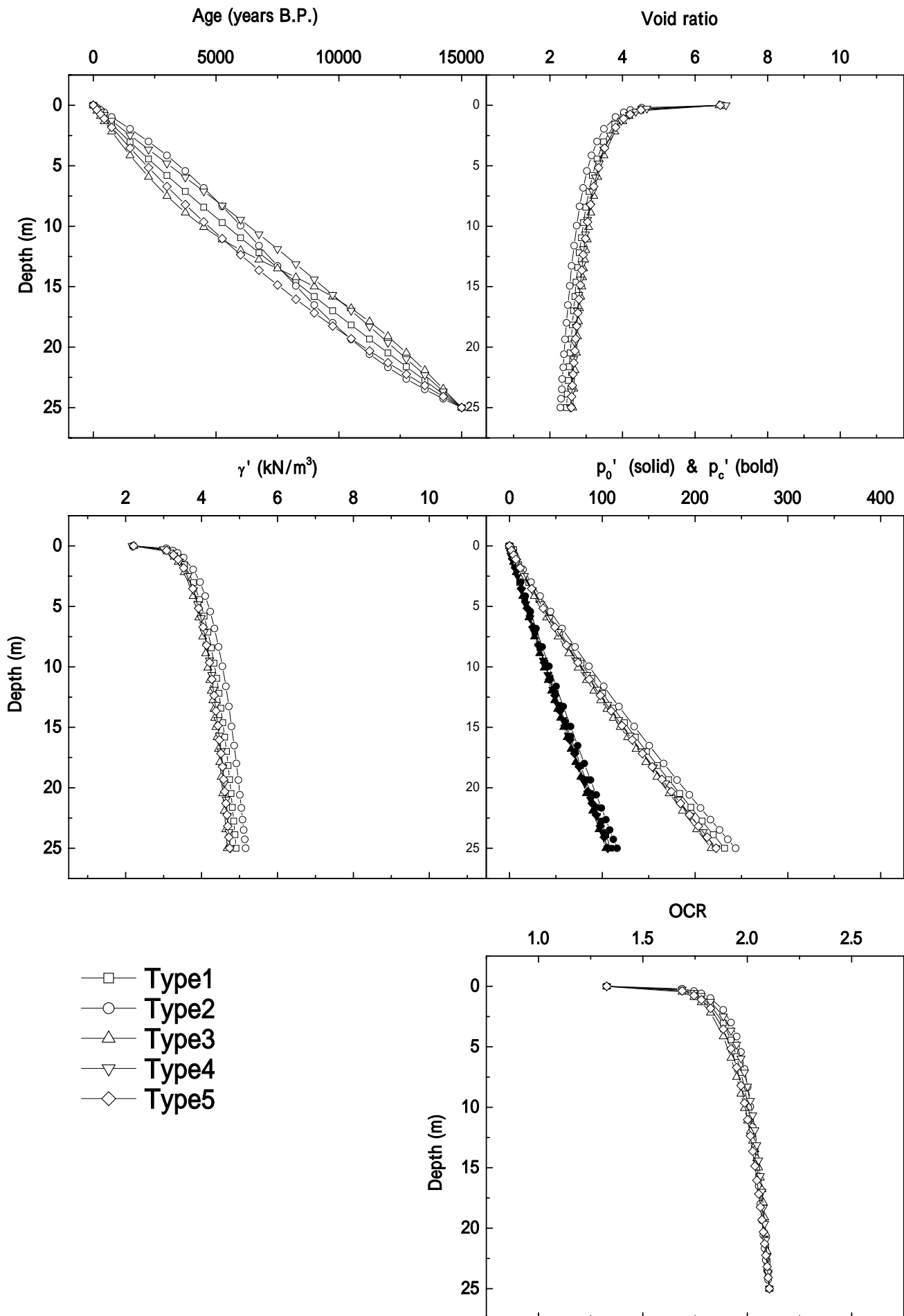
Figs.3.4 The effect of the depositional rate 2 of 5. $t, e, '$ and Po' ($T_0=10,000$)



Figs.3.5 The effect of the depositional rate 3 of 5. $t, e, '$ and Po' ($T_0=15,000$)



Figs.3.6 The effect of the depositional rate 4 of 5.
Po',Pc'and OCR (To=5000, 10000, 15000 years)



Figs.3.7 The effect of the depositional rate 5 of 5
 Enlarged diagrams of calculated parameters(PI=60, T0=15,000 years B.P.)

Table 3.3 Parameters lists of the calculations of Figs.3.3 and 3.6

To (years)	PI	Parameters of the V in Eqs. 3.1 - 3.5		e_{sd}	γ_{sd} (kN/m ³)	$T_{(10m)}$ (years)	,		
		C_1	C_2						
5,000	10	8.31×10^{-3}	0.0	1.940	5.782	1920	0.00213	0.0850	0.0156
		8.68×10^{-3}	4.0	1.979	5.707	2144			
		7.95×10^{-3}	4.0	1.933	5.796	1418			
		8.21×10^{-3}	4.0	1.997	5.672	2407			
		8.08×10^{-3}	4.0	1.941	5.780	1522			
5,000	20	9.91×10^{-3}	0.0	3.314	3.941	1879	0.00388	0.155	0.0470
		1.04×10^{-2}	4.0	3.369	3.891	2096			
		9.34×10^{-3}	4.0	3.300	3.953	1452			
		9.60×10^{-3}	4.0	3.395	3.825	2300			
		9.53×10^{-3}	4.0	3.311	3.943	1545			
5,000	40	1.18×10^{-2}	0.0	6.059	2.408	1833	0.00738	0.295	0.123
		1.24×10^{-2}	4.0	6.144	2.380	2042			
		1.10×10^{-2}	4.0	6.031	2.418	1470			
		1.14×10^{-2}	4.0	6.178	2.368	2186			
		1.12×10^{-2}	4.0	6.049	2.412	1553			
5,000	60	1.29×10^{-2}	0.0	8.801	1.735	1804	0.01088	0.435	0.208
		1.35×10^{-2}	4.0	8.916	1.714	2012			
		1.19×10^{-2}	4.0	8.759	1.742	1469			
		1.24×10^{-2}	4.0	8.957	1.707	2129			
		1.22×10^{-2}	4.0	8.786	1.734	1552			
5,000	80	1.36×10^{-2}	0.0	11.543	1.355	1788	0.01438	0.575	0.301
		1.43×10^{-2}	4.0	11.686	1.340	1990			
		1.25×10^{-2}	4.0	11.487	1.361	1468			
		1.31×10^{-2}	4.0	11.734	1.335	2095			
		1.28×10^{-2}	4.0	11.522	1.358	1550			
5,000	100	1.41×10^{-2}	0.0	14.284	1.112	1779	0.01788	0.715	0.397
		1.48×10^{-2}	4.0	14.457	1.100	1980			
		1.29×10^{-2}	4.0	14.214	1.117	1467			
		1.35×10^{-2}	4.0	14.511	1.096	2074			
		1.33×10^{-2}	4.0	14.258	1.114	1550			

Table 3.4 Parameters lists of the calculations of Figs.3.4 and 3.6

To (years)	PI	Parameters of the V in Eqs. 3.1 - 3.5		e_{sd}	γ_{sd} (kN/m ³)	$T_{(10m)}$ (years)	,		
		C_1	C_2						
10,000	10	4.24×10^{-3}	0.0	2.001	5.665	3841	0.00213	0.0850	0.0156
		4.42×10^{-3}	4.0	2.038	5.596	4286			
		4.06×10^{-3}	4.0	1.993	5.680	2854			
		4.19×10^{-3}	4.0	2.055	5.565	4790			
		4.13×10^{-3}	4.0	2.001	5.665	3055			
10,000	20	5.08×10^{-3}	0.0	3.425	3.842	3760	0.00388	0.155	0.0470
		5.31×10^{-3}	4.0	3.478	3.796	4192			
		4.79×10^{-3}	4.0	3.410	3.855	2923			
		4.97×10^{-3}	4.0	3.500	3.778	4564			
		4.89×10^{-3}	4.0	3.421	3.845	3101			
10,000	40	6.07×10^{-3}	0.0	6.269	2.339	3637	0.00738	0.295	0.123
		6.36×10^{-3}	4.0	6.359	2.312	4084			
		5.64×10^{-3}	4.0	6.241	2.348	2955			
		5.88×10^{-3}	4.0	6.382	2.303	4343			
		5.79×10^{-3}	4.0	6.259	2.342	3120			
10,000	60	6.65×10^{-3}	0.0	9.111	1.681	3612	0.01088	0.435	0.208
		6.98×10^{-3}	4.0	9.221	1.663	4015			
		6.13×10^{-3}	4.0	9.069	1.688	2956			
		6.39×10^{-3}	4.0	9.260	1.657	4232			
		6.29×10^{-3}	4.0	9.095	1.684	3120			
10,000	80	7.02×10^{-3}	0.0	11.951	1.313	3578	0.01438	0.575	0.301
		7.36×10^{-3}	4.0	12.091	1.299	3980			
		6.44×10^{-3}	4.0	11.897	1.318	2955			
		6.73×10^{-3}	4.0	12.135	1.294	4173			
		6.62×10^{-3}	4.0	11.930	1.315	3114			
10,000	100	7.29×10^{-3}	0.0	14.791	1.077	3552	0.01788	0.715	0.397
		7.65×10^{-3}	4.0	14.958	1.065	3947			
		6.66×10^{-3}	4.0	14.724	1.081	2951			
		6.96×10^{-3}	4.0	15.010	1.062	4130			
		6.84×10^{-3}	4.0	14.766	1.078	3113			

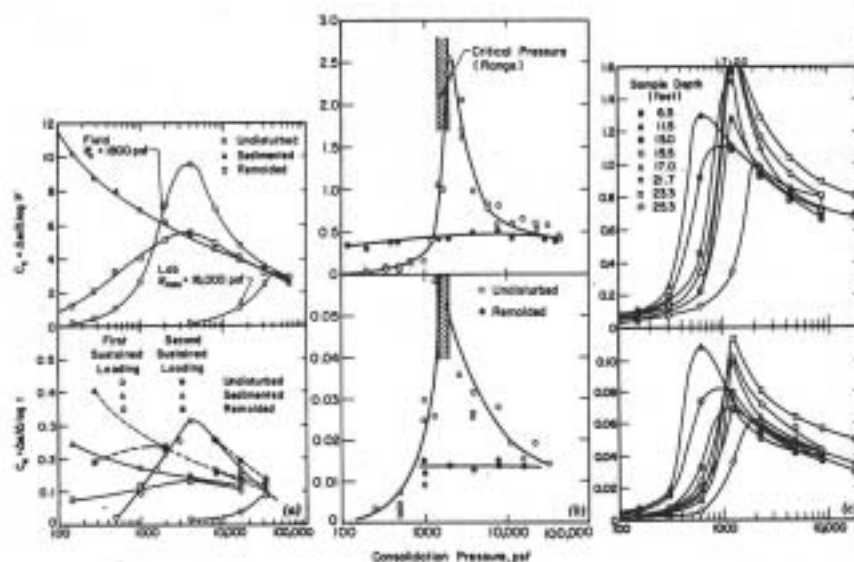
Table 3.5 Parameters lists of the calculations of Figs.3.5-3.7

To (years)	PI	Parameters of the V in Eqs. 3.1 - 3.5		e_{sd}	γ_{sd} (kN/m ³)	$T_{(10m)}$ (years)	,		
		C_1	C_2						
15,000	10	2.86×10^{-3}	0.0	2.036	5.599	5762	0.00213	0.0850	0.0156
		2.98×10^{-3}	4.0	2.073	5.532	6426			
		2.74×10^{-3}	4.0	2.029	5.612	4298			
		2.82×10^{-3}	4.0	2.090	5.502	7180			
		2.78×10^{-3}	4.0	2.036	5.599	4596			
15,000	20	3.43×10^{-3}	0.0	3.489	3.787	5644	0.00388	0.155	0.0470
		3.59×10^{-3}	4.0	3.542	3.744	6284			
		3.23×10^{-3}	4.0	3.475	3.799	4411			
		3.36×10^{-3}	4.0	3.563	3.726	6826			
		3.30×10^{-3}	4.0	3.485	3.790	4673			
15,000	40	4.12×10^{-3}	0.0	6.392	2.300	5505	0.00738	0.295	0.123
		4.31×10^{-3}	4.0	6.473	2.275	6120			
		3.82×10^{-3}	4.0	6.364	2.309	4450			
		3.98×10^{-3}	4.0	6.502	2.266	6506			
		3.92×10^{-3}	4.0	6.381	2.303	4692			
15,000	60	4.47×10^{-3}	0.0	9.355	1.642	5422	0.01088	0.435	0.208
		4.72×10^{-3}	4.0	9.401	1.634	6028			
		4.15×10^{-3}	4.0	9.251	1.658	4456			
		4.33×10^{-3}	4.0	9.438	1.629	6349			
		4.26×10^{-3}	4.0	9.277	1.654	4697			
15,000	80	4.76×10^{-3}	0.0	12.191	1.289	5373	0.01438	0.575	0.301
		4.99×10^{-3}	4.0	12.328	1.276	5968			
		4.37×10^{-3}	4.0	12.136	1.294	4447			
		4.56×10^{-3}	4.0	12.371	1.271	6248			
		4.48×10^{-3}	4.0	12.171	1.291	4694			
15,000	100	4.95×10^{-3}	0.0	15.088	1.057	5327	0.01788	0.715	0.397
		5.18×10^{-3}	4.0	15.254	1.046	5924			
		4.52×10^{-3}	4.0	15.022	1.061	4441			
		4.72×10^{-3}	4.0	15.303	1.043	6182			
		4.64×10^{-3}	4.0	15.064	1.058	4684			

3.4 Effect of material properties

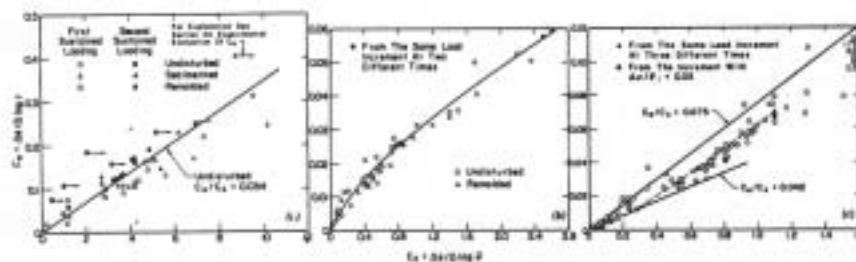
The effects of the material properties such as σ'_v , σ'_c , σ'_p are examined in this chapter. The material properties such as σ'_v , σ'_c , σ'_p are given by Fig.2.10 as follows: 1) Calculating according to PI . 2) σ'_v is given by substituting into σ'_v / σ'_c . 3) σ'_p is estimated by Karube's equation. The estimation chart shown in Fig.2.10 is supposed to be the value at the critical state. However the value of those material properties during the sedimentation or the consolidation in geological time might be smaller than the values at the critical state (e.g. Yasukawa and Kamon 1987; Morita et. al. 1988; Matsuo 1986).

Mesri and Godlewski(1977) showed the existence of the unique ratio C_u / C_c for natural clay independent of the consolidation pressure level or increment ratio (Figs.3.8 & 3.9). Mesri and Godlewski made a list of the ratio C_u / C_c which are in between 0.025-0.10 (Table 3.6).



Relationship Between C_c and C_u and Consolidation Pressure for: (a) Mexico City Clay; (b) Leda Clay; (c) Undisturbed New Haven Organic Silt (C_u from First Log Cycle after Transition, C_c from End of Primary e -Log $\bar{\sigma}$) (1 psf = 47.9 N/m²)

Figs.3.8 The relation between the C_u and C_c and consolidation pressure (After Mesri & Godlewski, 1977)



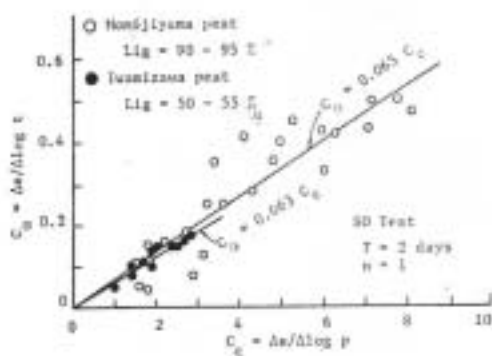
Relationship between C_u and C_c for: (a) Mexico City Clay; (b) Leda Clay; (c) Undisturbed New Haven Organic Clay Silt (C_u from First Cycle after Transition, C_c from End of Primary e -Log $\bar{\sigma}$)

Figs.3.9 The relation between the C_u and C_c (After Mesri & Godlewski, 1977)

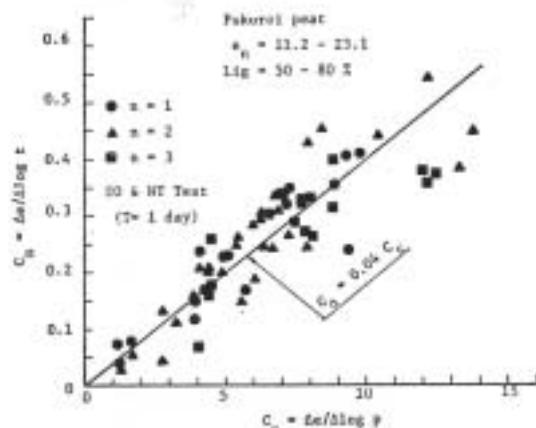
**Table 3.6 The list of the values of C_u / C_c for natural soil deposits
(After Mesri & Godlewski,1977)**

Values of C_u / C_c for Natural Soil Deposits		
Soil (1)	C_u / C_c (2)	Reference (3)
Whangamarino clay	0.03-0.04	Newland and Allely (22)
Norfolk organic silt	0.05	Barber (2)
Calcareous organic silt	0.035-0.06	Wahls (28)
Amorphous and fibrous peat	0.035-0.083	Lea and Brawner (13)
Canadian muskeg	0.09-0.10	Adams (1)
Leda clay	0.03-0.055	Walker and Raymond (31)
Leda clay	0.04-0.06	Walker and Raymond (32)
Peat	0.075-0.085	Weber (33)
Post-glacial organic clay	0.05-0.07	Chang (9)
Soft blue clay	0.026	Crawford and Sutherland (11)
Organic clays and silts	0.04-0.06	Ladd (12)
Sensitive clay, Portland	0.025-0.055	Ladd (12)
Peat	0.05-0.08	Samson and La Rochelle (25)
San Francisco Bay mud	0.04-0.06	Su and Prysock (26)
New Liskeard varved clay	0.03-0.06	Quigley and Ogunbadejo (23)
Silty clay C	0.032	Samson and Garneau (24)
Nearshore clays and silts	0.055-0.075	Brown and Rashid (6)
Fibrous peat	0.06-0.085	Berry and Vickers (3)
Mexico City clay	0.03-0.035	Mesri, et al. (19)
Hudson River silt	0.03-0.06	Mesri, Personal files
Leda clay	0.025-0.04	Present paper
New Haven organic clay silt	0.04-0.075	Present paper

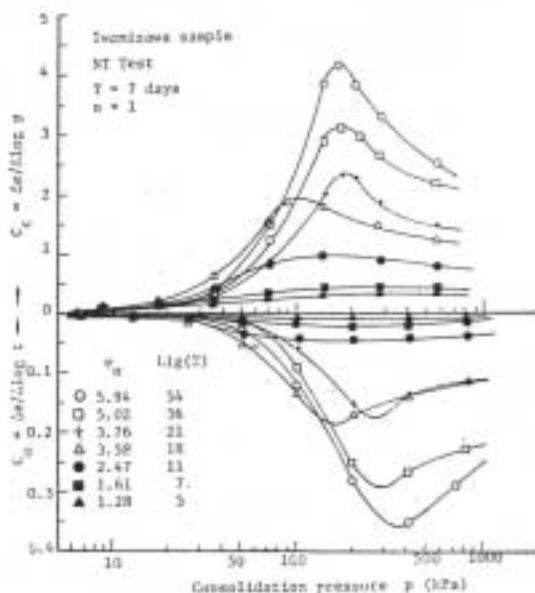
C_u and C_c represents σ'_v and σ'_c respectively as shown in Eq.(2.2). Matsuo et al. (1986) gave examples of the relation of the C_u and C_c together with the ratio C_u/C_c . Matsuo et al. examined the effect of the amount of organic materials (Figs.3.10), the loading increment (Figs.3.11), the period of the loading (Figs.3.12) and structures of the soils (Figs.3.13). Matsuo et al. concluded as follows: 1) The more the amount of organic material, the smaller the C_u and C_c . 2) The loading increment does not affect to C_u and C_c . 3) The longer the period of the loading, the smaller the C_u and C_c . 4) The initial structure affect the C_u and C_c in the smaller range of the consolidation pressure than P_c' . The diagram shows the relation of the ratio C_u/C_c and the C_u is illustrated by Matsuo et al. (Fig.3.14)



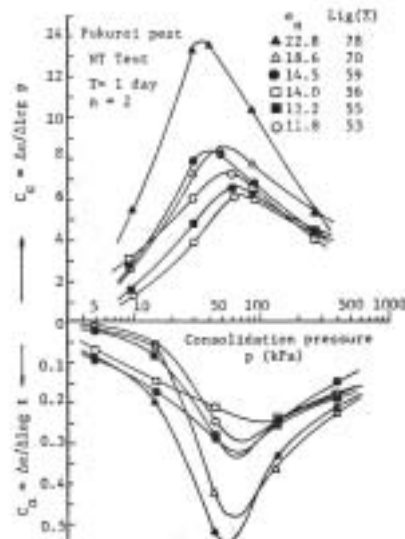
Relationship of C_c and C_u



Relationship of C_c and C_u



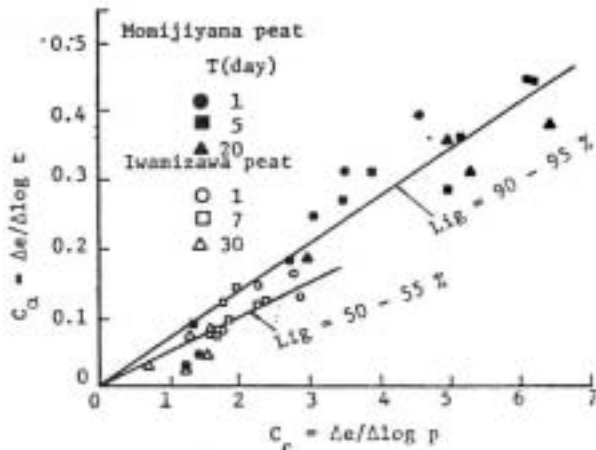
Change of C_c and C_u with respect to the range of consolidation pressure



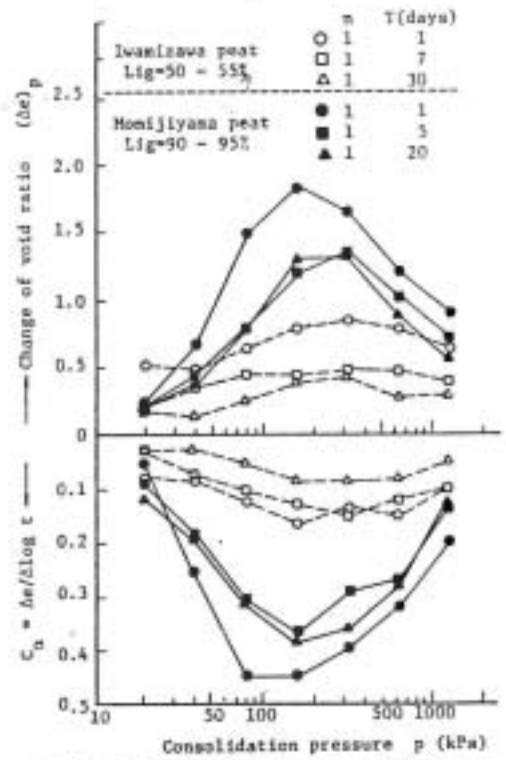
Change of C_c and C_u with respect to the range of consolidation pressure

Left Figs. 3.10 The effect of the amount of organic material in clay (After Matsuo et al., 1986)

Right Figs. 3.11 The effect of the loading increment (After Matsuo et al., 1986)

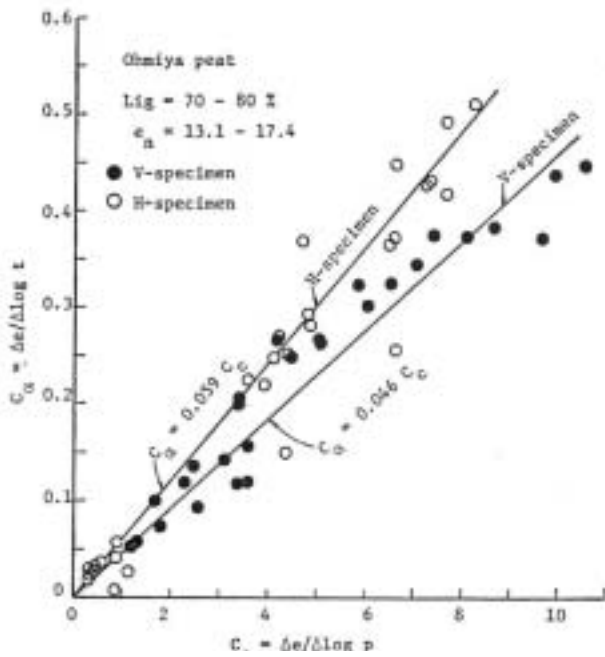


Relationship of C_c and C_a

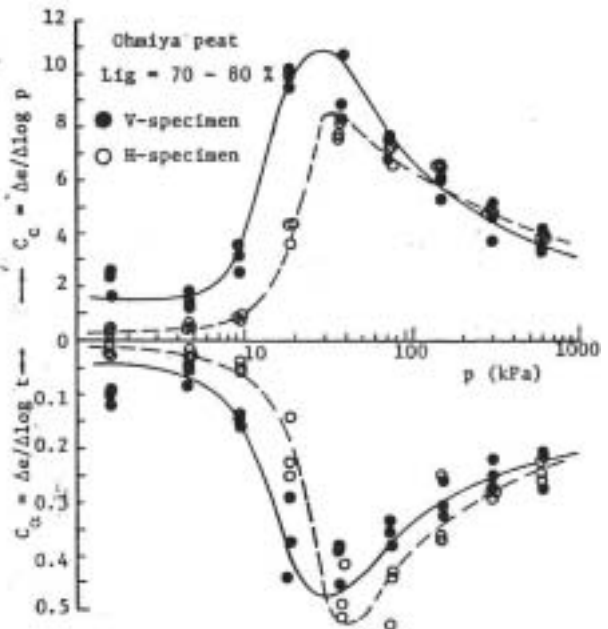


Relationship of $(e)p-C$ and $-\log p$

Figs. 3.12 The effect of the period of loading (After Matsuo et al., 1986)



Relationship of C_c and C_a



Change of C_c and C_a with respect to the range of consolidation pressure

Figs. 3.13 The effect of the initial structures of clay (After Matsuo et al., 1986)

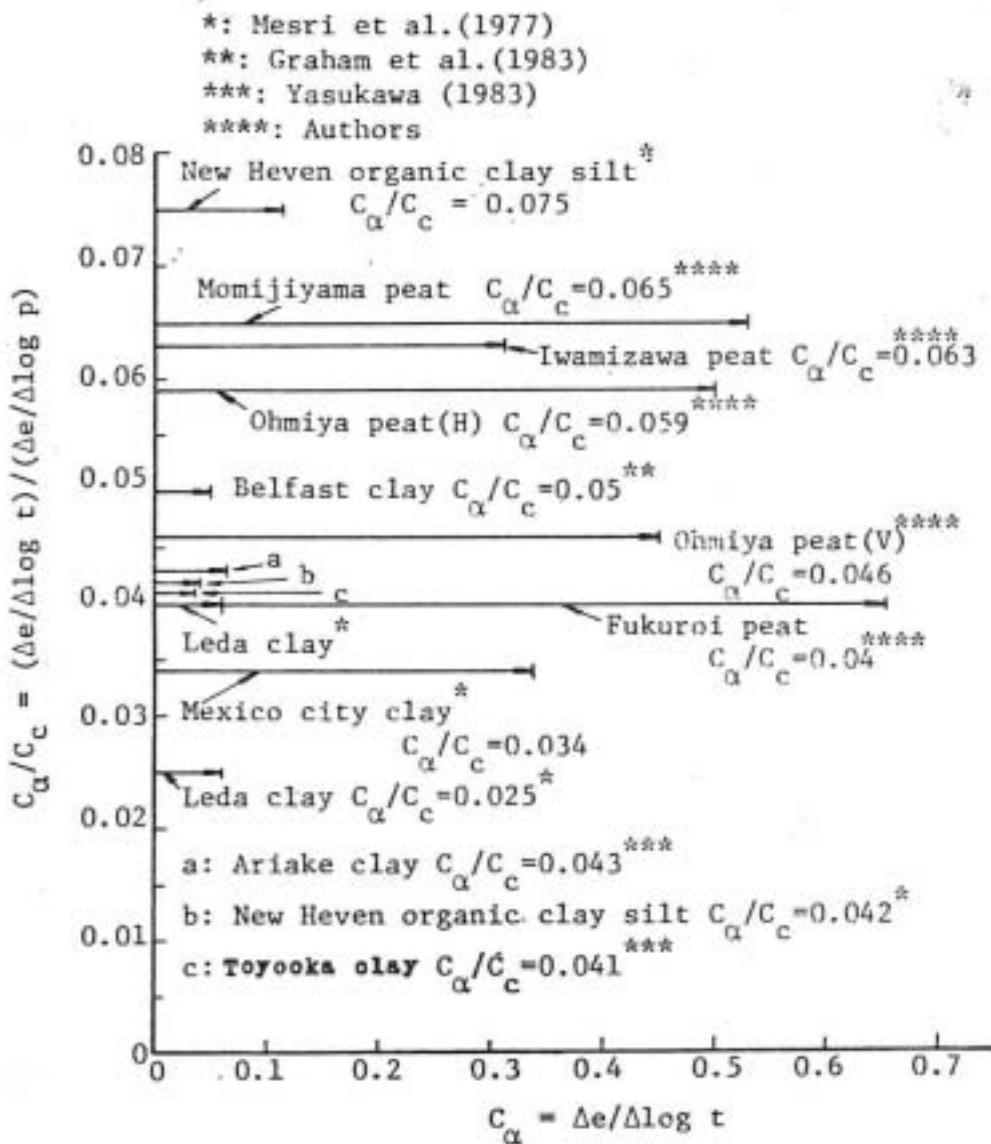


Fig. 3.14 Range of the C_α / C_c and the C_α (After Matsuo et al., 1986)

Those figures show the tendency that in the smaller range of the consolidation pressure than P_c the value of both C_α , C_α / C_c are smaller but the ratio of the C_α / C_c is the unique. There are no paper found enough to see any tendency or uniqueness of C_α / C_c depending on the consolidation pressure and so on.

In order to check the response of the soil parameters against the change of the material properties, three types of parametric study are carried out in this section as follows: 1) C_α , C_α / C_c times by 1.0, 0.75, 0.50, 0.25, 0.10. 2) C_α times by .0, 0.75, 0.50, 0.25, 0.10. 3) C_α / C_c times by .0, 0.75, 0.50, 0.25, 0.10.

The effect of the change of ' , ' ,

Figs.3.15-3.18

Range of age $T_0 = 5,000\text{years}, 10,000\text{years}, 15,000\text{years}$

Range of PI = 10, 20, 40, 60, 80, 100

Range of the factor to the material properties $\times 1.0, \times 0.75, \times 0.50, \times 0.25, \times 0.10$

The diagram shown in Figs.3.15-3.18 are arranged as follows (each box corresponding a graph in the figures) :

[Figs.3.15-3-17]

The corresponding depositional ages are $T_o=5,000$ years for Figs.3.15, $T_o=10,000$ for Figs.3.16 and $T_o=15,000$ for Figs.3.17.

Table 3.7 Arrangement of the graphs in Figs.3.15-3.17

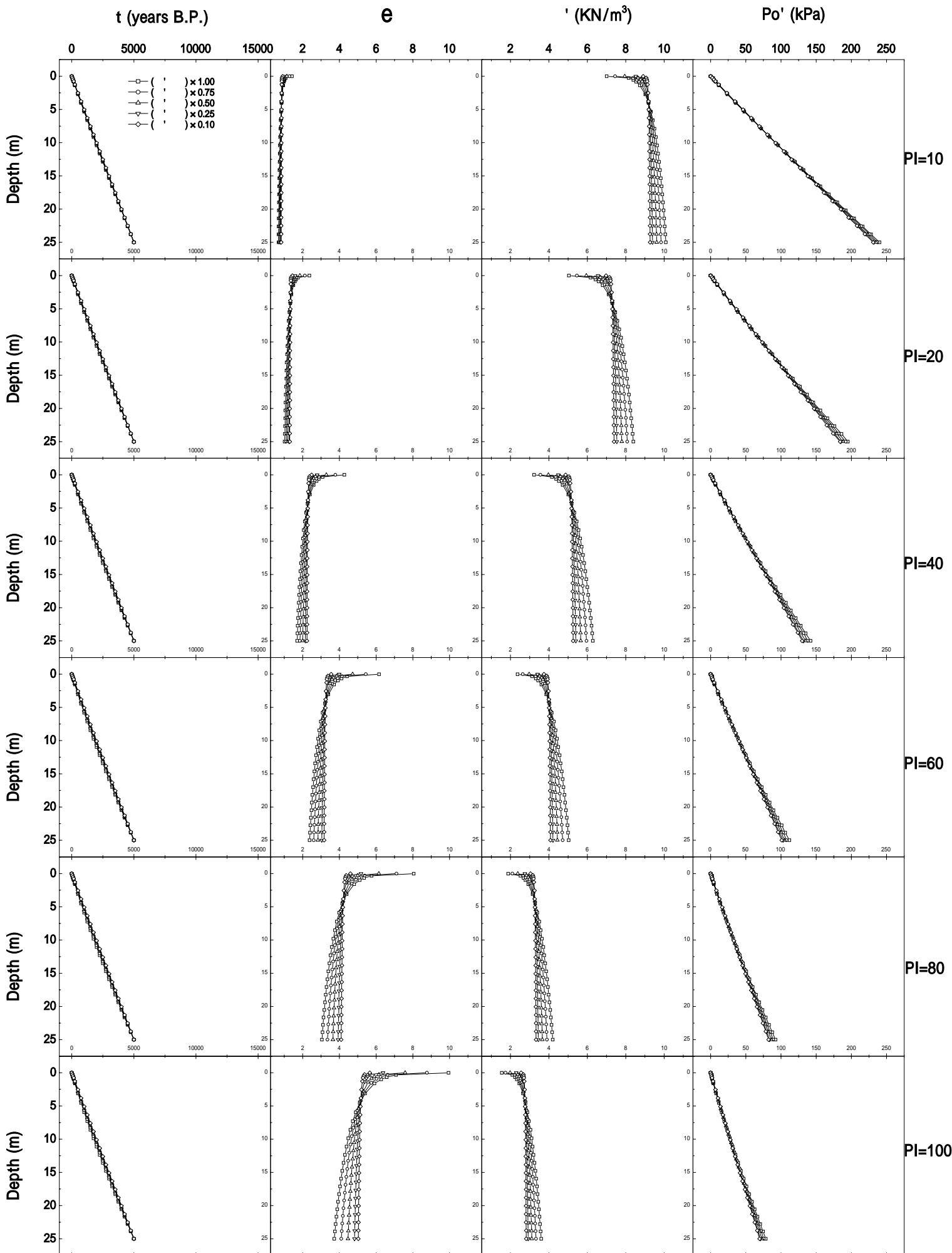
t-Depth PI=10 (' , ,) $\times 0.1 - 1.0$	e-Depth PI=10 (' , ,) $\times 0.1 - 1.0$	'-Depth PI=10 (' , ,) $\times 0.1 - 1.0$	Po'-Depth PI=10 (' , ,) $\times 0.1 - 1.0$
t-Depth PI=20 (' , ,) $\times 0.1 - 1.0$	e-Depth PI=20 (' , ,) $\times 0.1 - 1.0$	'-Depth PI=20 (' , ,) $\times 0.1 - 1.0$	Po'-Depth PI=20 (' , ,) $\times 0.1 - 1.0$
t-Depth PI=40 (' , ,) $\times 0.1 - 1.0$	e-Depth PI=40 (' , ,) $\times 0.1 - 1.0$	'-Depth PI=40 (' , ,) $\times 0.1 - 1.0$	Po'-Depth PI=40 (' , ,) $\times 0.1 - 1.0$
t-Depth PI=60 (' , ,) $\times 0.1 - 1.0$	e-Depth PI=60 (' , ,) $\times 0.1 - 1.0$	'-Depth PI=60 (' , ,) $\times 0.1 - 1.0$	Po'-Depth PI=60 (' , ,) $\times 0.1 - 1.0$
t-Depth PI=80 (' , ,) $\times 0.1 - 1.0$	e-Depth PI=80 (' , ,) $\times 0.1 - 1.0$	'-Depth PI=80 (' , ,) $\times 0.1 - 1.0$	Po'-Depth PI=80 (' , ,) $\times 0.1 - 1.0$
t-Depth PI=100 (' , ,) $\times 0.1 - 1.0$	e-Depth PI=100 (' , ,) $\times 0.1 - 1.0$	'-Depth PI=100 (' , ,) $\times 0.1 - 1.0$	Po'-Depth PI=100 (' , ,) $\times 0.1 - 1.0$

[Figs.3.18]

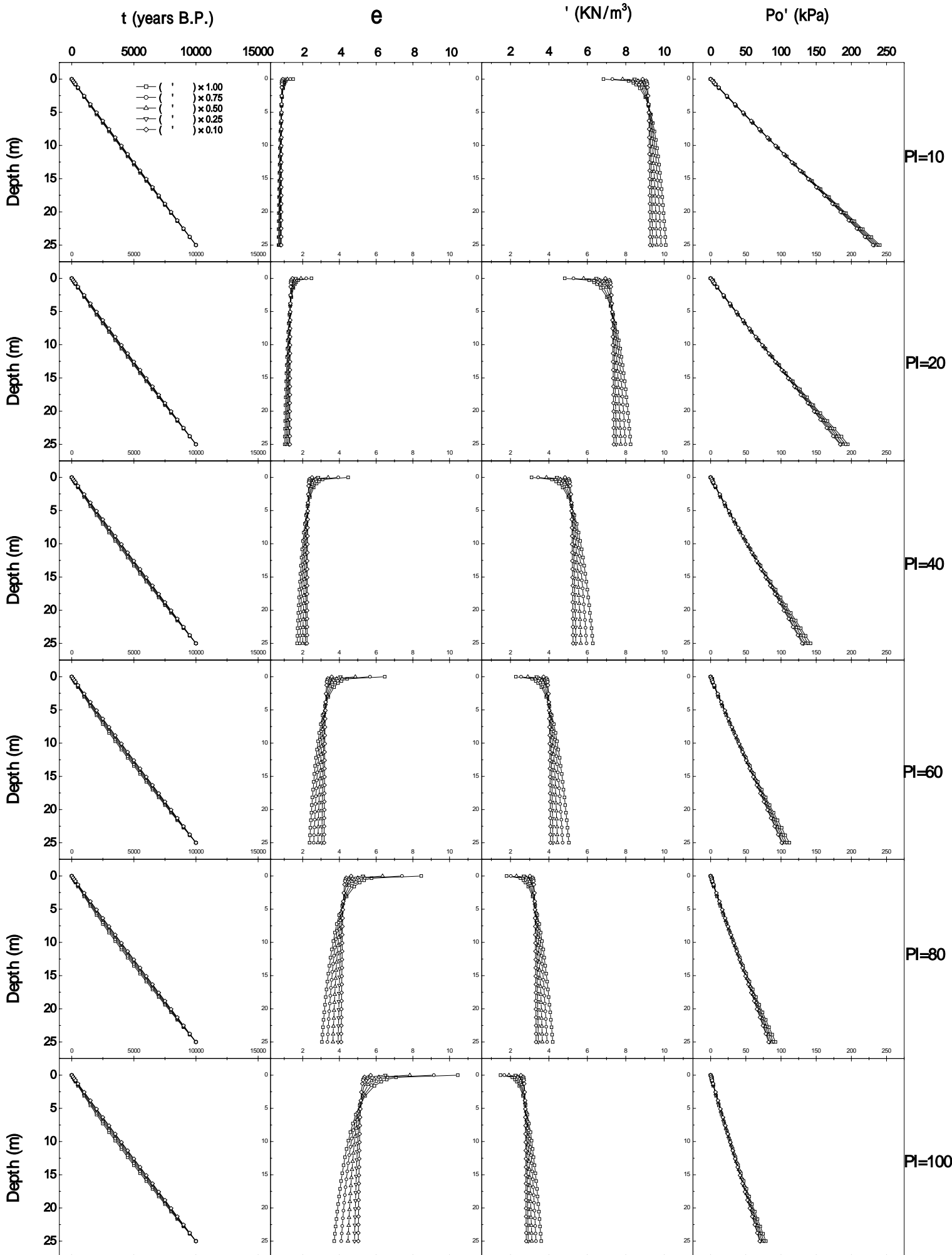
Table 3.8 Arrangement of the graphs in Figs.3.18

To=5,000 Po' & Pc'-Depth PI=10 (' , ,) $\times 0.1 - 1.0$	To=5,000 OCR-Depth PI=10 (' , ,) $\times 0.1 - 1.0$	To=10,000 Po' & Pc'-Depth PI=10 (' , ,) $\times 0.1 - 1.0$	To=10,000 OCR-Depth PI=10 (' , ,) $\times 0.1 - 1.0$	To=15,000 Po' & Pc'-Depth PI=10 (' , ,) $\times 0.1 - 1.0$	To=15,000 OCR-Depth PI=10 (' , ,) $\times 0.1 - 1.0$
To=5,000 Po' & Pc'-Depth PI=20 (' , ,) $\times 0.1 - 1.0$	To=5,000 OCR-Depth PI=20 (' , ,) $\times 0.1 - 1.0$	To=10,000 Po' & Pc'-Depth PI=20 (' , ,) $\times 0.1 - 1.0$	To=10,000 OCR-Depth PI=20 (' , ,) $\times 0.1 - 1.0$	To=15,000 Po' & Pc'-Depth PI=20 (' , ,) $\times 0.1 - 1.0$	To=15,000 OCR-Depth PI=20 (' , ,) $\times 0.1 - 1.0$
To=5,000 Po' & Pc'-Depth PI=40 (' , ,) $\times 0.1 - 1.0$	To=5,000 OCR-Depth PI=40 (' , ,) $\times 0.1 - 1.0$	To=10,000 Po' & Pc'-Depth PI=40 (' , ,) $\times 0.1 - 1.0$	To=10,000 OCR-Depth PI=40 (' , ,) $\times 0.1 - 1.0$	To=15,000 Po' & Pc'-Depth PI=40 (' , ,) $\times 0.1 - 1.0$	To=15,000 OCR-Depth PI=40 (' , ,) $\times 0.1 - 1.0$
To=5,000 Po' & Pc'-Depth PI=60 (' , ,) $\times 0.1 - 1.0$	To=5,000 OCR-Depth PI=60 (' , ,) $\times 0.1 - 1.0$	To=10,000 Po' & Pc'-Depth PI=60 (' , ,) $\times 0.1 - 1.0$	To=10,000 OCR-Depth PI=60 (' , ,) $\times 0.1 - 1.0$	To=15,000 Po' & Pc'-Depth PI=60 (' , ,) $\times 0.1 - 1.0$	To=15,000 OCR-Depth PI=60 (' , ,) $\times 0.1 - 1.0$
To=5,000 Po' & Pc'-Depth PI=80 (' , ,) $\times 0.1 - 1.0$	To=5,000 OCR-Depth PI=80 (' , ,) $\times 0.1 - 1.0$	To=10,000 Po' & Pc'-Depth PI=80 (' , ,) $\times 0.1 - 1.0$	To=10,000 OCR-Depth PI=80 (' , ,) $\times 0.1 - 1.0$	To=15,000 Po' & Pc'-Depth PI=80 (' , ,) $\times 0.1 - 1.0$	To=15,000 OCR-Depth PI=80 (' , ,) $\times 0.1 - 1.0$
To=5,000 Po' & Pc'-Depth PI=100 (' , ,) $\times 0.1 - 1.0$	To=5,000 OCR-Depth PI=100 (' , ,) $\times 0.1 - 1.0$	To=10,000 Po' & Pc'-Depth PI=100 (' , ,) $\times 0.1 - 1.0$	To=10,000 OCR-Depth PI=100 (' , ,) $\times 0.1 - 1.0$	To=15,000 Po' & Pc'-Depth PI=100 (' , ,) $\times 0.1 - 1.0$	To=15,000 OCR-Depth PI=100 (' , ,) $\times 0.1 - 1.0$

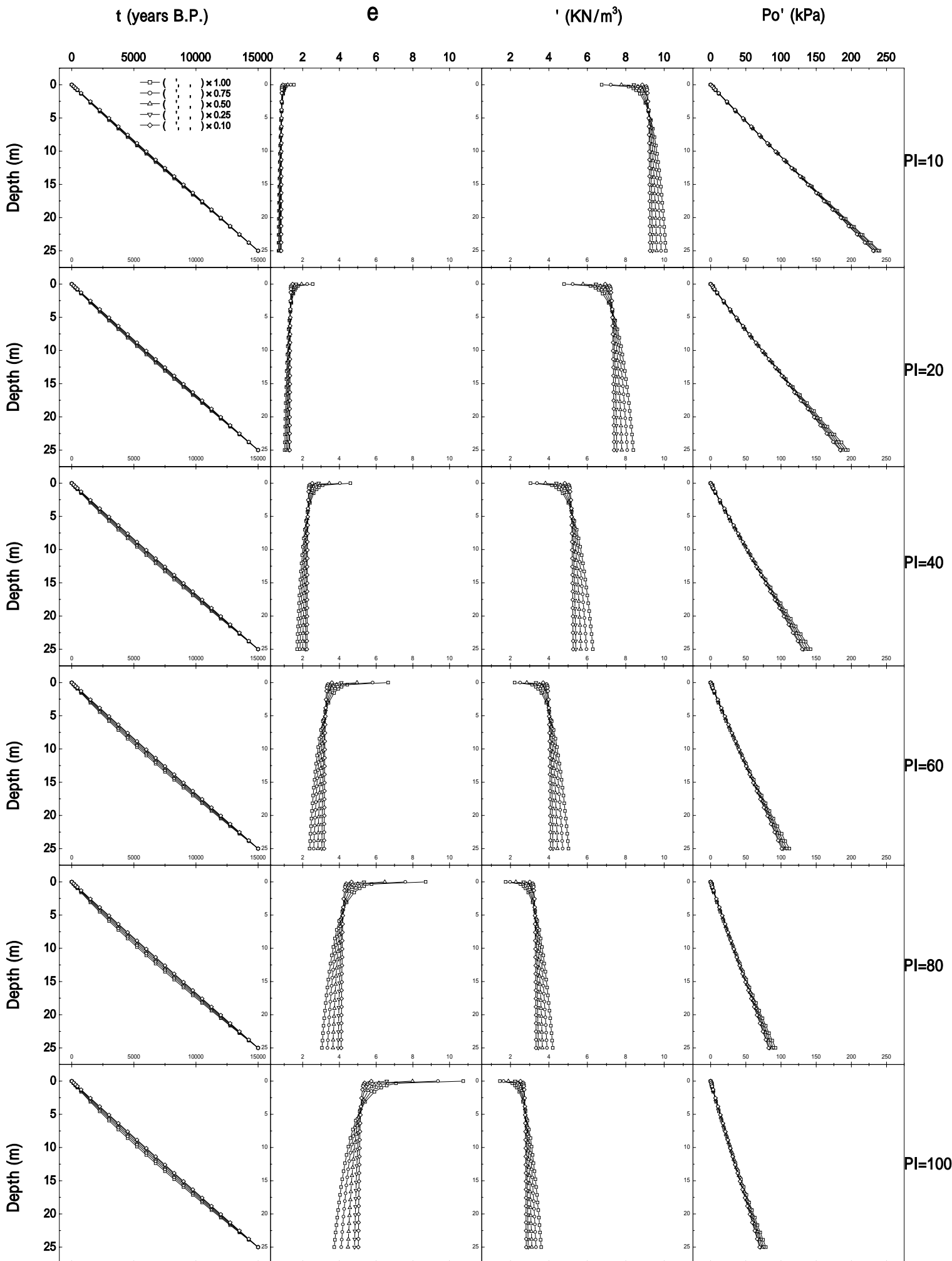
All the parameters and calculation are listed in Tables 3.9-3.11.



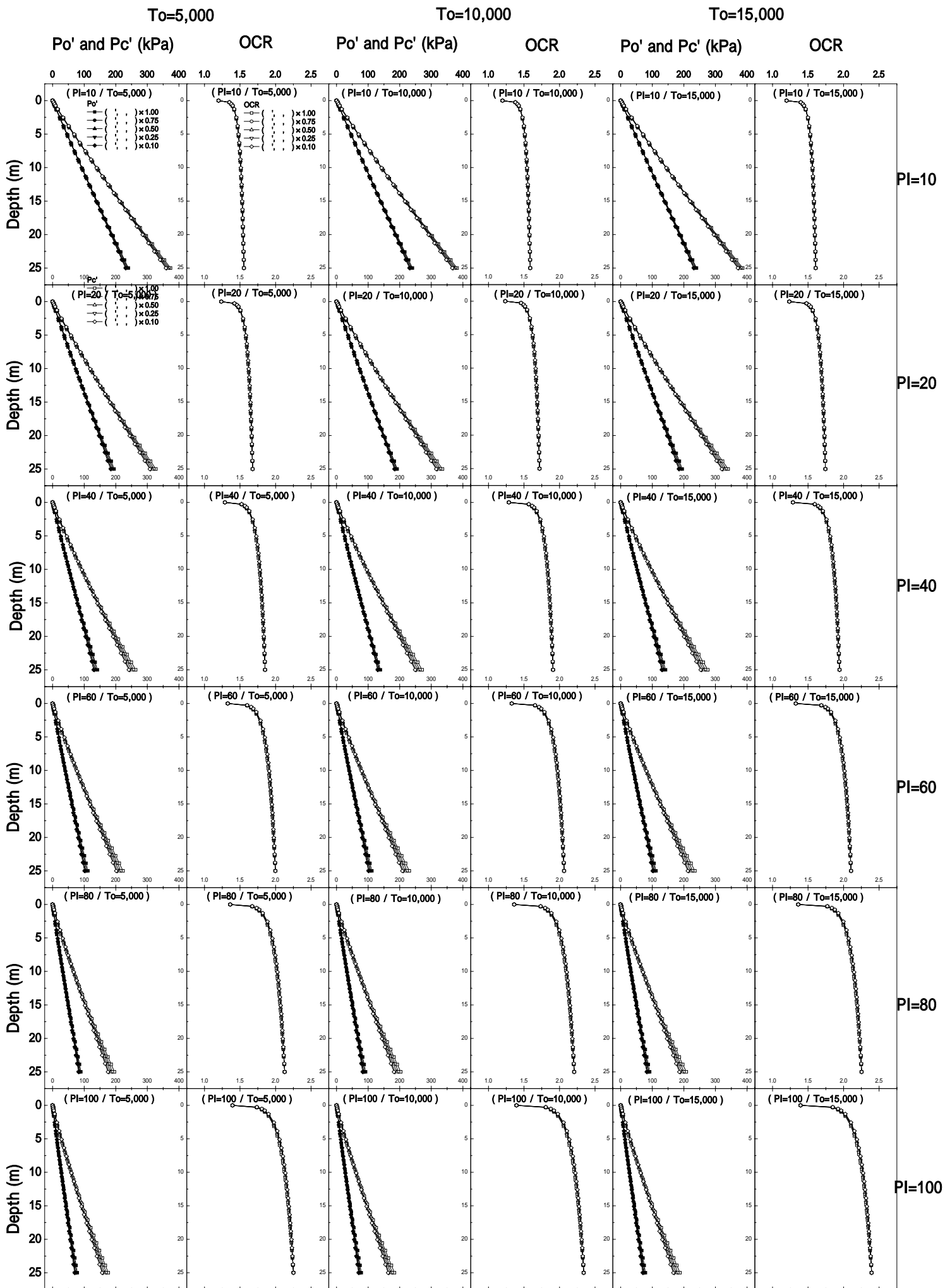
Figs.3.15 The effect of t , e , and Po' of 5. t , e , Po' and Po' ($To=5,000$)



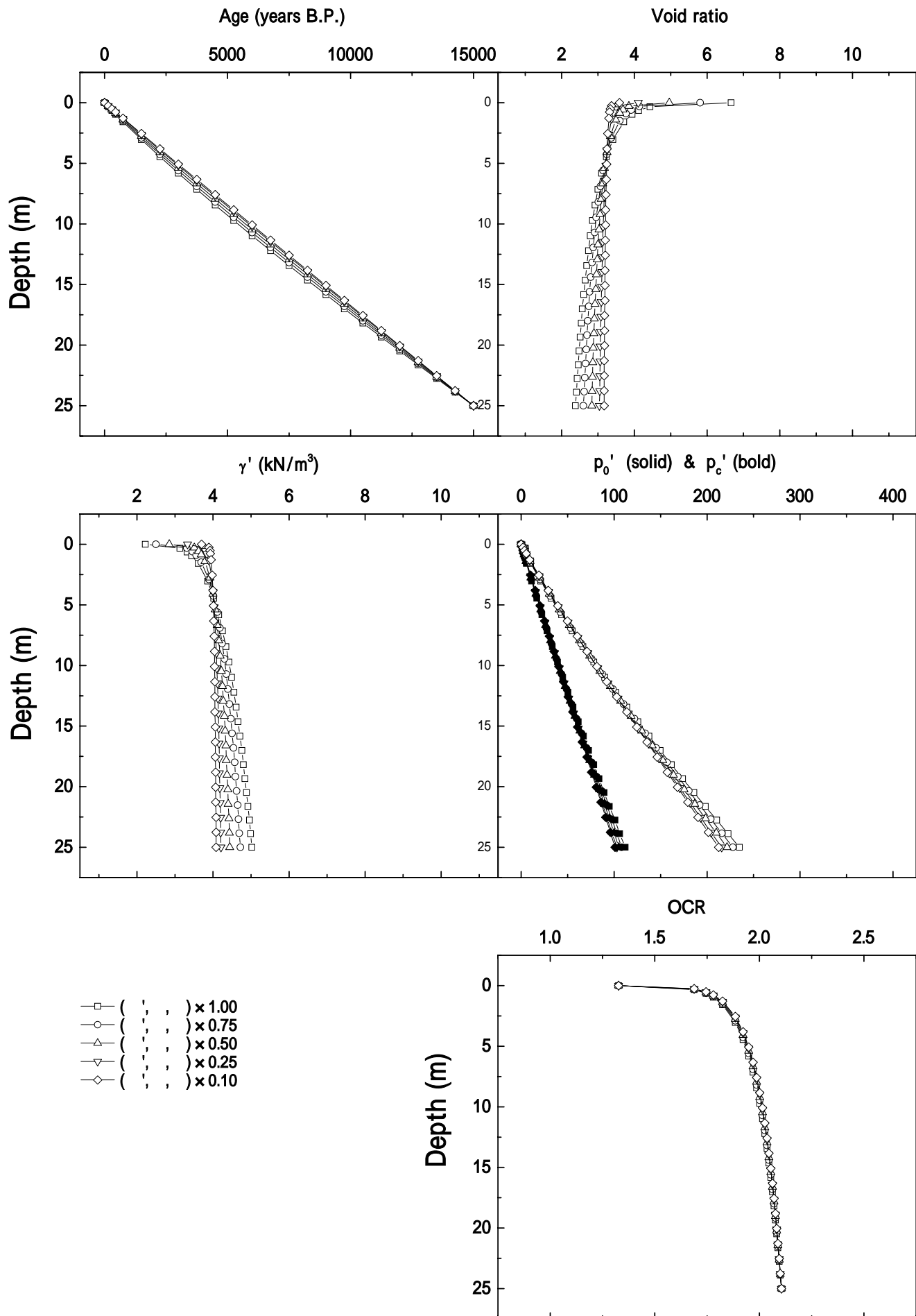
Figs.3.16 The effect of ' , and 2 of 5. t, e, 'and Po' (To=10,000)



Figs.3.17 The effect of ν , e , and γ of 3 of 5. t , e , γ and Po' ($To=15,000$)



Figs.3.18 The effect of σ_v' , σ_h' , and σ_v'/σ_h' of 5. Po' , Pc' and OCR ($To=5000,10000, 15000$)



Figs.3.19 The effect of γ_0' , γ_0' , and γ_0' of 5 of 5
 Enlarged diagrams of calculated parameters (PI=60, T0=15,000 years B.P.)

Table 3.9 Parameters lists of the calculations of Figs.3.15 and 3.18

To (years)	PI	V in Eq. 3.1	e_{sd}	γ'_{sd} (kN/m ³)	$T_{(10m)}$ (years)	γ		
		C_1						
5,000	10	8.31×10^{-3}	1.940	5.782	1920	0.00213	0.0850	0.0156
		7.45×10^{-3}	1.668	6.372	1942	0.00159	0.0638	0.0117
		6.62×10^{-3}	1.396	7.095	1961	0.00106	0.0425	0.0078
		5.80×10^{-3}	1.122	8.011	1981	0.00053	0.0213	0.0039
		5.32×10^{-3}	0.959	8.678	1993	0.00021	0.0085	0.0016
5,000	20	9.90×10^{-3}	3.315	3.940	1881	0.00388	0.1550	0.0470
		8.61×10^{-3}	2.820	4.450	1914	0.00291	0.1160	0.0352
		7.36×10^{-3}	2.325	5.113	1943	0.00194	0.0775	0.0235
		6.16×10^{-3}	1.828	6.011	1973	0.00097	0.0388	0.0117
		5.46×10^{-3}	1.529	6.722	1989	0.00039	0.0155	0.0047
5,000	40	1.18×10^{-2}	6.060	2.408	1835	0.00738	0.2950	0.1230
		9.96×10^{-3}	5.123	2.776	1880	0.00553	0.2210	0.0920
		8.22×10^{-3}	4.182	3.281	1922	0.00369	0.1480	0.0613
		6.58×10^{-3}	3.237	4.012	1962	0.00184	0.0738	0.0307
		5.62×10^{-3}	2.669	4.633	1986	0.00074	0.0295	0.0123
5,000	60	1.29×10^{-2}	8.802	1.734	1809	0.01090	0.4350	0.2080
		1.07×10^{-2}	7.424	2.018	1861	0.00816	0.3260	0.1560
		8.71×10^{-3}	6.038	2.415	1911	0.00544	0.2180	0.1040
		6.81×10^{-3}	4.647	3.010	1955	0.00272	0.1090	0.0521
		5.71×10^{-3}	3.809	3.535	1983	0.00109	0.0435	0.0208
5,000	80	1.36×10^{-2}	11.544	1.355	1791	0.01440	0.5750	0.3010
		1.12×10^{-2}	9.724	1.585	1849	0.01080	0.4310	0.2250
		9.01×10^{-3}	7.895	1.911	1903	0.00719	0.2880	0.1500
		6.95×10^{-3}	6.056	2.409	1953	0.00359	0.1440	0.0751
		5.77×10^{-3}	4.949	2.858	1982	0.00144	0.0575	0.0301
5,000	100	1.41×10^{-2}	14.284	1.112	1779	0.01790	0.7150	0.3970
		1.16×10^{-2}	12.024	1.305	1841	0.01340	0.5360	0.2980
		9.23×10^{-3}	9.751	1.581	1898	0.00894	0.3580	0.1990
		7.05×10^{-3}	7.465	2.008	1951	0.00447	0.1790	0.0994
		5.81×10^{-3}	6.089	2.398	1981	0.00179	0.0715	0.0397

Table 3.10 Parameters lists of the calculations of Figs.3.16 and 3.18

To (years)	PI	V in Eq. 3.1	e_{sd}	γ'_{sd} (kN/m ³)	$T_{(10m)}$ (years)	γ		
		C_1						
10,000	10	4.24×10^{-3}	2.001	5.665	3841	0.00213	0.0850	0.0156
		3.79×10^{-3}	1.714	6.264	3882	0.00159	0.0638	0.0117
		3.35×10^{-3}	1.426	7.007	3923	0.00106	0.0425	0.0078
		2.92×10^{-3}	1.138	7.951	3963	0.00053	0.0213	0.0039
		2.67×10^{-3}	0.965	8.651	3986	0.00021	0.0085	0.0016
10,000	20	5.08×10^{-3}	3.425	3.842	3763	0.00388	0.1550	0.0470
		4.40×10^{-3}	2.903	4.356	3826	0.00291	0.1160	0.0352
		3.74×10^{-3}	2.380	5.030	3887	0.00194	0.0775	0.0235
		3.11×10^{-3}	1.856	5.952	3945	0.00097	0.0388	0.0117
		2.74×10^{-3}	1.540	6.693	3978	0.00039	0.0155	0.0047
10,000	40	6.07×10^{-3}	6.269	2.339	3670	0.00738	0.2950	0.1230
		5.11×10^{-3}	5.280	2.707	3760	0.00553	0.2210	0.0920
		4.20×10^{-3}	4.287	3.215	3845	0.00369	0.1480	0.0613
		3.33×10^{-3}	3.290	3.963	3925	0.00184	0.0738	0.0307
		2.83×10^{-3}	2.690	4.607	3971	0.00074	0.0295	0.0123
10,000	60	6.64×10^{-3}	9.111	1.681	3618	0.01090	0.4350	0.2080
		5.51×10^{-3}	7.656	1.964	3722	0.00816	0.3260	0.1560
		4.45×10^{-3}	6.193	2.363	3822	0.00544	0.2180	0.1040
		3.45×10^{-3}	4.724	2.970	3914	0.00272	0.1090	0.0521
		2.87×10^{-3}	3.840	3.512	3966	0.00109	0.0435	0.0208
10,000	80	7.01×10^{-3}	11.952	1.313	3582	0.01440	0.5750	0.3010
		5.77×10^{-3}	10.031	1.541	3698	0.01080	0.4310	0.2250
		4.61×10^{-3}	8.099	1.868	3806	0.00719	0.2880	0.1500
		3.52×10^{-3}	6.158	2.375	3908	0.00359	0.1440	0.0751
		2.90×10^{-3}	4.990	2.838	3964	0.00144	0.0575	0.0301
10,000	100	7.27×10^{-3}	14.792	1.076	3558	0.01790	0.7150	0.3970
		5.95×10^{-3}	12.405	1.268	3682	0.01340	0.5360	0.2980
		4.72×10^{-3}	10.005	1.545	3796	0.00894	0.3580	0.1990
		3.58×10^{-3}	7.592	1.979	3903	0.00447	0.1790	0.0994
		2.92×10^{-3}	6.133	2.383	3963	0.00179	0.0715	0.0397

Table 3.11 Parameters lists of the calculations of Figs.3.17-3.19

To (years)	PI	V in Eq. 3.1	e_{sd}	γ'_{sd} (kN/m ³)	$T_{(10m)}$ (years)	γ		
		C_1						
15,000	10	2.86×10^{-3}	2.036	5.599	5761	0.00213	0.0850	0.0156
		2.55×10^{-3}	1.740	6.204	5824	0.00159	0.0638	0.0117
		2.25×10^{-3}	1.444	6.954	5885	0.00106	0.0425	0.0078
		1.95×10^{-3}	1.147	7.918	5944	0.00053	0.0213	0.0039
		1.78×10^{-3}	0.969	8.634	5978	0.00021	0.0085	0.0016
15,000	20	3.43×10^{-3}	3.489	3.787	5644	0.00388	0.1550	0.0470
		2.97×10^{-3}	2.951	4.303	5741	0.00291	0.1160	0.0352
		2.52×10^{-3}	2.412	4.982	5831	0.00194	0.0775	0.0235
		2.09×10^{-3}	1.872	5.919	5918	0.00097	0.0388	0.0117
		1.83×10^{-3}	1.547	6.675	5968	0.00039	0.0155	0.0047
15,000	40	4.12×10^{-3}	6.392	2.300	5506	0.00738	0.2950	0.1230
		3.45×10^{-3}	5.372	2.668	5641	0.00553	0.2210	0.0920
		2.83×10^{-3}	4.348	3.179	5768	0.00369	0.1480	0.0613
		2.23×10^{-3}	3.321	3.934	5888	0.00184	0.0738	0.0307
		1.89×10^{-3}	2.703	4.591	5956	0.00074	0.0295	0.0123
15,000	60	4.50×10^{-3}	9.293	1.652	5431	0.01090	0.4350	0.2080
		3.73×10^{-3}	7.791	1.934	5585	0.00816	0.3260	0.1560
		3.00×10^{-3}	6.283	2.334	5732	0.00544	0.2180	0.1040
		2.32×10^{-3}	4.769	2.947	5871	0.00272	0.1090	0.0521
		1.92×10^{-3}	3.858	3.499	5949	0.00109	0.0435	0.0208
15,000	80	4.76×10^{-3}	12.191	1.289	5373	0.01440	0.5750	0.3010
		3.91×10^{-3}	10.210	1.517	5547	0.01080	0.4310	0.2250
		3.11×10^{-3}	8.218	1.844	5710	0.00719	0.2880	0.1500
		2.37×10^{-3}	6.218	2.355	5861	0.00359	0.1440	0.0751
		1.94×10^{-3}	5.014	2.827	5946	0.00144	0.0575	0.0301
15,000	100	4.94×10^{-3}	15.089	1.057	5337	0.01790	0.7150	0.3970
		4.03×10^{-3}	12.628	1.247	5522	0.01340	0.5360	0.2980
		3.19×10^{-3}	10.153	1.524	5694	0.00894	0.3580	0.1990
		2.41×10^{-3}	7.667	1.961	5853	0.00447	0.1790	0.0994
		1.96×10^{-3}	6.170	2.371	5944	0.00179	0.0715	0.0397

The effect of the change of

Figs.3.20

Range of age $T_0 = 5,000\text{years}, 10,000\text{years}, 15,000\text{years}$

Range of $PI = 10, 20, 40, 60, 80, 100$

Range of the factor to the material properties $\times 1.0, \times 0.75, \times 0.50, \times 0.25, \times 0.10$

Note that has no relations except OCR and P_c '

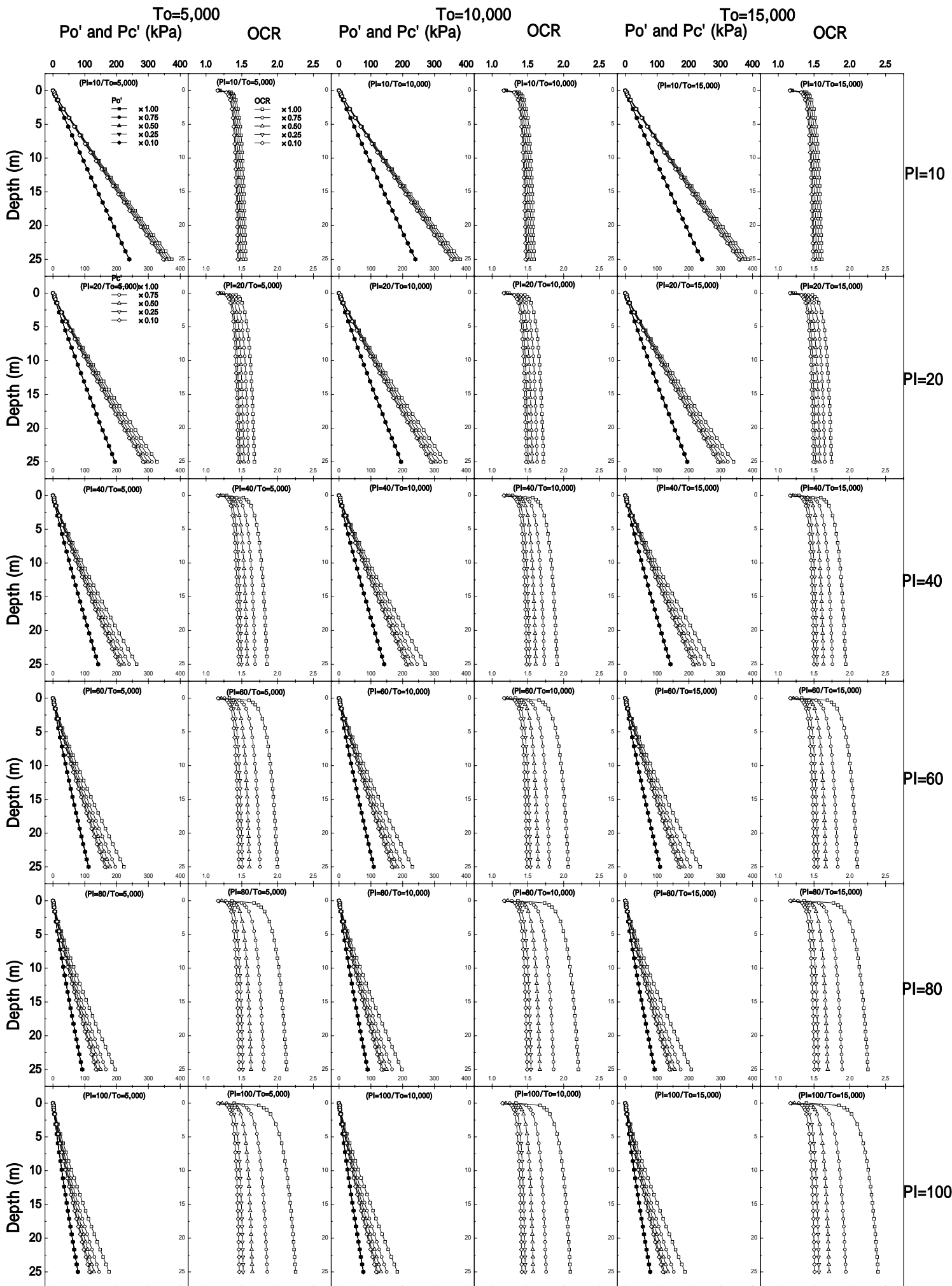
The diagram shown in Figs.3.20 is arranged as follows (each box corresponding a graph in the figures) :

[Figs.3.20]

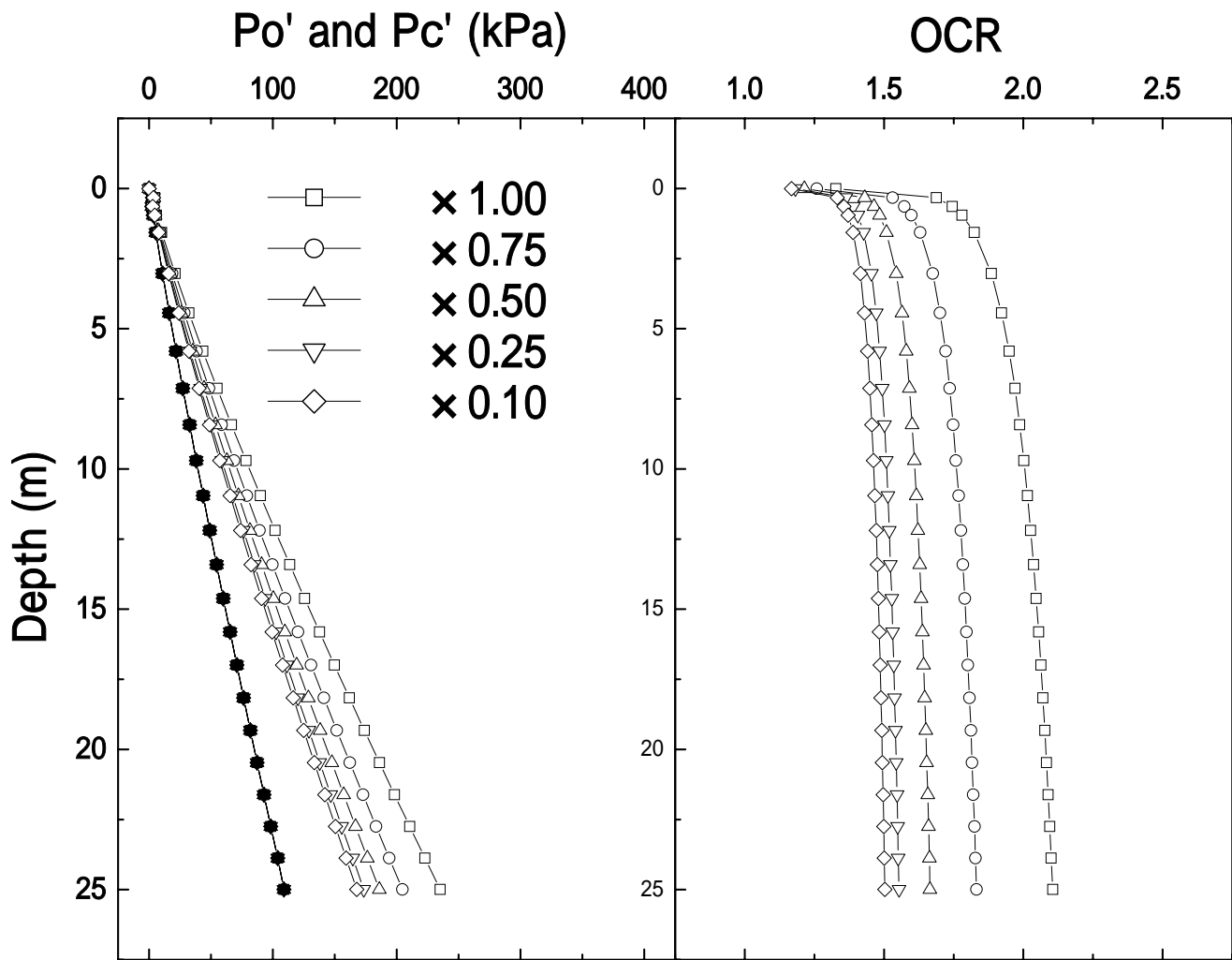
Table 3.12 Arrangement of the graphs in Figs.3.20

To=5,000 Po' & Pc'-Depth PI=10 x 0.1 – 1.0	To=5,000 OCR-Depth PI=10 x 0.1 – 1.0	To=10,000 Po' & Pc'-Depth PI=10 x 0.1 – 1.0	To=10,000 OCR-Depth PI=10 x 0.1 – 1.0	To=15,000 Po' & Pc'-Depth PI=10 x 0.1 – 1.0	To=15,000 OCR-Depth PI=10 x 0.1 – 1.0
To=5,000 Po' & Pc'-Depth PI=20 x 0.1 – 1.0	To=5,000 OCR-Depth PI=20 x 0.1 – 1.0	To=10,000 Po' & Pc'-Depth PI=20 x 0.1 – 1.0	To=10,000 OCR-Depth PI=20 x 0.1 – 1.0	To=15,000 Po' & Pc'-Depth PI=20 x 0.1 – 1.0	To=15,000 OCR-Depth PI=20 x 0.1 – 1.0
To=5,000 Po' & Pc'-Depth PI=40 x 0.1 – 1.0	To=5,000 OCR-Depth PI=40 x 0.1 – 1.0	To=10,000 Po' & Pc'-Depth PI=40 x 0.1 – 1.0	To=10,000 OCR-Depth PI=40 x 0.1 – 1.0	To=15,000 Po' & Pc'-Depth PI=40 x 0.1 – 1.0	To=15,000 OCR-Depth PI=40 x 0.1 – 1.0
To=5,000 Po' & Pc'-Depth PI=60 x 0.1 – 1.0	To=5,000 OCR-Depth PI=60 x 0.1 – 1.0	To=10,000 Po' & Pc'-Depth PI=60 x 0.1 – 1.0	To=10,000 OCR-Depth PI=60 x 0.1 – 1.0	To=15,000 Po' & Pc'-Depth PI=60 x 0.1 – 1.0	To=15,000 OCR-Depth PI=60 x 0.1 – 1.0
To=5,000 Po' & Pc'-Depth PI=80 x 0.1 – 1.0	To=5,000 OCR-Depth PI=80 x 0.1 – 1.0	To=10,000 Po' & Pc'-Depth PI=80 x 0.1 – 1.0	To=10,000 OCR-Depth PI=80 x 0.1 – 1.0	To=15,000 Po' & Pc'-Depth PI=80 x 0.1 – 1.0	To=15,000 OCR-Depth PI=80 x 0.1 – 1.0
To=5,000 Po' & Pc'-Depth PI=100 x 0.1 – 1.0	To=5,000 OCR-Depth PI=100 x 0.1 – 1.0	To=10,000 Po' & Pc'-Depth PI=100 x 0.1 – 1.0	To=10,000 OCR-Depth PI=100 x 0.1 – 1.0	To=15,000 Po' & Pc'-Depth PI=100 x 0.1 – 1.0	To=15,000 OCR-Depth PI=100 x 0.1 – 1.0

All the parameters and calculation are listed in Tables 3.13-3.15. Note that the changing in does not affect t, e, ' nor Po' at all.



Figs.3.20 The effect of 1 of 2. Po',Pc'and OCR (To=5000,10000, 15000)



Figs.3.21 The effect of λ 2 of 2
 Enlarged diagrams of Po',Pc'and OCR (PI=60,To=15000)

Table 3.13 Parameters lists of the calculations of Figs.3.20 and 3.21

To (years)	PI	V in Eq. 3.1	e_{sd}	γ'_{sd} (kN/m ³)	$T_{(10m)}$ (years)	γ		
		C_1						
5,000	10	8.31×10^{-3}	1.940	5.782	1920	0.00213	0.0850	0.0156
								0.0117
								0.0078
								0.0039
								0.0016
5,000	20	9.90×10^{-3}	3.315	3.940	1881	0.00388	0.1550	0.0470
								0.0352
								0.0235
								0.0117
								0.0047
5,000	40	1.18×10^{-2}	6.060	2.408	1835	0.00738	0.2950	0.1230
								0.0920
								0.0613
								0.0307
								0.0123
5,000	60	1.29×10^{-2}	8.802	1.734	1808	0.01090	0.4350	0.2080
								0.1560
								0.1040
								0.0521
								0.0208
5,000	80	1.36×10^{-2}	11.543	1.355	1791	0.01440	0.5750	0.3010
								0.2250
								0.1500
								0.0751
								0.0301
5,000	100	1.41×10^{-2}	14.284	1.112	1779	0.01790	0.7150	0.3970
								0.2980
								0.1990
								0.0994
								0.0397

Table 3.14 Parameters lists of the calculations of Figs.3.20 and 3.21

To (years)	PI	V in Eq. 3.1	e_{sd}	σ'_{sd} (kN/m ³)	$T_{(10m)}$ (years)	γ		
		C_1						
10,000	10	4.24×10^{-3}	2.001	5.665	3841	0.00213	0.0850	0.0156
								0.0117
								0.0078
								0.0039
								0.0016
10,000	20	5.08×10^{-3}	3.425	3.842	3763	0.00388	0.1550	0.0470
								0.0352
								0.0235
								0.0117
								0.0047
10,000	40	6.07×10^{-3}	6.269	2.339	3670	0.00738	0.2950	0.1230
								0.0920
								0.0613
								0.0307
								0.0123
10,000	60	6.64×10^{-3}	9.111	1.681	3617	0.01090	0.4350	0.2080
								0.1560
								0.1040
								0.0521
								0.0208
10,000	80	7.01×10^{-3}	12.077	1.300	3594	0.01440	0.5750	0.3010
								0.2250
								0.1500
								0.0751
								0.0301
10,000	100	7.27×10^{-3}	14.792	1.076	3558	0.01790	0.7150	0.3970
								0.2980
								0.1990
								0.0994
								0.0397

Table 3.15 Parameters lists of the calculations of Figs.3.20 and 3.21

To (years)	PI	V in Eq. 3.1	e_{sd}	$'_{sd}$ (kN/m ³)	$T_{(10m)}$ (years)	,		
		C_1						
15,000	10	2.86×10^{-3}	2.036	5.599	5761	0.00213	0.0850	0.0156
								0.0117
								0.0078
								0.0039
								0.0016
15,000	20	3.43×10^{-3}	3.489	3.787	5644	0.00388	0.1550	0.0470
								0.0352
								0.0235
								0.0117
								0.0047
15,000	40	4.12×10^{-3}	6.392	2.300	5506	0.00738	0.2950	0.1230
								0.0920
								0.0613
								0.0307
								0.0123
15,000	60	4.50×10^{-3}	9.292	1.652	5425	0.01090	0.4350	0.2080
								0.1560
								0.1040
								0.0521
								0.0208
15,000	80	4.76×10^{-3}	12.191	1.289	5373	0.01440	0.5750	0.3010
								0.2250
								0.1500
								0.0751
								0.0301
15,000	100	4.94×10^{-3}	15.089	1.057	5337	0.01790	0.7150	0.3970
								0.2980
								0.1990
								0.0994
								0.0397

The effect of the change of γ'

Figs.3.22-3.25

Range of age $T_0 = 5,000\text{years}, 10,000\text{years}, 15,000\text{years}$

Range of $PI = 10, 20, 40, 60, 80, 100$

Range of the material property γ' $0.025, 0.0375, 0.0500, 0.0625, 0.0750$

The diagram shown in Figs.3.22-3.25 are arranged as follows (each box corresponding a graph in the figures) :

[Figs.3.22-3-24]

The corresponding depositional ages are $T_o=5,000$ years for Figs.3.22, $T_o=10,000$ for Figs.3.23 and $T_o=15,000$ for Figs.3.24.

Table 3.16 Arrangement of the graphs in Figs.3.22-3.24

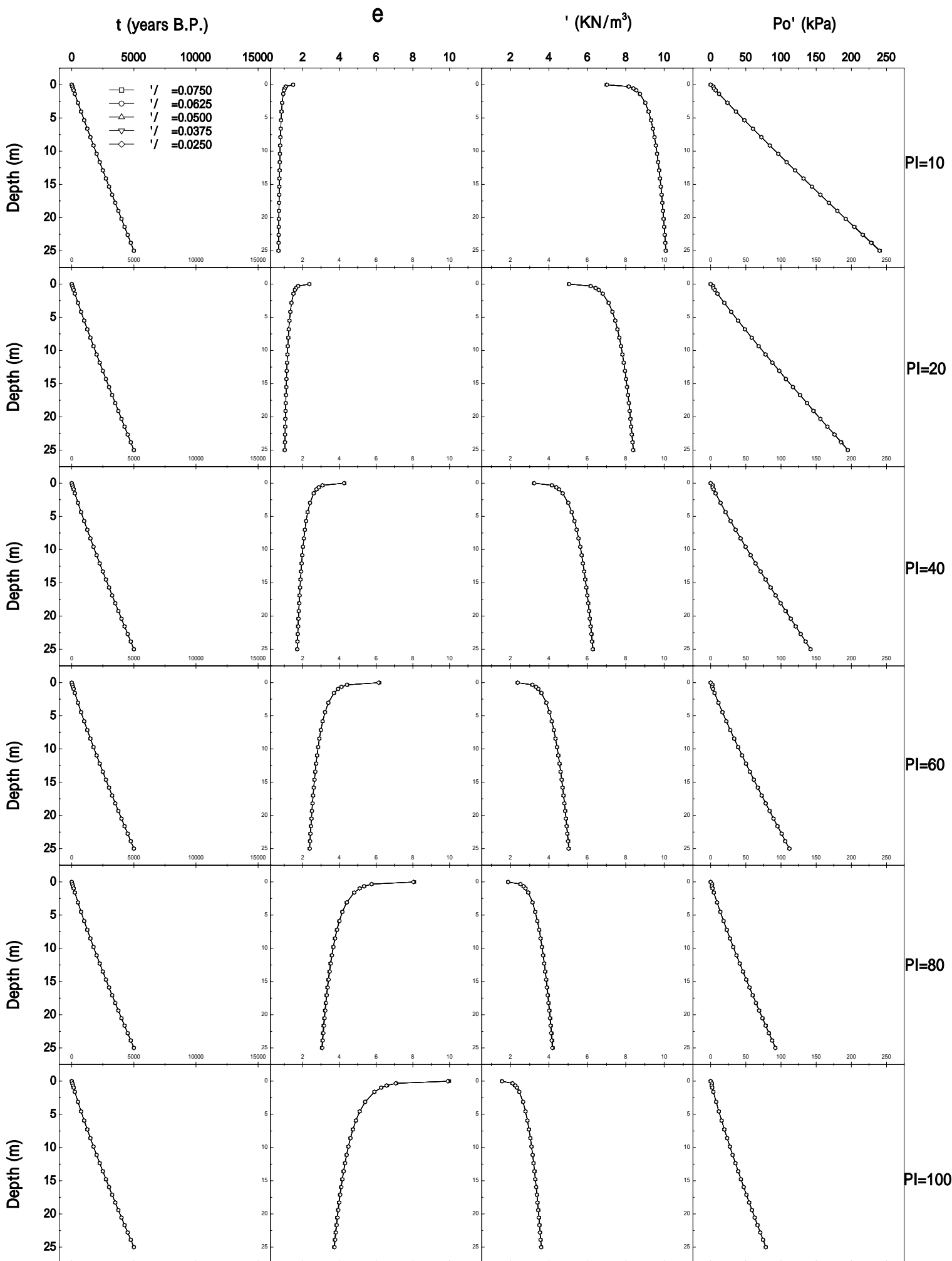
t-Depth PI=10 γ/δ : 0.025 – 0.075	e-Depth PI=10 γ/δ : 0.025 – 0.075	'-Depth PI=10 γ/δ : 0.025 – 0.075	Po'-Depth PI=10 γ/δ : 0.025 – 0.075
t-Depth PI=20 γ/δ : 0.025 – 0.075	e-Depth PI=20 γ/δ : 0.025 – 0.075	'-Depth PI=20 γ/δ : 0.025 – 0.075	Po'-Depth PI=20 γ/δ : 0.025 – 0.075
t-Depth PI=40 γ/δ : 0.025 – 0.075	e-Depth PI=40 γ/δ : 0.025 – 0.075	'-Depth PI=40 γ/δ : 0.025 – 0.075	Po'-Depth PI=40 γ/δ : 0.025 – 0.075
t-Depth PI=60 γ/δ : 0.025 – 0.075	e-Depth PI=60 γ/δ : 0.025 – 0.075	'-Depth PI=60 γ/δ : 0.025 – 0.075	Po'-Depth PI=60 γ/δ : 0.025 – 0.075
t-Depth PI=80 γ/δ : 0.025 – 0.075	e-Depth PI=80 γ/δ : 0.025 – 0.075	'-Depth PI=80 γ/δ : 0.025 – 0.075	Po'-Depth PI=80 γ/δ : 0.025 – 0.075
t-Depth PI=100 γ/δ : 0.025 – 0.075	e-Depth PI=100 γ/δ : 0.025 – 0.075	'-Depth PI=100 γ/δ : 0.025 – 0.075	Po'-Depth PI=100 γ/δ : 0.025 – 0.075

[Figs.3.25]

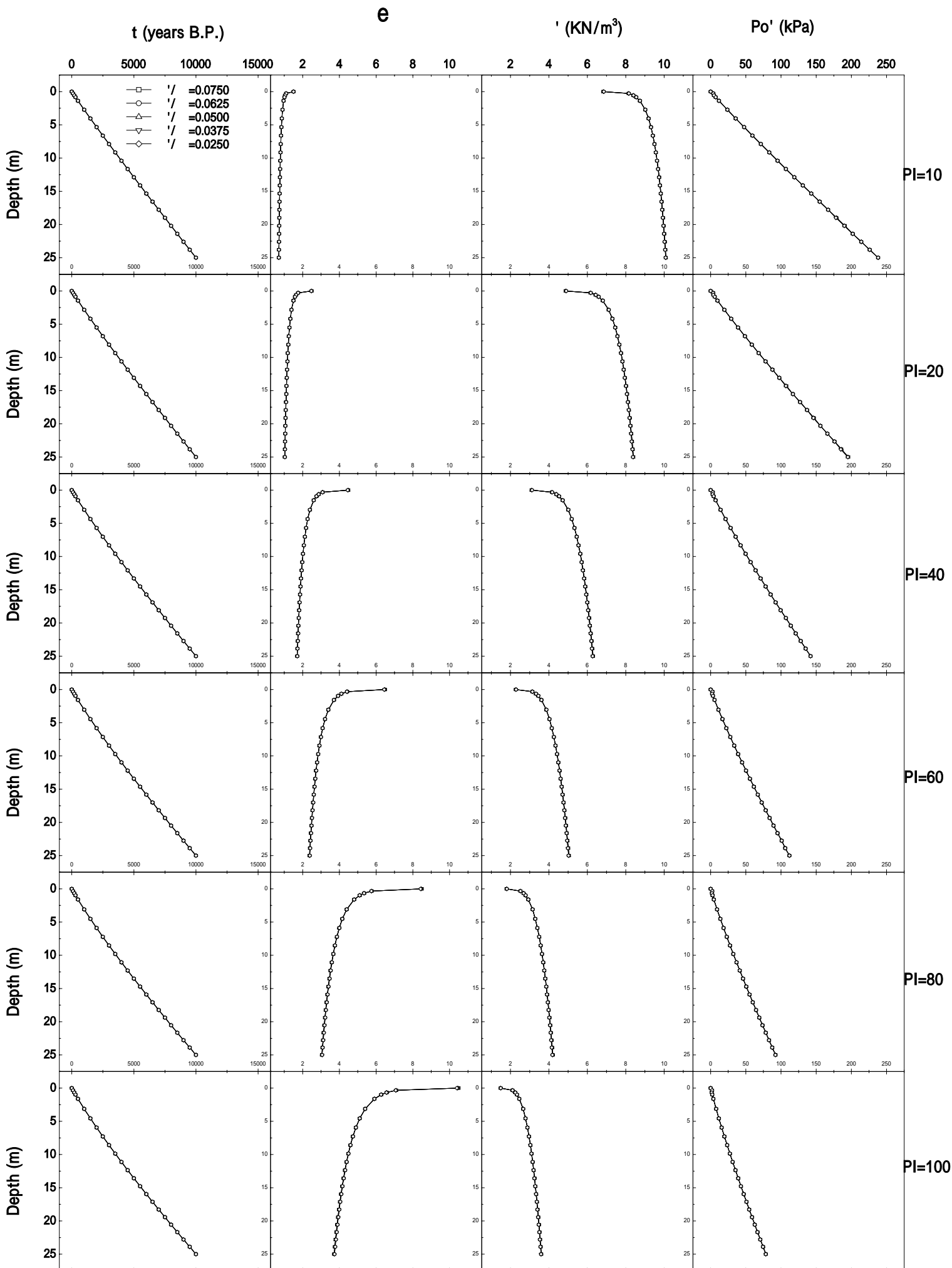
Table 3.17 Arrangement of the graphs in Figs.3.25

To=5,000 Po' & Pc'-Depth PI=10 γ/δ : 0.025 – 0.075	To=5,000 OCR-Depth PI=10 γ/δ : 0.025 – 0.075	To=10,000 Po' & Pc'-Depth PI=10 γ/δ : 0.025 – 0.075	To=10,000 OCR-Depth PI=10 γ/δ : 0.025 – 0.075	To=15,000 Po' & Pc'-Depth PI=10 γ/δ : 0.025 – 0.075	To=15,000 OCR-Depth PI=10 γ/δ : 0.025 – 0.075
To=5,000 Po' & Pc'-Depth PI=20 γ/δ : 0.025 – 0.075	To=5,000 OCR-Depth PI=20 γ/δ : 0.025 – 0.075	To=10,000 Po' & Pc'-Depth PI=20 γ/δ : 0.025 – 0.075	To=10,000 OCR-Depth PI=20 γ/δ : 0.025 – 0.075	To=15,000 Po' & Pc'-Depth PI=20 γ/δ : 0.025 – 0.075	To=15,000 OCR-Depth PI=20 γ/δ : 0.025 – 0.075
To=5,000 Po' & Pc'-Depth PI=40 γ/δ : 0.025 – 0.075	To=5,000 OCR-Depth PI=40 γ/δ : 0.025 – 0.075	To=10,000 Po' & Pc'-Depth PI=40 γ/δ : 0.025 – 0.075	To=10,000 OCR-Depth PI=40 γ/δ : 0.025 – 0.075	To=15,000 Po' & Pc'-Depth PI=40 γ/δ : 0.025 – 0.075	To=15,000 OCR-Depth PI=40 γ/δ : 0.025 – 0.075
To=5,000 Po' & Pc'-Depth PI=60 γ/δ : 0.025 – 0.075	To=5,000 OCR-Depth PI=60 γ/δ : 0.025 – 0.075	To=10,000 Po' & Pc'-Depth PI=60 γ/δ : 0.025 – 0.075	To=10,000 OCR-Depth PI=60 γ/δ : 0.025 – 0.075	To=15,000 Po' & Pc'-Depth PI=60 γ/δ : 0.025 – 0.075	To=15,000 OCR-Depth PI=60 γ/δ : 0.025 – 0.075
To=5,000 Po' & Pc'-Depth PI=80 γ/δ : 0.025 – 0.075	To=5,000 OCR-Depth PI=80 γ/δ : 0.025 – 0.075	To=10,000 Po' & Pc'-Depth PI=80 γ/δ : 0.025 – 0.075	To=10,000 OCR-Depth PI=80 γ/δ : 0.025 – 0.075	To=15,000 Po' & Pc'-Depth PI=80 γ/δ : 0.025 – 0.075	To=15,000 OCR-Depth PI=80 γ/δ : 0.025 – 0.075
To=5,000 Po' & Pc'-Depth PI=100 γ/δ : 0.025 – 0.075	To=5,000 OCR-Depth PI=100 γ/δ : 0.025 – 0.075	To=10,000 Po' & Pc'-Depth PI=100 γ/δ : 0.025 – 0.075	To=10,000 OCR-Depth PI=100 γ/δ : 0.025 – 0.075	To=15,000 Po' & Pc'-Depth PI=100 γ/δ : 0.025 – 0.075	To=15,000 OCR-Depth PI=100 γ/δ : 0.025 – 0.075

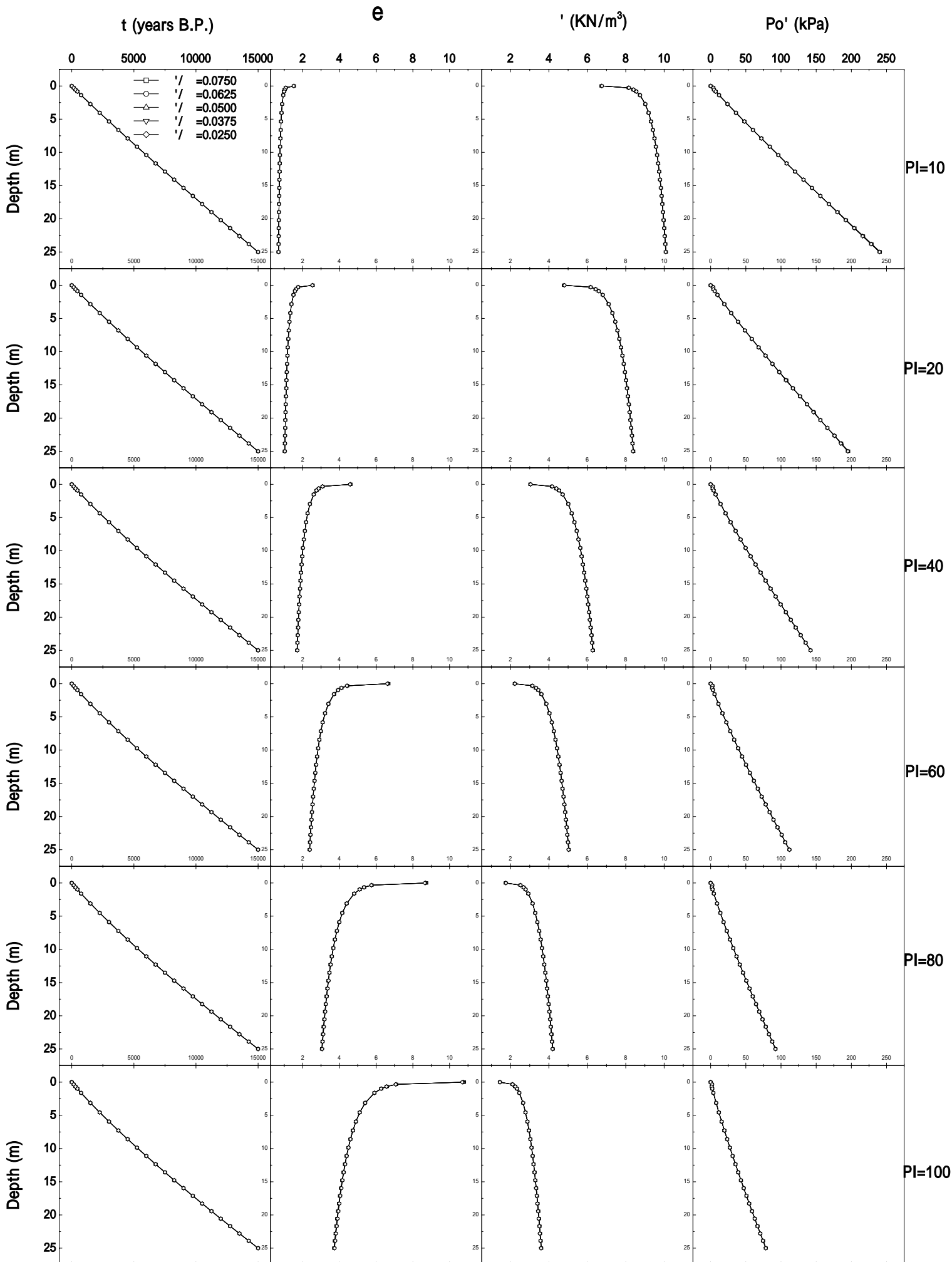
All the parameters and calculation are listed in Tables 3.18-3.20.



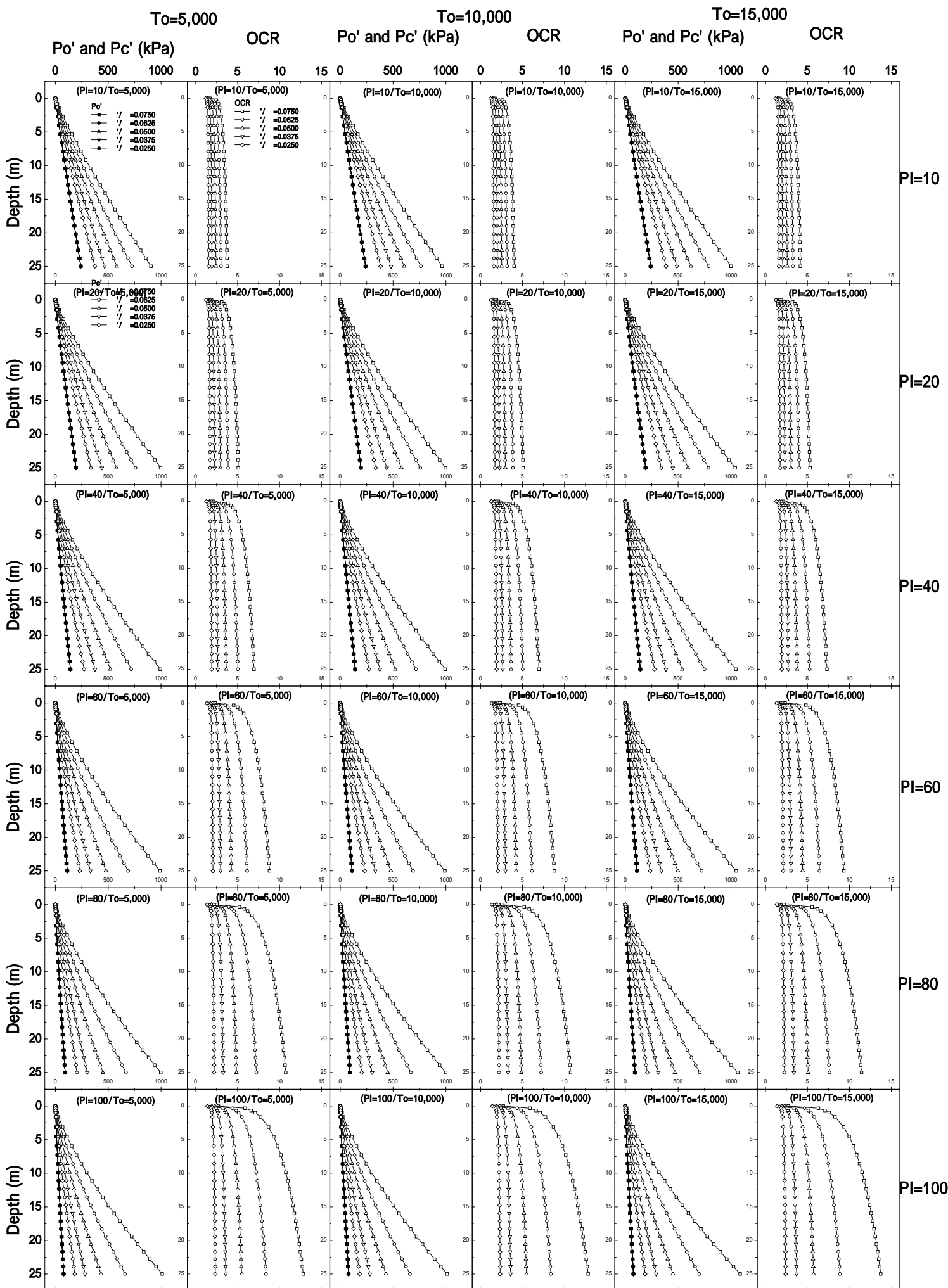
Figs.3.22 The effect of σ_v' / σ_v of 5. t , e , σ_v' and Po' ($To=5,000$)



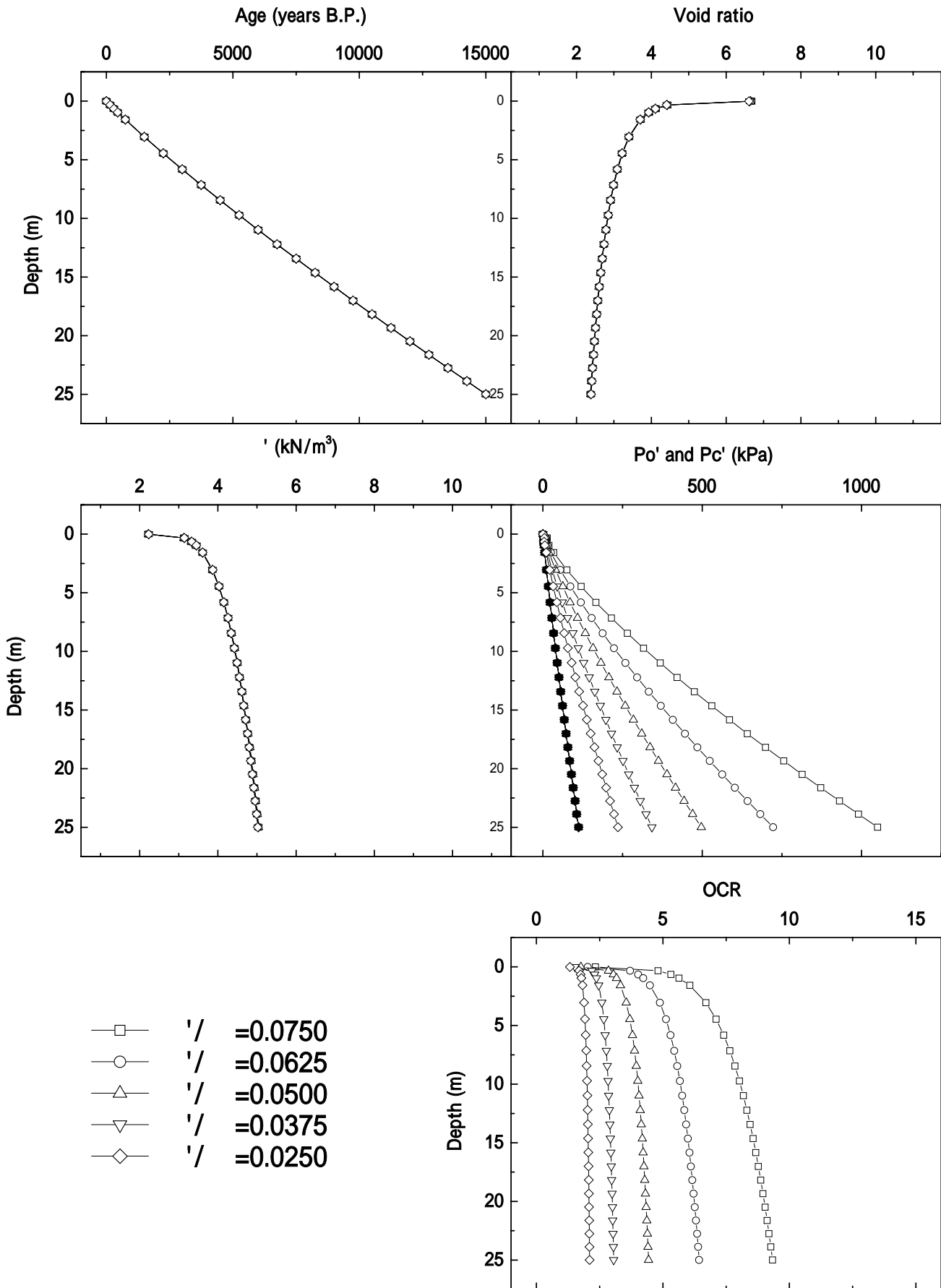
Figs.3.23 The effect of c_v of 5. t , e , σ' and Po' ($T_0=10,000$)



Figs.3.24 The effect of k_v/k_h of 5. t , e , σ_v and Po' ($To=15,000$)



Figs.3.25 The effect of ' of 5. Po',Pc' and OCR (To=5000,10000, 15000)



Figs.3.26 Enlarged diagrams of the t , e , σ' and Po' ($PI=60$, $To=15,000$)
The effect of σ'/σ_v' of 5

Table 3.18 Parameters lists of the calculations of Figs.3.22 and 3.25

To (years)	PI	V in Eq. 3.1	e_{sd}	γ'_{sd} (kN/m ³)	$T_{(10m)}$ (years)	γ		
		C_1						
5,000	10	8.48×10^{-3}	1.993	5.680	1916	0.00683	0.0850	0.0156
		8.44×10^{-3}	1.980	5.705	1916	0.00531		
		8.40×10^{-3}	1.967	5.730	1916	0.00425		
		8.36×10^{-3}	1.953	5.757	1917	0.00319		
		8.31×10^{-3}	1.940	5.782	1920	0.00213		
5,000	20	1.02×10^{-2}	3.411	3.854	1874	0.01160	0.1550	0.0470
		1.01×10^{-2}	3.387	3.857	1875	0.00969		
		1.00×10^{-2}	3.363	3.896	1876	0.00775		
		9.98×10^{-3}	3.338	3.916	1877	0.00581		
		9.91×10^{-3}	3.314	3.941	1879	0.00388		
5,000	40	1.22×10^{-2}	6.242	2.347	1824	0.02210	0.2950	0.1230
		1.21×10^{-2}	6.197	2.362	1830	0.01840		
		1.20×10^{-2}	6.151	2.377	1829	0.01480		
		1.19×10^{-2}	6.105	2.393	1831	0.01110		
		1.18×10^{-2}	6.059	2.408	1833	0.00738		
5,000	60	1.33×10^{-2}	9.069	1.688	1794	0.03260	0.4350	0.2080
		1.32×10^{-2}	9.003	1.699	1801	0.02720		
		1.31×10^{-2}	8.936	1.711	1802	0.02180		
		1.30×10^{-2}	8.869	1.723	1803	0.01630		
		1.29×10^{-2}	8.801	1.735	1804	0.01090		
5,000	80	1.41×10^{-2}	11.895	1.318	1774	0.04310	0.5750	0.3010
		1.40×10^{-2}	11.807	1.327	1778	0.03590		
		1.38×10^{-2}	11.720	1.336	1784	0.02880		
		1.37×10^{-2}	11.632	1.346	1788	0.02160		
		1.36×10^{-2}	11.542	1.355	1788	0.01440		
5,000	100	1.46×10^{-2}	14.723	1.081	1767	0.05360	0.7150	0.3970
		1.45×10^{-2}	14.611	1.089	1765	0.04470		
		1.44×10^{-2}	14.502	1.097	1768	0.03580		
		1.42×10^{-2}	14.394	1.104	1776	0.02680		
		1.41×10^{-2}	14.282	1.112	1776	0.01790		

Table 3.19 Parameters lists of the calculations of Figs.3.23 and 3.25

To (years)	PI	V in Eq. 3.1	e_{sd}	γ'_{sd} (kN/m ³)	$T_{(10m)}$ (years)	γ		
		C_1						
10,000	10	4.33×10^{-3}	2.056	5.563	3832	0.00638	0.0850	0.0156
		4.30×10^{-3}	2.043	5.587	3840	0.00531		
		4.28×10^{-3}	2.029	5.612	3840	0.00425		
		4.26×10^{-3}	2.015	5.638	3840	0.00319		
		4.25×10^{-3}	2.000	5.667	3835	0.00213		
10,000	20	5.22×10^{-3}	3.526	3.756	3745	0.01160	0.1550	0.0470
		5.18×10^{-3}	3.501	3.777	3752	0.00969		
		5.15×10^{-3}	3.475	3.799	3753	0.00775		
		5.11×10^{-3}	3.450	3.820	3760	0.00581		
		5.08×10^{-3}	3.425	3.842	3760	0.00388		
10,000	40	6.27×10^{-3}	6.462	2.278	3648	0.02210	0.2950	0.1230
		6.22×10^{-3}	6.414	2.293	3654	0.01840		
		6.18×10^{-3}	6.365	2.308	3653	0.01480		
		6.13×10^{-3}	6.317	2.323	3658	0.01110		
		6.08×10^{-3}	6.269	2.339	3664	0.00738		
10,000	60	6.88×10^{-3}	9.394	1.636	3591	0.03260	0.4350	0.2080
		6.83×10^{-3}	9.322	1.647	3592	0.02720		
		6.77×10^{-3}	9.252	1.658	3598	0.02180		
		6.70×10^{-3}	9.182	1.670	3611	0.01630		
		6.65×10^{-3}	9.111	1.681	3612	0.01090		
10,000	80	7.28×10^{-3}	12.324	1.276	3552	0.04310	0.5750	0.3010
		7.20×10^{-3}	12.232	1.285	3566	0.03590		
		7.15×10^{-3}	12.138	1.294	3565	0.02880		
		7.08×10^{-3}	12.045	1.303	3574	0.02160		
		7.03×10^{-3}	11.950	1.313	3573	0.01440		
10,000	100	7.54×10^{-3}	15.256	1.046	3536	0.05360	0.7150	0.3970
		7.48×10^{-3}	15.140	1.053	3537	0.04470		
		7.42×10^{-3}	15.023	1.061	3540	0.03580		
		7.35×10^{-3}	14.907	1.069	3547	0.02680		
		7.28×10^{-3}	14.791	1.077	3555	0.01790		

Table 3.20 Parameters lists of the calculations of Figs.3.24 and 3.25

To (years)	PI	V in Eq. 3.1	e_{sd}	γ'_{sd} (kN/m ³)	$T_{(10m)}$ (years)	γ		
		C_1						
15,000	10	2.92×10^{-3}	2.094	5.495	5750	0.00638	0.0850	0.0156
		2.91×10^{-3}	2.079	5.521	5753	0.00531		
		2.89×10^{-3}	2.065	5.546	5755	0.00425		
		2.87×10^{-3}	2.050	5.574	5769	0.00319		
		2.86×10^{-3}	2.036	5.599	5760	0.00213		
15,000	20	3.53×10^{-3}	3.594	3.700	5620	0.01160	0.1550	0.0470
		3.51×10^{-3}	3.567	3.722	5620	0.00969		
		3.48×10^{-3}	3.542	3.743	5635	0.00775		
		3.46×10^{-3}	3.515	3.765	5635	0.00581		
		3.44×10^{-3}	3.489	3.787	5634	0.00388		
15,000	40	4.25×10^{-3}	6.590	2.240	5477	0.02210	0.2950	0.1230
		4.22×10^{-3}	6.540	2.255	5479	0.01840		
		4.19×10^{-3}	6.491	2.269	5480	0.01480		
		4.15×10^{-3}	6.441	2.285	5497	0.01110		
		4.12×10^{-3}	6.392	2.300	5498	0.00738		
15,000	60	4.67×10^{-3}	9.584	1.606	5387	0.03260	0.4350	0.2080
		4.63×10^{-3}	9.511	1.617	5395	0.02720		
		4.59×10^{-3}	9.438	1.629	5404	0.02180		
		4.55×10^{-3}	9.365	1.640	5413	0.01630		
		4.51×10^{-3}	9.291	1.652	5422	0.01090		
15,000	80	4.95×10^{-3}	12.574	1.252	5323	0.04310	0.5750	0.3010
		4.89×10^{-3}	12.480	1.261	5350	0.03590		
		4.85×10^{-3}	12.393	1.269	5347	0.02880		
		4.81×10^{-3}	12.287	1.279	5359	0.02160		
		4.77×10^{-3}	12.190	1.289	5364	0.01440		
15,000	100	5.14×10^{-3}	15.566	1.026	5285	0.05360	0.7150	0.3970
		5.09×10^{-3}	15.447	1.034	5298	0.04470		
		5.04×10^{-3}	15.327	1.041	5311	0.03580		
		5.00×10^{-3}	15.206	1.049	5314	0.02680		
		4.95×10^{-3}	15.088	1.057	5327	0.01790		

3.5 Effect of the *PI* transition

Actual depthwise distribution of *PI* may not be constant because of the transition of the depositional environment during the geological time. The effects of the *PI* transition on the mechanical properties are investigated in this section. The parameters used for the calculations are listed in Table 3.21. The results of the calculations are plotted in Figs. 3.27 and listed in Tables 3.21-3.25. $T_o=10,000$ years 25 m of the present thickness is assumed in the calculations.

Table 3.21 Parameters lists of the calculations of Figs.3.27

T_o (years)	<i>PI</i>	V in Eq. 3.1	e_{sd}	γ'_{sd} (kN/m ³)	$T_{(10m)}$ (years)	γ	γ_w	γ_{sat}
		C_1 (m/year)						
10,000	10	4.27×10^{-3}	1.97	5.39	3817	2.13E-03	8.50E-02	1.56E-02
	15	4.74×10^{-3}	2.67	4.36	3768	3.00E-03	1.20E-01	3.05E-02
	20	5.13×10^{-3}	3.38	3.66	3728	3.88E-03	1.55E-01	4.70E-02
	40	6.16×10^{-3}	6.18	2.23	3621	7.38E-03	2.95E-01	1.23E-01
	60	6.76×10^{-3}	8.99	1.60	3560	1.09E-02	4.35E-01	2.08E-01
	80	7.15×10^{-3}	11.79	1.25	3520	1.44E-02	5.75E-01	3.01E-01
	90	7.30×10^{-3}	13.19	1.13	3504	1.61E-02	6.45E-01	3.49E-01
	100	7.43×10^{-3}	14.59	1.03	3491	1.79E-02	7.15E-01	3.97E-01

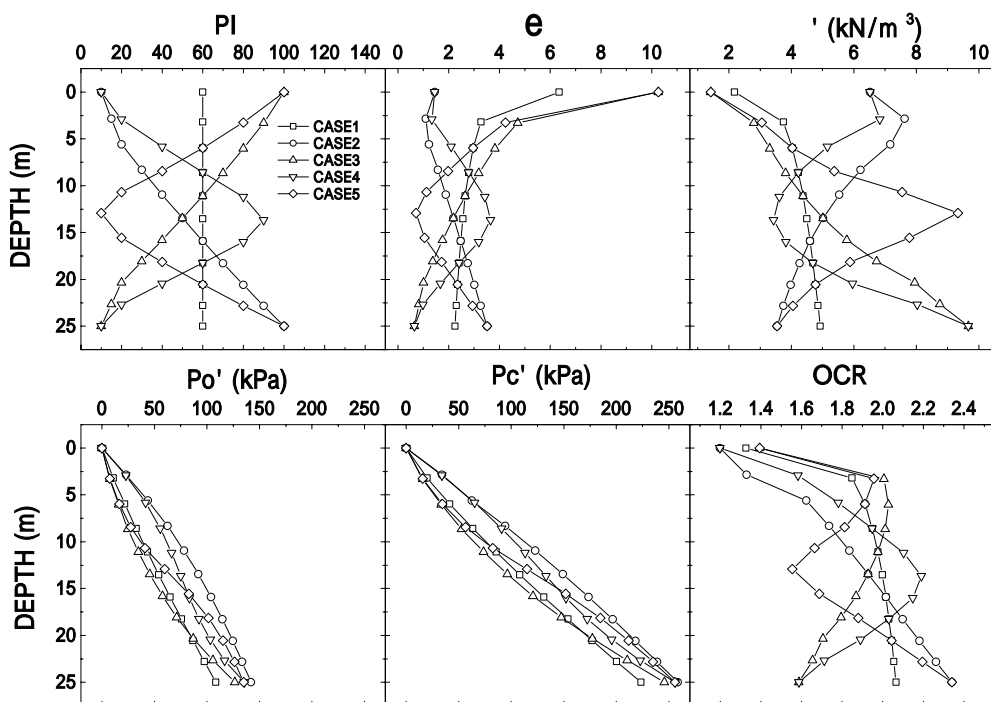


Fig.3.27 Effects of the transition of *PI* on the mechanical parameters

Table 3.22 Results of the calculations Case1 of Fig.3.24

[Case1]

t (years)	PI	Depth (m)	e	' (kN/m ³)	Po' (kPa)	Pc' (kPa)	OCR
1	60	0.007	6.355	2.176	0.011	0.014	1.327
1000	60	3.196	3.275	3.743	10.829	20.023	1.849
2000	60	5.973	2.966	4.035	21.658	41.401	1.912
3000	60	8.591	2.785	4.228	32.487	63.321	1.949
4000	60	11.108	2.656	4.376	43.316	85.602	1.976
5000	60	13.547	2.557	4.498	54.145	108.155	1.998
6000	60	15.926	2.476	4.603	64.974	130.926	2.015
7000	60	18.255	2.407	4.696	75.803	153.881	2.030
8000	60	20.540	2.347	4.780	86.632	176.995	2.043
9000	60	22.788	2.295	4.856	97.461	200.248	2.055
10000	60	25.001	2.248	4.926	108.290	223.626	2.065

Table 3.23 Results of the calculations Case2 of Fig.3.24

[Case2]

t (years)	PI	Depth (m)	e	' (kN/m ³)	Po' (kPa)	Pc' (kPa)	OCR
1	10	0.004	1.456	6.514	0.023	0.028	1.198
1000	15	2.865	1.098	7.627	22.978	34.012	1.330
2000	20	5.600	1.231	7.173	43.617	62.322	1.623
3000	30	8.326	1.572	6.220	62.363	94.081	1.736
4000	40	10.952	1.890	5.536	78.203	122.844	1.836
5000	50	13.482	2.190	5.016	91.924	149.240	1.928
6000	60	15.926	2.476	4.603	104.027	173.741	2.015
7000	70	18.293	2.749	4.267	114.856	196.696	2.099
8000	80	20.590	3.013	3.987	124.655	218.371	2.181
9000	90	22.824	3.267	3.749	133.602	238.972	2.262
10000	100	25.002	3.514	3.545	141.834	258.661	2.341

Table 3.24 Results of the calculations Case3 of Fig.3.24

[Case3]

t (years)	PI	Depth (m)	e	' (kN/m ³)	Po' (kPa)	Pc' (kPa)	OCR
1	100	0.007	10.264	1.420	0.008	0.011	1.394
1000	90	3.285	4.720	2.797	7.624	15.679	2.007
2000	80	6.062	3.830	3.313	15.856	33.470	2.028
3000	70	8.646	3.188	3.820	24.803	52.786	2.012
4000	60	11.108	2.656	4.376	34.602	73.644	1.976
5000	50	13.482	2.190	5.016	45.431	96.197	1.928
6000	40	15.796	1.767	5.782	57.534	120.697	1.868
7000	30	18.071	1.377	6.732	71.255	147.513	1.795
8000	20	20.333	1.010	7.958	87.095	177.162	1.706
9000	15	22.651	0.828	8.755	105.841	210.353	1.654
10000	10	25.001	0.654	9.675	126.484	245.699	1.588

Table 3.25 Results of the calculations Case4 of Fig.3.24

[Case4]

t (years)	PI	Depth (m)	e	' (kN/m ³)	Po' (kPa)	Pc' (kPa)	OCR
1	10	0.004	1.456	6.514	0.023	0.028	1.198
1000	20	2.930	1.341	6.835	22.978	34.012	1.583
2000	40	5.836	2.100	5.162	41.723	65.181	1.782
3000	60	8.591	2.785	4.228	55.444	90.916	1.949
4000	80	11.210	3.421	3.619	66.273	113.197	2.103
5000	90	13.681	3.656	3.436	75.220	133.122	2.190
6000	80	16.012	3.182	3.826	83.452	152.233	2.148
7000	60	18.255	2.407	4.696	92.399	172.546	2.030
8000	40	20.464	1.680	5.969	103.228	195.659	1.891
9000	20	22.677	0.992	8.033	116.949	222.786	1.713
10000	10	25.001	0.654	9.675	135.694	256.109	1.588

Table 3.26 Results of the calculations Case5 of Fig.3.24

[Case5]

t (years)	PI	Depth (m)	e	' (kN/m ³)	Po' (kPa)	Pc' (kPa)	OCR
1	100	0.007	10.264	1.420	0.008	0.011	1.394
1000	80	3.260	4.238	3.054	7.624	15.679	1.956
2000	60	5.973	2.966	4.035	16.571	34.473	1.912
3000	40	8.438	1.977	5.374	27.400	56.394	1.813
4000	20	10.683	1.121	7.545	41.120	82.506	1.664
5000	10	12.934	0.714	9.335	59.866	114.947	1.555
6000	20	15.571	1.056	7.782	82.844	151.877	1.688
7000	40	18.149	1.721	5.881	101.589	184.750	1.880
8000	60	20.540	2.347	4.780	115.309	211.731	2.043
9000	80	22.814	2.943	4.057	126.138	234.984	2.195
10000	100	25.002	3.514	3.545	135.086	255.706	2.341

3.6 Conclusions

The conclusions obtained in this chapter are as follows:

- (1) The parametric studies were carried out based on the proposed theory in this paper. It enables us to estimate the depthwise distribution of the soil parameters. Moreover effects of the history and properties of the soil such as age, depositional rate, PI , γ , ρ and the ratio γ'/ρ are investigated in this chapter.
- (2) The effect of PI is considerably strong to each parameter. Transition of PI gives a strong effect on the mechanical parameters except OCR.
- (3) Age T_o at the bottom of the formation does not effect to the depthwise distribution of age, void ratio and unit weight. T_o give effect to OCR and P_c' , however, the effect is not so strong because the effect is proportional to the logarithm of the age and it is possible to obtain the age with in the error of one order.
- (4) Depositional rate influences the depthwise distribution of all the parameters. The difference of the calculated value caused by the difference of the depositional rate is about 5%-10%.
- (5) The effect of the same changes of material properties γ , ρ to the age, P_o' , OCR and P_c' are negligible. However the effect to the shape of the depthwise distribution of void ratio and unit weight is that the smaller the those parameters the smaller the depthwise changes of the void ratio and unit weight.
- (6) The changes of γ (in this case ρ , ρ are not changed) give a strong impact to the depthwise distribution of OCR and P_c' . The bigger the value of γ , the larger the OCR and P_c' . Note that ρ does not have any relation with the distribution of the age, void ratio, unit weight and P_o' .
- (7) The changes of the ratio γ'/ρ give a effect only to the OCR and P_c' . The bigger the value of the ratio γ'/ρ , the larger the OCR and P_c' .

Summary of the parametric study is shown in Table 3.27.

Table 3.27 Summary of the parametric study

Parameters	t_{age}	e	γ	P_o'	OCR	P_c'
T_o	×	×	×	×		
V						
PI						
(γ , ρ , ρ)						
	×	×	×	×		
γ'/ρ	×	×	×	×		

: Strong effect, : Moderate effect, ; Weak effect, × : Negligible effect

References

- Bjerrum, L. (1967): Engineering geology of Norwegian Normally-consolidated Marine Clays as related to Settlements of Buildings. *Geotechnique*, Vol.17, pp.83-118.
- Crawford, C.B. (1964): Interpretation of Consolidation Test, *J. Soil Mech. Found. Div.,ASCE*, 90 SM5), p.87-102.
- Iizuka, A. (1997): Significance of Reference and Initial Conditions in Elasto-Viscoplastic Settlement Prediction. *Tsuchi-To-Kiso JGS*, Vol.45, No.2, pp.11-14. (in Japanese)
- Iizuka, A and Ohta, H. (1987): A Determination Procedure of Input Parameters in Elasto-Viscoplastic Finite Element Analysis. *Soils and Foundations*, Vol.27, No. 3, pp.71-87.
- Karube, D. (1975): Unstandardized Triaxial Testing Procedures and Related Subjects for Inquiry. *Proc. 20th Symp. on Geotech. Eng.* pp.45-60.
- Kenney, T.C. (1959): Discussion on Proc. Paper 1732(Wu,1958). *Proc. ASCE*, Vol.85, SM3, pp.67-79.
- Lambe, T.W. and Whitman, R. V. (1969): *Soil Mechanics*. New York: John Wiley & Sons.
- Matsuo, K., Yamaguchi, Y. and Ohira, Y. (1986): Coefficient of Secondary Consolidation of Peats, *Soils and Foundations*, Vol.26, No.1, pp. 139-150. (in Japanese)
- Mesri, G (1973): Coefficient of Secondary Compression. *Proc. ASCE*, Vol.99, No.SM1,pp.123-137.
- Mesri, G. and Choi, Y.K. (1979): Discussion on “Strain Rate Behaviour of Saint-Jean-Vianney Clay” by VAID,Y.P. et.al.. *Can. Geotech. J.*, 16, pp.831-834.
- Mesri, G. and Godlewski, P.M. (1977): Time-and Stress-compressibility Interrelationship, *J. Geotech.Eng.Div.,ASCE*, 103(GT5), pp.417-430.
- Mesri, G. and Castro, A. (1987): C / C_c Concept and K_0 during Secondary Compression. *J. Geotech. Div.,ASCE*, Vol.113(GT3), pp.230-247.
- Morita, Y., Sasao K., Yasuhara K., Suzuki D. and Hirano T. (1988): Characteristics of the Long-term Consolidation of Over-consolidated Clay, *Proc. Symp. on the Special Consolidation Test*, pp.1-6. (in Japanese)
- Ohta, H. (1992): Chapter 4 Deformation of Soft Ground (71-142) in *Soft Ground -Theory and Practice-*. Tokyo: ed. by the Japanese Society of Soil Mechanics and Foundation Engineering.(in Japanese)
- Sekiguchi, H. (1983): Effects of Time on the Compressibility of Clay Skelton. *Proc. 18th Japan National Conference of Soil Mech. and Foundation Eng.*, pp.209-210. (in Japanese)
- Yasukawa, I and Kamon, M (1987): Effect of Loading Conditions on Secondary Consolidation of Cohesive Soils, *Soils and Foundations*, Vol.27, No.2, pp. 93-106, 1987. (in Japanese)

APPLICATIONS OF THE THEORY & INTERPRETATIONS OF THE DEPOSITIONAL ENVIRONMENT

4.1 Introduction

The examples of the applications of the theory to the field observations are given in this chapter together with the geological interpretation. The distributions of soil parameters in several sites are being estimated by means of the geological information such as boring logs and basic soil properties. The distributions of the age of soils are usually hard to obtain. In that case the age was assumed based on the printed papers. The depositional rate is assumed to be constant according to the results of the parametric study carried out in chapter 3.

Change of the depositional environment seems to give effects to the characteristics of soils. Examples of the characteristic differences of marine and freshwater clays are given in Table 4.1(after Kamon et al., 1995). *PI* represents the change of the depositional environment in this study because *PI* is one of the basic properties reflecting the difference in nature of clays. Geological analysis and its interpretation were also carried out in this chapter in order to explain how the depositional environment changed and gave the effect on the characteristics of natural clays.

Understanding the change of the depositional environment in the concerning location helps engineers to interpret the limited information such as boring logs. Several methods have been proposed in order to distinguish the depositional environment (e.g. Sato and Yokoyama, 1987; Horie et al. 1988; Ohtsubo, 1995; Fukusawa, 1997; Masuda, 1997; Kamei, 1997; Kitamura, 1998). Fig.4.1 shows schematic drawing how the understanding of the depositional environment is related to civil engineering. Microfossils analyses are very useful to reconstruct sedimentary environment from core samples. Because core samples are large enough to collect microfossils, but are too small to obtain megafossils such as molluscs. The existence of coccolith is an index of marine sediments and suggests that diagenetic alternation of the sample was negligible. The volume percentage of diatom remains is also very important to predict physical property. Table 4.2 is the lists of the methods to distinguish depositional environment of soil for civil engineers.

Table 4.1 Differences of marine and freshwater clays (after Kamon et al., 1995)

	Characteristics	Marine clay	Freshwater clays
Physical characteristics	Clay content	over 30% Mostly classified into clays, partially silty clays	20-30% Mostly classified into clayey silt, particle size distributes widely
	Activity	slightly high	slightly low
	Consistency	LL=50-130% PI=20-90 Highly plastic	LL=40-70% PI=15-40 Medium to highly plastic
	Unit weight	slightly light	slightly heavy
	Void ratio	slightly high	slightly low
Observation of outcrop	Color	dark grayish blue	bluish green, grayish green
	Breaking shape	Small shell shape tips Outcrop is easily collapsed	Large block Outcrop seems to be wall
	Educts	Yellow sulfur powder Needle-like gypsum	Vivianite (Fresh Vivianite is blue color and it turns to be brown)
	pH	2 - 5	6 - 8

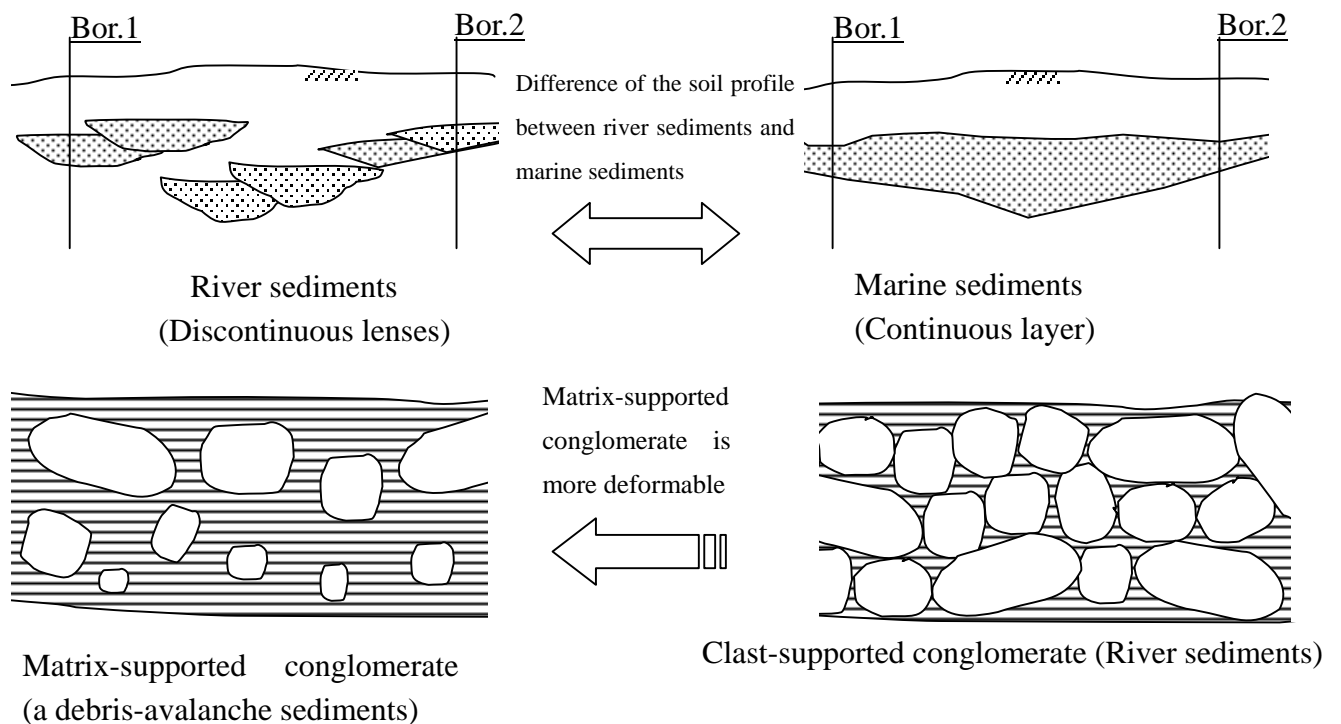


Fig.4.1 Examples of the importance of understanding depositional environment

Addition to the relationship between depositional environment and mechanical properties of clays, having the information of the depositional environment may help an engineer a lot (e.g. Kitamura, 1998). For example soil profile has to be prepared at the beginning of the planning, designing and analysis of any construction project. The quality of the soil profile dominates the success of the project. Accuracy of the analysis is also depending on the quality of the soil profile together with the accuracy of the soil parameters. Present soil formations are the results of the change of the depositional environment. The difference of the depositional environment is reflected to the facies of the sediments (Einsel, 1992).

Table 4.2 Lists of geological analysis

Geological analysis	Target material	Target information
Observation of core	Core sample	Facies fossils such as molluscs show depositional environment. Roots represent shallow water or on shore environment. Tephra can be a time marker.
Particle size	Particle size distribution curve foraminifer	Existence of water flow: Coarse particles are piled up under faster water flow. Fine particle such as silt or clay is piled up under no water flow.
Smear slide	Micro fossil (Diatom, Coccolith, Foraminifer)	Coccolith (CaCO_3) and Foraminifer (SiO_2) exist only in marine sediments. Different types of Diatom (SiO_2) species exist in marine, brackish and fresh water sediments.
Soft X-ray photograph	Soft X-ray photograph of Boring core	Laminae represents brackish environment
Electric conductivity	Stirred water with fine particles	Marine sediments show higher conductivity. Fresh water sediments show lower conductivity.
pH	Stirred water with fine particles	Marine sediments show lower pH. Fresh water sediments show higher pH.
XRF	Quantitative element analysis	Higher sulfur content represents marine environment.
C^{14} dating	C^{14} in organic material	C^{14} age

4.2 Meade’s void ratio (San Joaquin valley, California)

Fig.4.2 shows the estimated distribution compared with the field data reported by Meade (1963) and Velde (1996). Both of those data are the distribution of the void ratio in the field. The former data are taken at the east of the San Joaquin Valley, California, USA. The tendency of the depthwise distribution of void ration is that the deeper the depth, the larger the void ratio (Meade, 1963). The latter data are taken from deep-sea clay-rich deposit all over the world. Theoretical distributions are calculated by assuming w_n equals to w_L ($a = 1.0$) in Eq.(2.20). The age of deposits are assumed to be 2 Ma (2 million ages or 2 million years before present) at the depth of 500m, since the lower part of the San Joaquin which depth of 500m-600m is suppose to be a part of late Pliocene (San Joaquin formation).

All the data shown in Fig.4.2 are in the range of theoretical data where PI is in between ten to hundred. The data reported by Meade (1963) are shown in Figs.4.3 with the different scale from Fig.4.2. Meade describes that the distribution of the void ratio increases with increasing depth of burial. Meade also shows the results of chemical analysis (but no PI is shown) such as percentage of montmorillonite in clay fraction, adsorbed cation, pH together with diatom remains percentage of sediment and median diameter. The percentage of montmorillonite in clay mineral and adsorbed cation Na increases with increasing void ratio. Regarding the amount of clay fraction and activity, the more clay fraction (in this case clay means montmorillonite), the higher the PI (Skempton, 1953, Lambe and Whitman, 1969, see Fig.4.4). In addition to the montmorillonite and PI relation, the more Na in the adsorbed cation of montmorillonite, the higher the PI (Grim, 1962; Lambe and Whitman, 1969, see Table 4.3). Though there is no mention about PI in the Meade’s paper, it is reasonable to conclude that PI must increase with increasing depth burial.

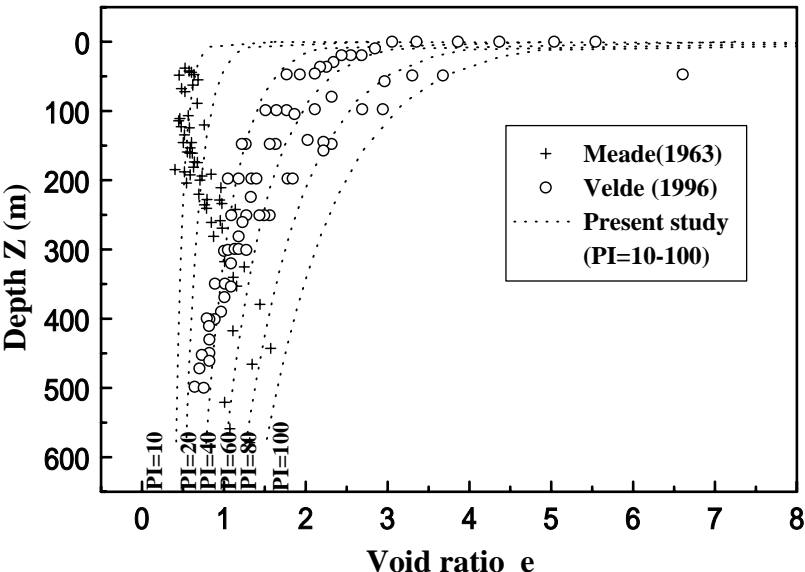
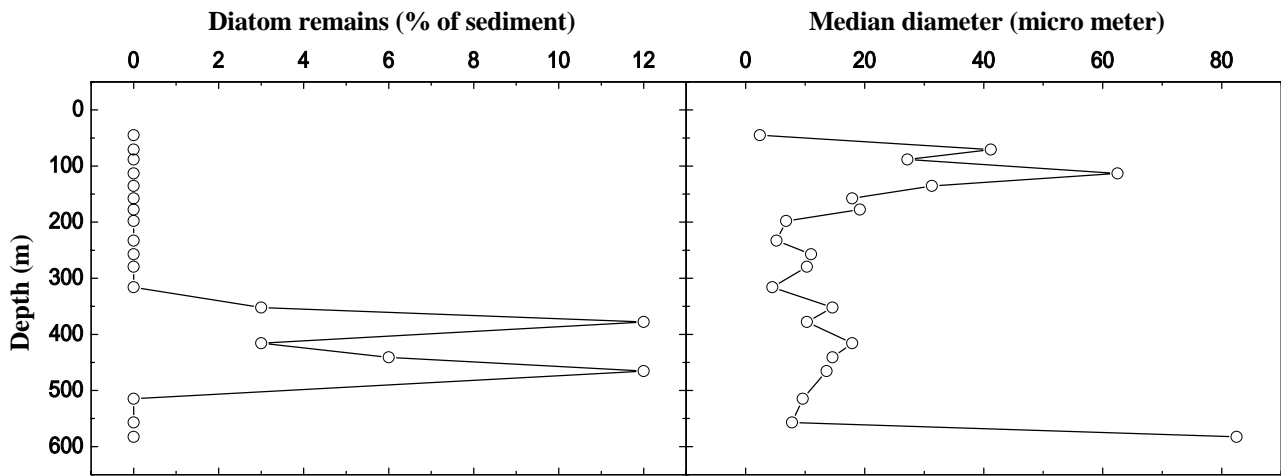
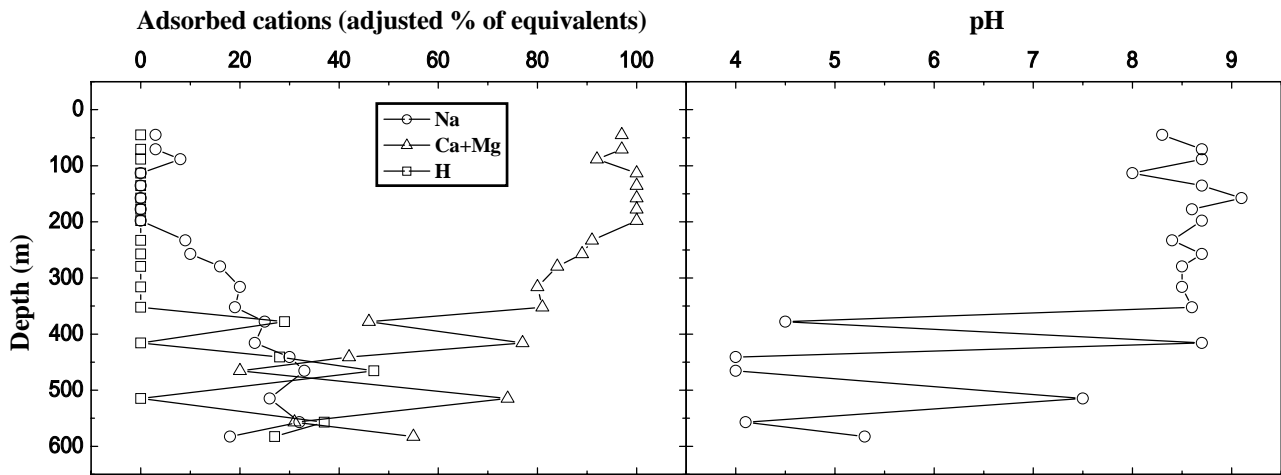
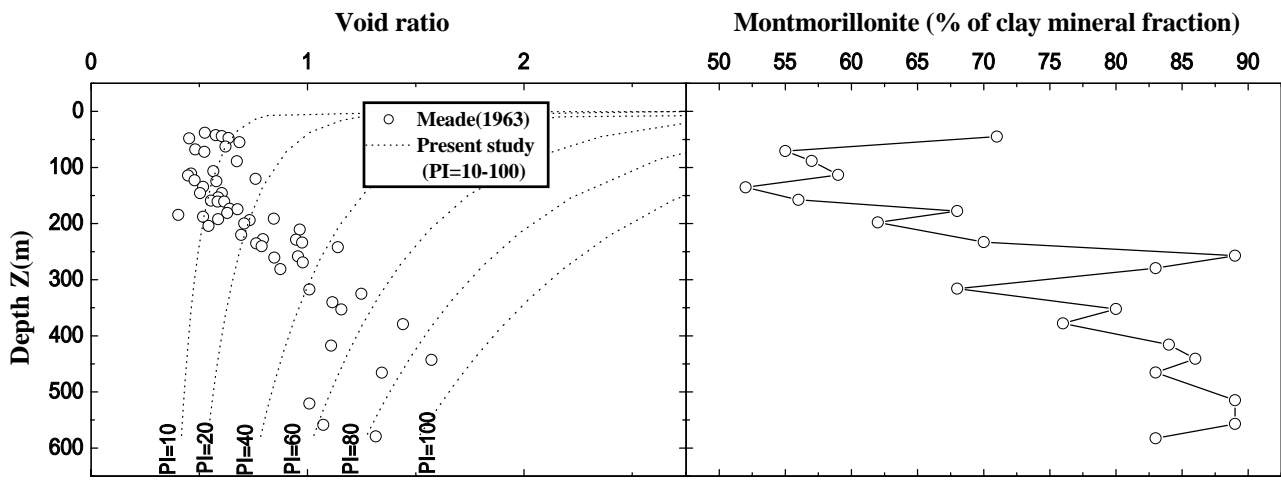


Fig.4.2 Comparison with the field observation by Meade (1963) and Velde (1996)

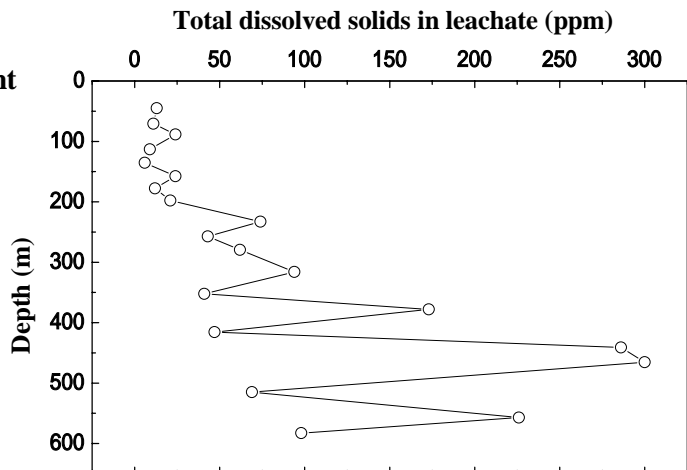


Geology & the change of depositional environment

Depth 0-230m Lenses of sand, silt, clay and gravel : alluvial

Depth 230-580m Siltstone with intercalated thin-bedded sands : mainly marine

Depth deeper than 580m Well sorted sand : marine



Figs. 4.3 Properties of sediments at San Joaquin valley, California(after Meade, R. H.,1963)

Table 4.3 Fraction and PI (after Lambe and Whitman, 1969)

Atterberg Limits of Clay Minerals					
Mineral	Exchangeable Ion	Liquid Limit (%)	Plastic Limit (%)	Plasticity Index (%)	Shrinkage Limit (%)
Montmorillonite	Na	710	54	656	9.9
	K	660	98	562	9.3
	Ca	510	81	429	10.5
	Mg	410	60	350	14.7
	Fe	290	75	215	10.3
	Fe ^a	140	73	67	—
Illite	Na	120	53	67	15.4
	K	120	60	60	17.5
	Ca	100	45	55	16.8
	Mg	95	46	49	14.7
	Fe	110	49	61	15.3
	Fe ^a	79	46	33	—
Kaolinite	Na	53	32	21	26.8
	K	49	29	20	—
	Ca	38	27	11	24.5
	Mg	54	31	23	28.7
	Fe	59	37	22	29.2
	Fe ^a	56	35	21	—
Attapulgitic	H	270	150	120	7.6

Data from Cornell, 1951.

^a After five cycles of wetting and drying.

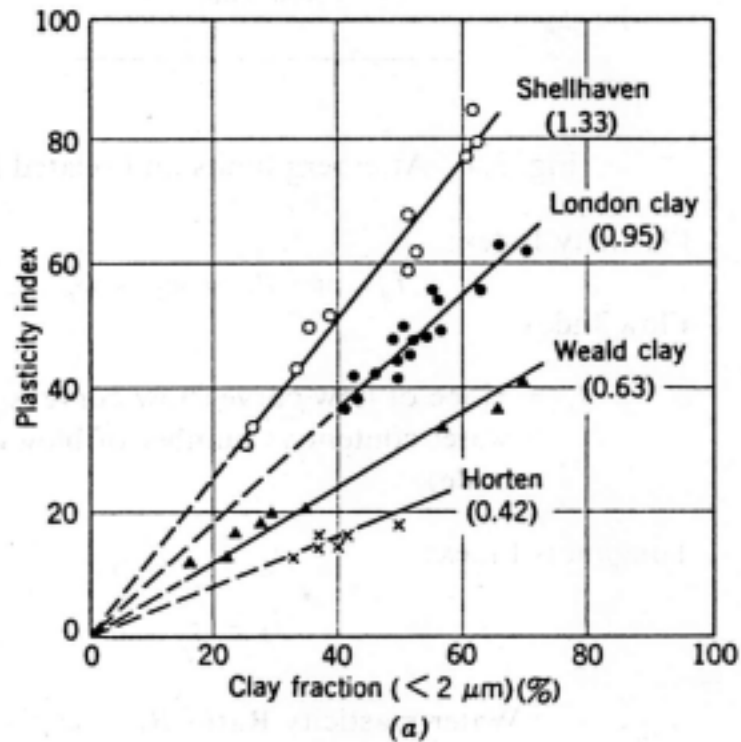


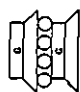
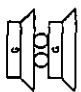


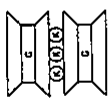
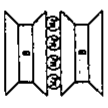
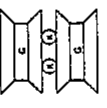

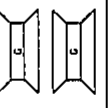
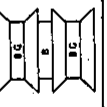


Fig.4.4 Clay mineral, adsorbed cation and PI (after Lambe and Whitman, 1969)

Mineral	Structure Symbol	Isomorphous Substitution (nature and amount)	Linkage between Sheets (type and strength)	Specific Surface (m^2/g)	$\frac{1}{\text{Charge Density}} (\text{\AA}^2/\text{ion})$	Potential Exchange Capacity (me/100 g)	Actual Exchange Capacity (me/100 g)	Particle Shape	Particle Size
Serpentine		none	H-bonding + secondary valence			1	1	Platy or fibrous	
Kaolinite		Al for Si 1 in 400	H-bonding + secondary valence	10-20	83	3	3	Platy	$d = 0.3 \text{ to } 3 \mu\text{m}$ thickness $= \frac{1}{3} \text{ to } \frac{1}{10} d$
Halloysite ($4H_2O$)		Al for Si 1 in 100	Secondary valence	40	55	12	12	Hollow rod	OD = $0.07 \mu\text{m}$ ID = $0.04 \mu\text{m}$ L = $0.5 \mu\text{m}$
Halloysite ($2H_2O$)		Al for Si 1 in 100	Secondary valence	40	55	12	12	Hollow rod	OD = $0.07 \mu\text{m}$ ID = $0.04 \mu\text{m}$ L = $0.5 \mu\text{m}$
Talc		none	Secondary valence			1	1	Platy	
Pyrophyllite		none	Secondary valence			1	1	Platy	

Sheet silicate minerals.

Table 4.4 Clay minerals (1/2), after Lambe & Whitman (1969)

Muscovite		Al for Si, 1 in 4	Secondary valence + K linkage		250	5-20	Platy	
Vermiculite		Al, Fe, for Mg Al for Si	Secondary valence + Mg linkage	5-400	150	150	Platy	$t = \frac{1}{10}d$ to $\frac{1}{30}d$
Illite		Al for Si, 1 in 7 Mg, Fe for Al Fe, Al for Mg	Secondary valence + K linkage	80-100	150	25	Platy	$d = 0.1$ to $2 \mu\text{m}$ $t = \frac{1}{10}d$
Montmorillonite		Mg for Al, 1 in 6	Secondary valence + exchangeable ion linkage	800	100	100	Platy	$d = 0.1$ to $1 \mu\text{m}$ $t = \frac{1}{100}d$
Nontronite		Al for Si, 1 in 6	Secondary valence + exchangeable ion linkage	800	100	100	Lath	$t = 0.4$ to $2 \mu\text{m}$ $t = \frac{1}{100}d$
Chlorite		Al for Si, Fe, Al for Mg	Secondary valence + brucite linkage	5-50	20	20	Platy	

Sheet silicate minerals.

Table 4.5 Clay minerals (2/2), after Lambe and Whitman(1969)

The differences of the characteristics of clay according to the depositional environment seem to be related to the size and the structure of clay minerals (Table 4.4 and 4.5). Sulfide might play a role in destruction of the mineral structure and leaching of Ca or Mg of montmorillonite during the weathering (Grim, 1953; Ichihara, 1960).

Meade (1963) concluded that the distribution of the void ratio in San Joaquin is related to the distribution of median of diameter, percent adsorbed Na and electrolyte concentration. And he mentioned that the skeleton of the diatom contributes significantly to the pore volume as his impression. According to Meade (1963) the change of the depositional environment at San Joaquin is as follows:

- 0-230m: Lenses of sand, silt, clay and gravel (alluvial)
- 230-580m: Siltstone with intercalated thin-bedded sands (mainly marine)
- deeper than 580m: Well sorted sand (marine)

The distribution of pH seems to support that the lower part of the formation is marine sediments. On the other hand the upper part of the formation seems to be fresh water sediments. Moreover, since the upper part of the medium diameter of the sediments is becoming larger than the lower ones, the depositional environment seems to have changed from the environment without current to with current. Therefore, it seems reasonable to conclude that the depositional environment changed sometime in the period of sedimentation from marine to fresh water. Consequently the plasticity of sediments changed from high to low. Thus the distribution of void ratio increases with increasing depth of burial. The change of the depositional environment could be confirmed by the geological analysis mentioned in 4.3.

The value of σ' and σ is supposed to be stress dependent (e.g. Mesri, 1973). σ' and σ during the consolidation must be considerably smaller than the value at the sedimentation. The parameters for the present theory are assumed to be constant in spite of the depth and the age of clays in this study in order to make the theory easier and simpler as much as possible. Thus the value of σ' and σ in this study might be larger than true value through the sedimentation. On the other hand the ratio σ'/σ in this study seems to be reasonable because the ratio σ'/σ are supposed to be independent of the stress (e.g. Mesri, 1973). Moreover there is little study on the stress dependency of the parameter σ (or $\sigma = 1 - \sigma'/\sigma$). Further study on the parameters concerning with the stress dependency is needed.

4.3 Shiunji lagoon (Northeast of Niigata)

Many lagoons are recognized behind sand dune in the Echigo Plain, Niigata, central Japan. Shiunji lagoon and was one of them and was located in Kajikawa village where is northeast of Niigata City. Shiunji lagoon was a fresh pond with an area of 36 km², a water depth of about 6 meters. Shiunji Lagoon has been reclaimed by 1733. The tidal range around the Echigo Plain is 20 cm.

The test results (see Appendix.1) and boring core are obtained through the courtesy of Japan Highway Public Corporation. The sediments of boring core is divided into three parts. The lower part is gravelly sediment. The middle part represents fining-upward succession and the upper part indicates coarsening-upward lithologies.

The burial distributions of the mechanical properties of alluvial formations are estimated based on PI and age of the formations the estimation chart proposed in this study. Geological analysis was carried out and the changes of the depositional environment are explained. Fig.4.5 indicates the flowchart of the geological analysis of the boring core of B1-71.

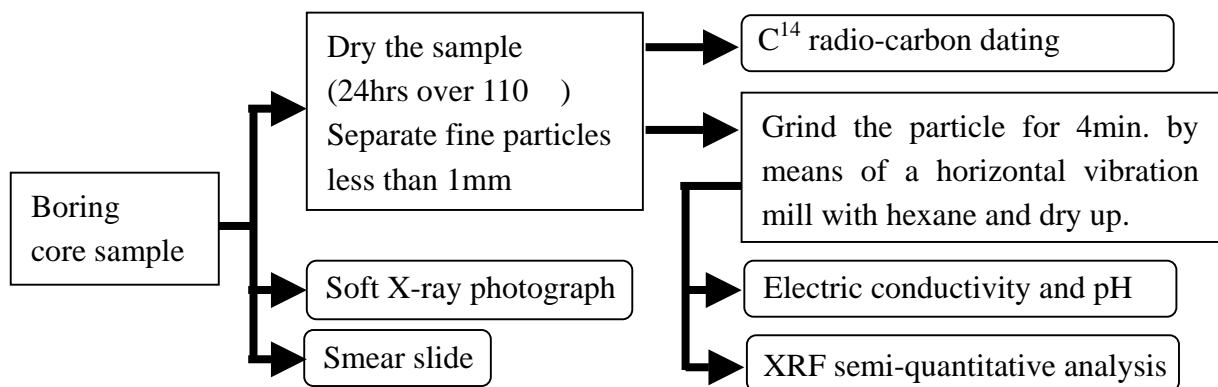


Fig.4.5 Flowchart of the geological analysis in section 4.3

4.3.1 Location and Boring log

Fig.4.6 indicates the location of Shiunji lagoon. The boring log B1-71 is shown in Fig.4.7. Fine fraction increased from the bottom of the sand with silt at the depth of 34m of B1-71. Silty clay at the depth of 26m to 16m contains fine fraction the most.



**Fig.4.6 The location of Shiunji lagoon
 (URBAN KUBOTA, No.17, p51, 1979)**

Depth (m) [Altitude T.P.+(m)]	Symbol	Soil component	Sample number	Fraction %				Liquid limit W _L %	Plastic limit W _P %	Natural water content W _n %	C14 Age
				Clay	Silt	Sand	Gravel				
				20	40	60	80				
4.26		Sandy	P-1								
7.80		Silt	P-2								
2.26		Peaty	P-3								
4.40		Silt	P-4								
-0.14		Sand	P-5								
			P-6								
-4.74		Peat	P-7								
			P-8								
-5.04		Sand with	P-9								
11.20		Silt	P-10								
-6.94		Silt	P-11								
			P-12								
15.50		Silty Clay	P-13								
			P-14								
-11.24		Silty Clay	P-15								
			P-16								
			P-17								
26.30		Silt with Sand	P-18								
			P-19								
-22.24		Sand with Silt	P-20								
			P-21								
32.15		Sand with Silt	P-22								
			P-23								
-27.89		Sand & Cg	P-24								
			P-25								
34.60		Sand & Cg	P-26								
			P-27								
-30.34		Sand & Cg	P-28								
			P-29								
39.12		Sand & Cg	P-30								
			P-31								
-34.86		Sand & Cg	P-32								
			P-33								

Fig.4.7 Boring data B1-71 (G.L.=T.P.+4.26m)

4.3.2 Smear slide

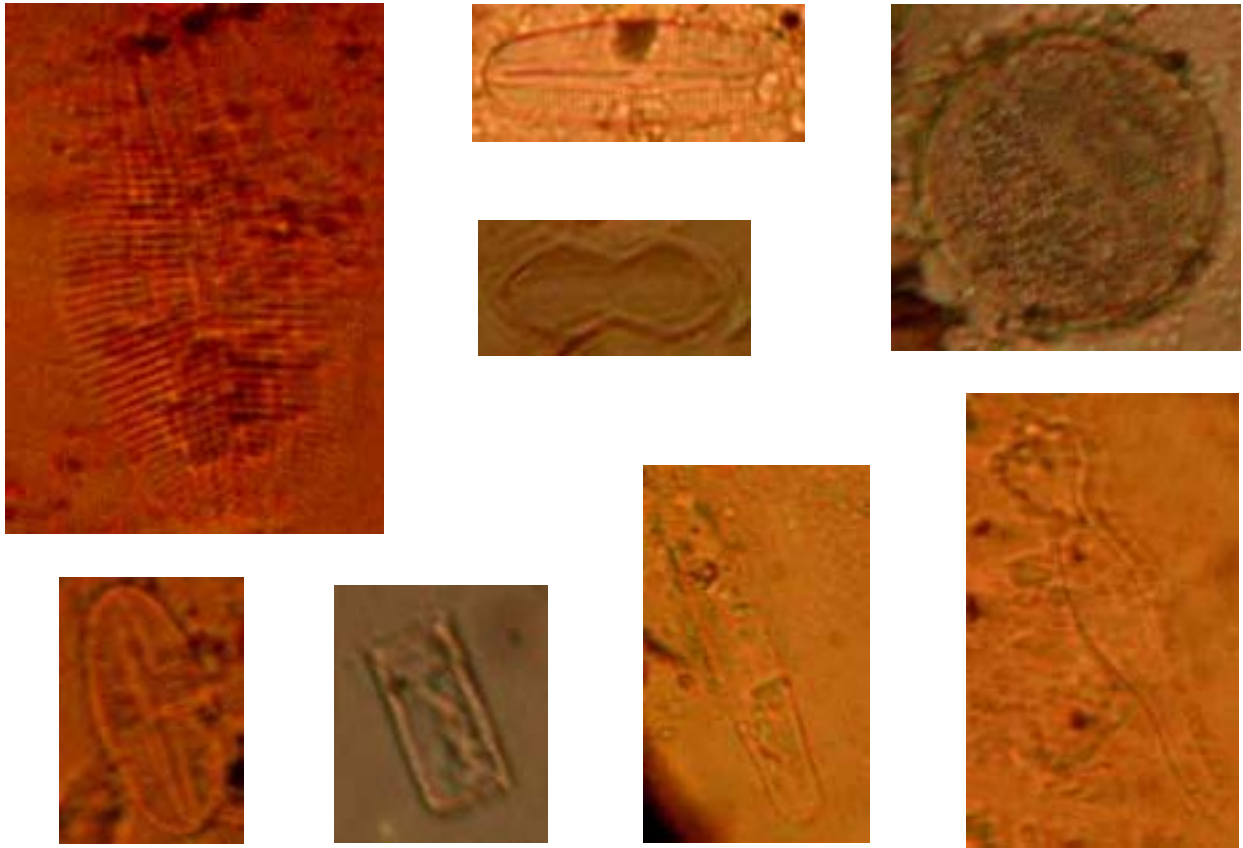
Smear slide is one of the basic methods to observe the soil particle directly under the microscope. The size and the volumetric percent of particles can be checked roughly by means of the smear slide (Photos.4.1). Microfossils of the diatom or coccolith can be the marker showing the depositional environment.

The preparation of the smear slides is as follows:

- (1) Wiping the slide glass and cover glass.
- (2) Picking up the small amount of the sample with the tooth stick. The tooth stick must be changed sample by sample in order to prevent contamination of the samples.
- (3) Smear the sample on the slide with one or two drops of the distilled water.
- (4) Drying up the slide on the Hot plate.
- (5) Putting one or two drops of enclosure on the slide.
- (6) Setting the cover glass on the sample.
- (7) Drying until the enclosure hardened completely on the horizontal table.
- (8) Observe the smear slide under the microscope.

The difference of the depositional environment can be expected by means of the microfossil such as diatom, coccolith and so on. Unfortunately judging and distinguishing the species of the microfossil are so difficult that one has to ask a professional for that. For example a professional of the microfossil memorize several thousands of species or more. However it is still important for engineers to observe particles of sediments and at least one can observe if the sediments contain microfossil or not. Also an engineer can observe the mineral contained roughly and can check the shape of the particles. Photos.4.1 shows the typical photograph of smear slides under the microscope.

Microscopic observation of the smear slides of B1-71 and B1-69 was carried out by Dr. A. Kitamura (Associate professor, Department of Geoscience, Shizuoka University) in order to check micro fossils. Fig.4.8 shows the distribution of the areal percentages of Diatom against burial depth. There is a peak of the areal percentages of Diatom at the depth of 16m-20m (T.P.-11.74m-T.P.-15.74m). Note that no Foraminifer or Coccolith was observed in the smear slides. Generally speaking both Foraminifer and Coccolith exist only in marine environment. On the other hand Diatom exist in fresh, brackish and sea water. Therefore it is inferred from the observation of the smear slides to suppose that the depositional environment at the depth of 16m-20m (T.P.-11.74m-T.P.-15.74m) was not marine environment but freshwater or brackish water environment.



Photos.4.1 Photographs of several kinds of Diatom in the smear slides of B1-69 & B1-71 under microscope (x2.0 of the photos. x400)

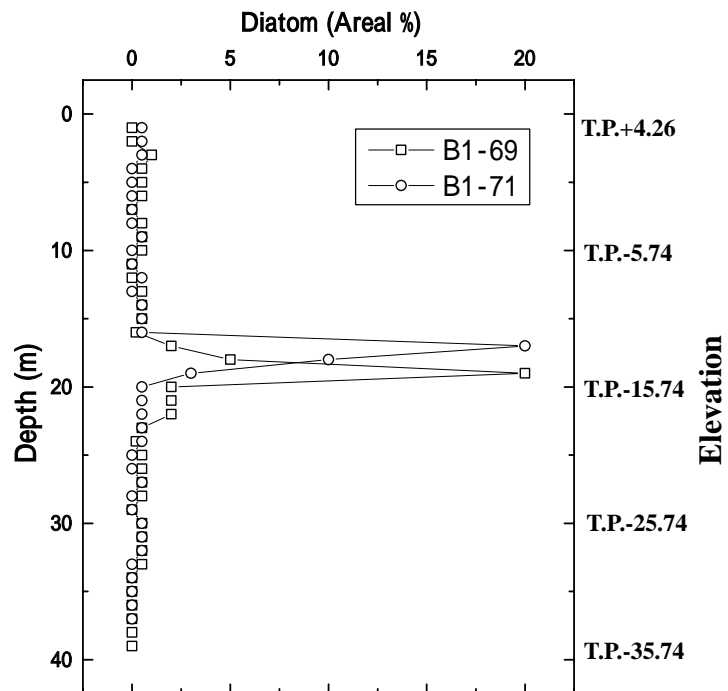


Fig.4.8 Burial depth distribution of the areal percentages of diatom in the smear slides

4.3.3 Soft X-ray photograph

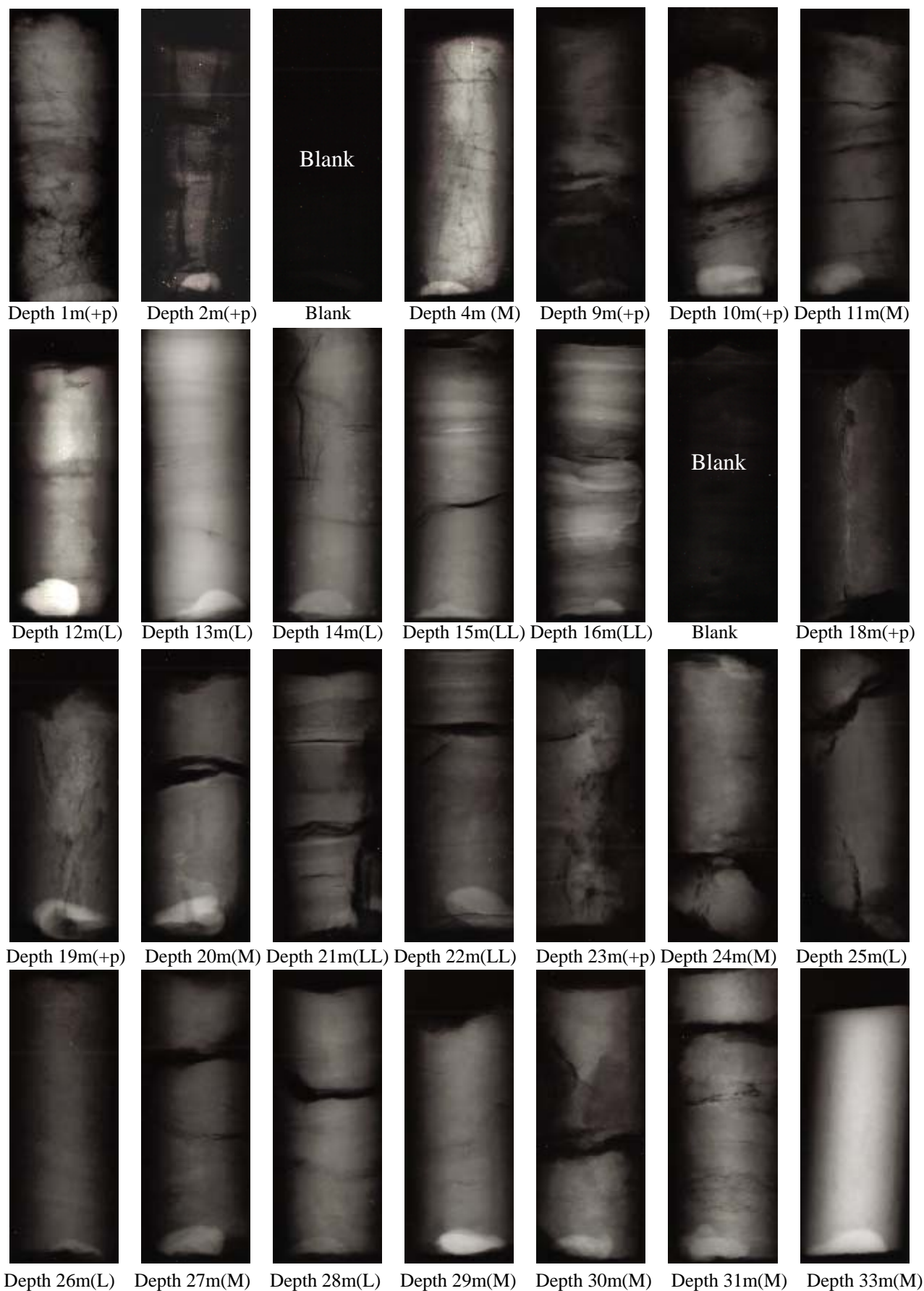
Soft X-ray photograph is a method to investigate the inner structure of boring core by means of the soft X-ray. For the study of the aged clay thin stripe of the core sample called 'laminae' is important. For many reasons, lake water tends to become stratified either permanently or seasonally. Permanent stratification is characteristic of lakes in which the bottom water is more saline than surface water. Consequently, the bottom water can become completely stagnant and be depleted in oxygen. Such condition is maintained for a long time period, laminated mud rich in organic matter can accumulate. Thus the laminae is the proof that the soil is deposit under the brackish-water environment such as lagoon (e.g. Einsel, 1992; Kitamura, 1995). Soft X-ray photographs of the core sample of Shiunji lagoon were taken at the department of Geoscience of Shizuoka university

The method of taking a soft X-ray photograph is as follows:

- (1) Setting a sensitive film paper in the plate
- (2) Putting 35 mm core samples on the plate by means of the plastic material so that the samples are fixed in the Soft X-ray photographic machine. Note that it is not necessary to take the sample core out of the plastic case. Do not put the sample core upside down.
- (3) Putting the sample on the plate into the soft X-ray photographic machine.
- (4) Setting the strength and the emission time (50kV, 4.5mA and 270sec.). Then take the X-ray photograph. Note down the name of the sample core and film number together with the emission time.
- (5) Developing and fixing the film in the dark room.
- (6) Drying up the film paper.

The soft X-ray photographs of the boring No. 71 of Shiunji lagoon are shown in Photos.4.2. The structures such as laminae in the core of the soft X-ray photographs cannot be observed by naked eyes because of the disturbance, slurry and mold. The laminae in the core represent the brackish depositional environment. Note that it is possible for us to take soft X-ray photographs and distinguish lamina structure of old and dried samples even covered with mold. Additionally the samples need not to be taken out from the core cases.

Clear laminae are observed at the depth of 15m, 16m, 21m and 22m, which are marked 'LL' in Photos.4.2. Weak laminae are observed at the depth of 12m, 13m, 24m, 25m, 26m and 28m, which are marked 'L' in Photos.4.2. Two blanks in Photos.4.2 are peaty material, which can be distinguished by naked eyes easily. Therefore Soft X-ray photos are not taken. The samples contain peaty materials partly are marked '+p' in Photos.4.2, which are at the depth of 1m, 2m, 9m, 10m, 18m, 19m and 23m. Massive, Dense homogeneous samples without laminae are marked 'M' in Photos.4.2, which are at the depths of 4m, 24m, 27m, 29m, 30m, 31m and 33m.



Photos.4.2 Soft X-ray photographs of Bor. B1-71 (G.L.=T.P.+4.26m)

4.3.4 Electrical conductivity and pH

pH and electrical conductivity (E/C) of the stirred water indicate the depositional environment (e.g. Yokoyama and Sato,1987; Sato and Yokoyama,1992). Yokoyama and Sato (1987, 1992) reason out the relation of the depositional environment and the plot of pH and E/C with the help of microfossil analysis. According to the study of Yokoyama and Sato (1987, 1992), high pH with low E/C represents fresh water environment, low pH with high E/C represents marine water environment, medium pH with relatively low E/C represents brackish water environment (Fig.4.9 and Table 4.6).

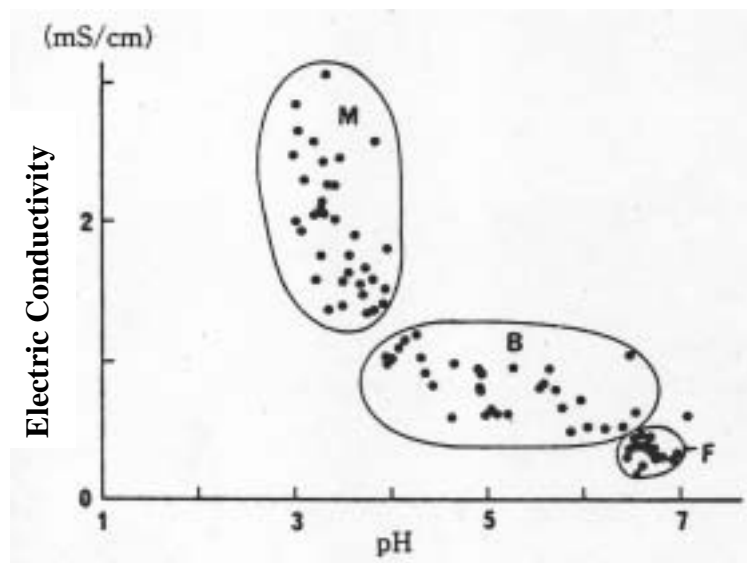


Fig.4.9 Relation of pH and E/C of the stirred water (after Yokoyama and Sato, 1987)

Table 4.6 Depositional environment with pH and E/C (after Yokoyama and Sato, 1987)

	SEC—Core			1400 m—Core
E/C (mS/cm)	Marine Clay 1.3-3.0	Brackish Clay 0.4-1.2	Fresh Clay 0.2-0.4	Fresh Clay 0.2-0.3
pH	3-4	4-6.5	6-7	7-8

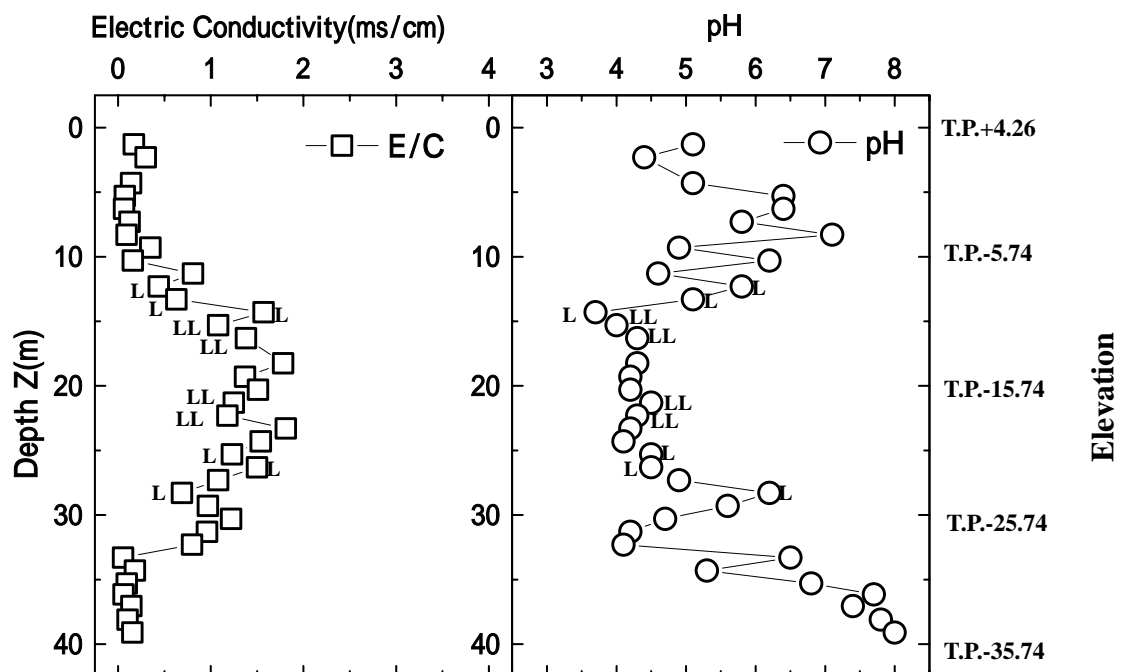
Measurement of the pH and E/C of the stirred water of the core sample taken from Shiunji lagoon, northeast Niigata are carried out. Fine particles are separated by means of sieve in order to obtain the good response of sand or even the matrix of the conglomerate. The procedure of the measurement is as follows:

- (1) Drying up the sample with the temperature of 110 for 24 hours.
- (2) Taking out fine particles which diameter are less than 1mm by means of sieve in order to obtain the good response of sand or even the matrix of the conglomerate.
- (3) Crashing the sample by means of horizontal shaking mill for 4 minuetts with hexane.

- (4) Drying up the sample with the temperature of 110 for 24 hours.
- (5) Measuring 10.0g of the sample and putting it into a beaker with 120 ml of the distilled water
- (6) Stirring 3 minutes by means of a stirrer
- (7) Measuring the pH and E/C one-hour after the stirring.
- (8) Repeating the same procedures as (6) and (7) five days later.

The results of the measure were shown in Figs.4.10 and 4.11. The depthwise distribution is obtained continuously even if the formation is sand or the matrix of the conglomerate. This is because of the separation of the fine particle from the sand and the conglomerate. The possibility of the application of pH and E/C to the sand and conglomerate can be proposed because the same tendency of the change of the depositional environment was obtained by the depthwise distribution of sulfur (see section 4.3.5). The depthwise distribution of sulfur obtained by means of XRF is shown in the following section.

According to the information obtained from Photos 4.2, Figs.4.10 and Fig. 4.11, the depositional environment changed from fresh water to brackish water at the depth of 32m to 12m then went back to fresh water up to now. The environment changed to be brackish but it might not to be marine environment because of the existence of laminae in the core and the value of pH stopped at around 3.75-4.0, which is about the upper limit pH of marine environment.



Figs.4.10 Distribution of pH and E/C of the stirred water of Shiunji lagoon, Niigata
LL: Clear laminae, L: Laminae. Neither pH nor E/C is measured because of the lack of the sample at the depth of 3m.

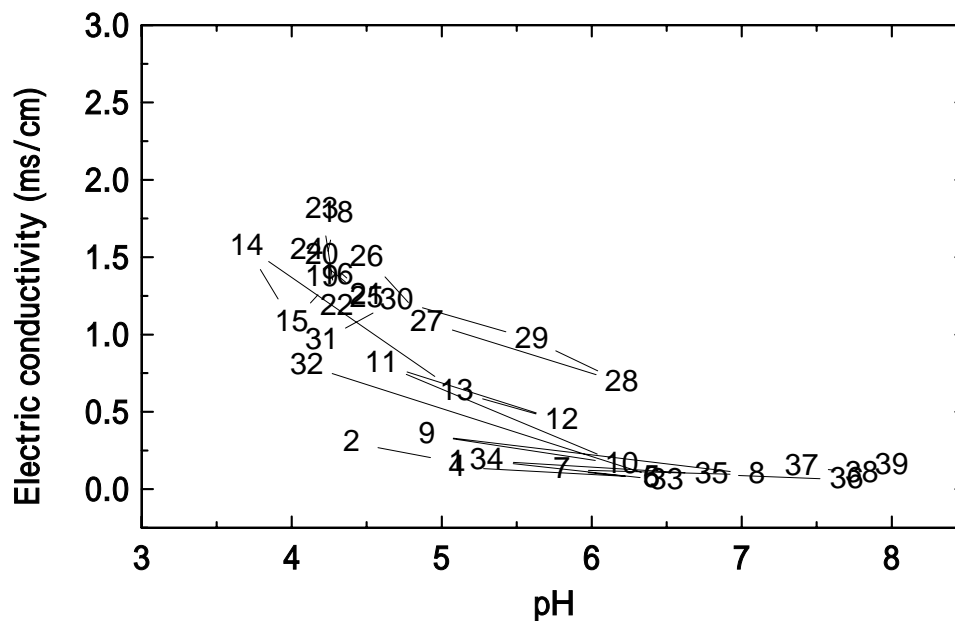


Fig.4.11 Relation of pH and E/C of the stirred water of Shiunji lagoon, Niigata
Numbers in the graph represent the depth of the measured sample(G.L.=T.P.+4.26)

4.3.5 XRF analysis

The quantitative element analysis by means of X-ray Fluorescence (XRF) was carried out by means of PW2404 (Philips) at the research corporation section of Tokyo Institute of Technology. The quantitative element analysis by XRF is available for almost all the elements except light elements such as carbon, hydrogen, nitrogen, oxygen, fluorine, boron and beryllium.

In order to carry out quantitative element analysis, standard samples were analyzed first. Those standards are prepared by Japan Geological Society. The standards used in this study are JH-1, JR-3, JMn-1, JSy-1, JGb-2, JLk-1 and Jh-1. The tables of the chemical analysis of standard samples proposed by JGS are shown in Appendix.2. Calibration curves of main and minor elements are shown in Appendix.2. All the calibration curves are linear and the quantity of the standards covers the range of the results of the boring sample analysis. The lists of the calibration curves are shown in Appendix.2.

Preparation of the samples is as follows:

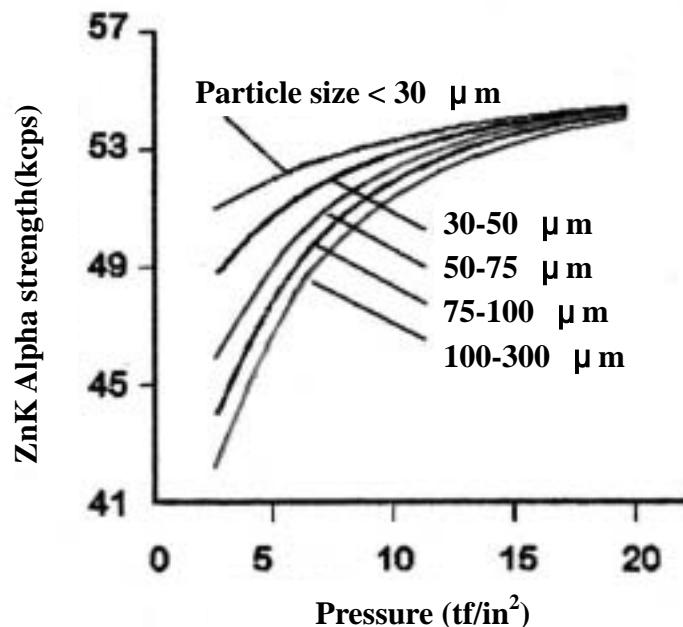
- (1) Drying the sample with the temperature of 100 for 24 hours.
- (2) Separating the fine particles less than 1mm by means of sieve.
- (3) Crashing the particles by means of horizontal shaking mill for 4 minutes with hexane.

- (4) Drying the sample with the temperature of 100 for 24 hours.
- (5) Packing 5g of the sample powder into the 27mm vinyl chloride ring.
- (6) Setting the sample powder in between the dice.
- (7) Pressing the packed sample powder under the 30tf of axial force for 1 minuets.
- (8) Unloading the press slowly.
- (9) Making the calibration line of the standard samples.

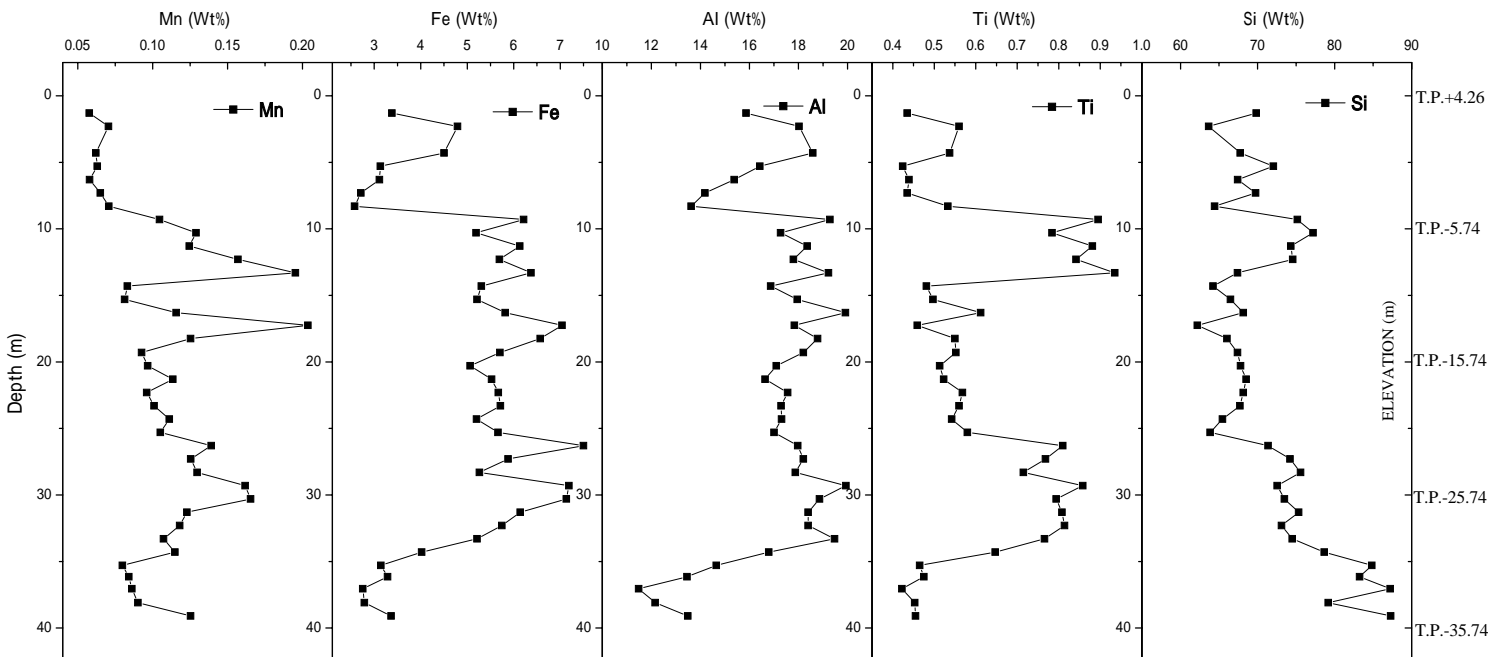
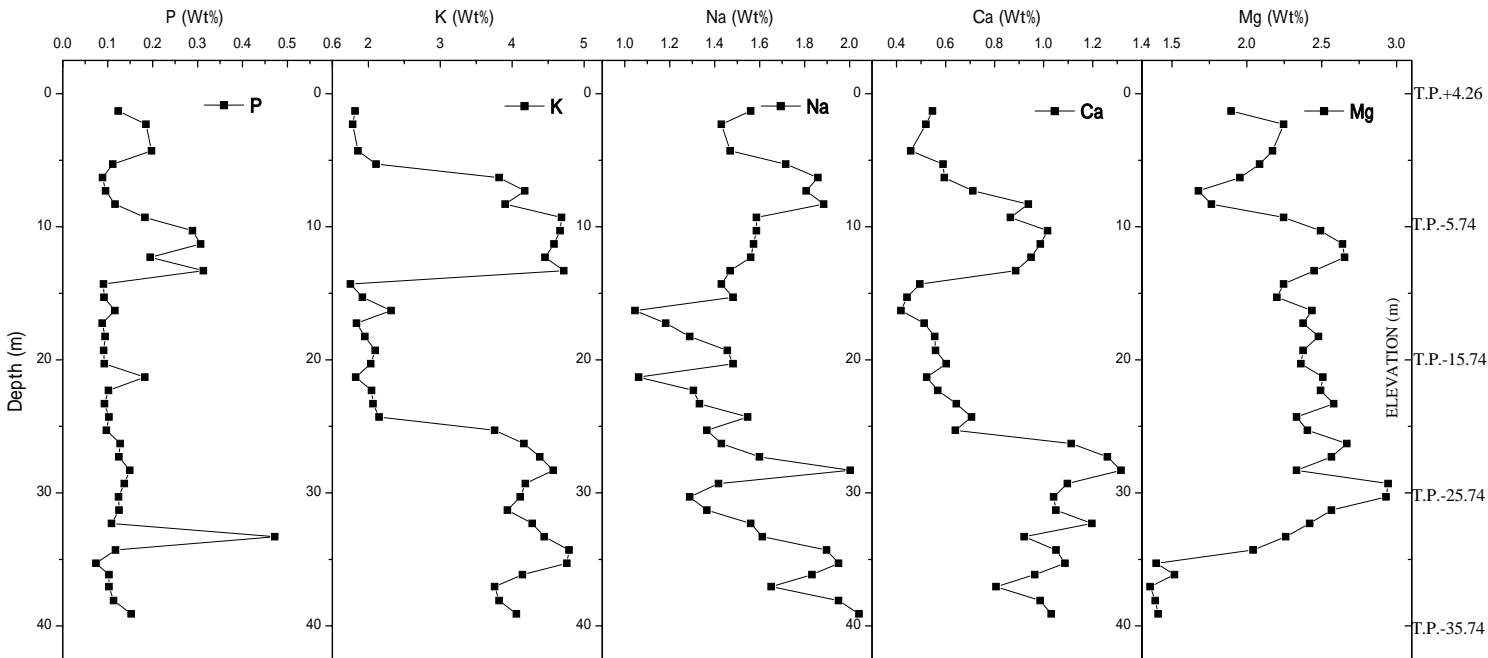
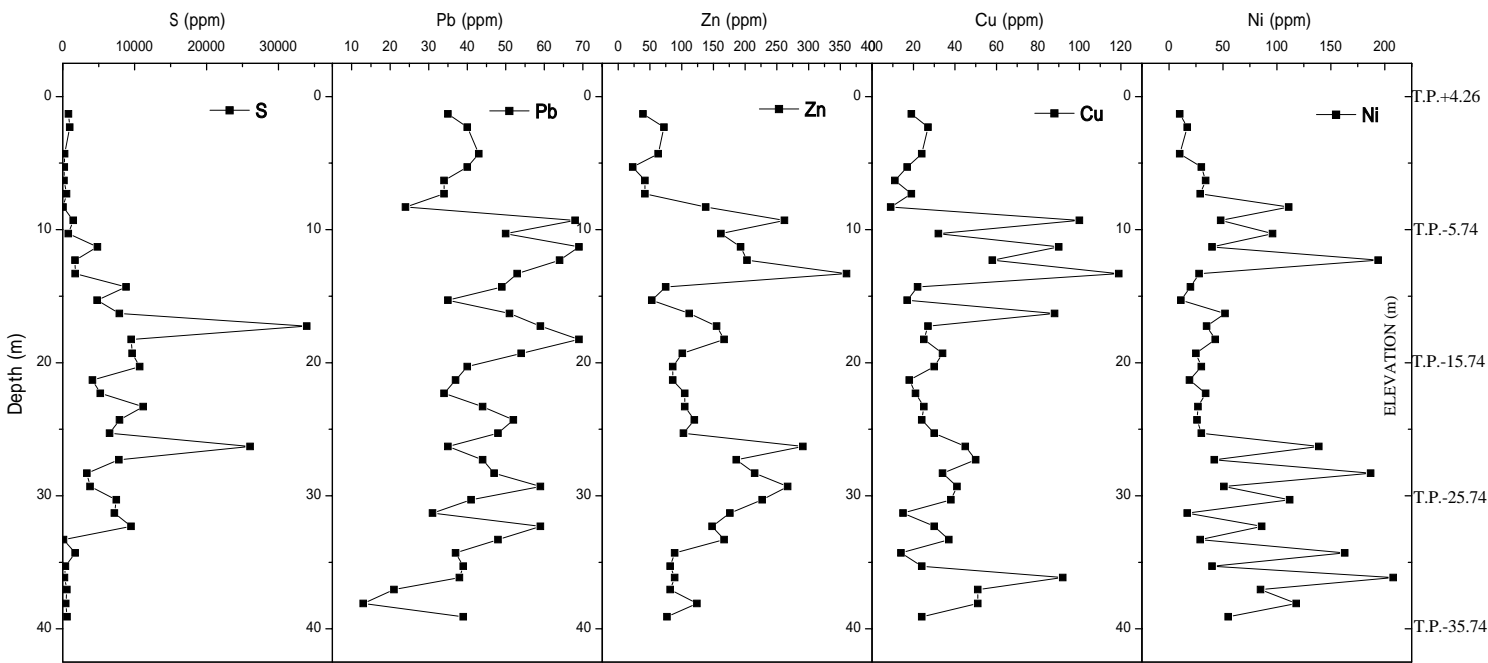
Both obtaining fine particle of the sample and pressing the sample under enough axial force are important for the analysis (Fig.4.12). Several cases are carried out in this study and finally 4 min. of crashing and 30 tf (it is about 424 MPa) of axial force are chosen.

Fig.4.13 is the results of the semi-quantitative XRF element analysis of the boring B1-71 of the Shiunji lagoon sample. The distribution of sulfur shows that the contents of sulfur increase between at the depth of 34m and 10m. Because the contents of sulfur in saline water is over 500-1000 times of that in fresh water (e.g. Horibe and Tsubota, 1977; Nakai et al., 1982; Kamei et al., 1997).

The relation between other elements and depositional environment are not so clear so far. Because the phenomena is so complex that it is not enough to explain only by means of the contents of elements. It seemed to be required the information of the status of molecule and ion together with the information about organic material (e.g. Kamei et al., 1997).



**Fig.4.12 Particle size, axial force vs. count of an element
(Internal document of PHILLIPS, 2000)**



Figs.4.13 The results of the quantitative XRF analysis of boring No.71 of Shiunji lagoon

4.3.6 Radiocarbon dating

5 samples were then dated using an accelerator mass spectrometry. The measurements are ordered to BETA ANALYTIC INC. in U.S.A. via GEO-SCIENCE LABORATORY. The results of the radio carbon dating are as follows:

Table 4.7 Results of the radio carbon dating

Depth (m)	Altitude T.P.+(m)	Material	14C AGE		Method	Code number
			(yBP)	1		
9.0	-4.74	Wood	5,280	50	AMS	Beta-148183
16.0	-11.74	Peaty clay	11,270	60	AMS	Beta-148182
24.0	-19.74	Peaty clay	9,800	40	AMS	Beta-152326
25.0	-20.74	Plant stalk	5,170	40	AMS	Beta-148181
25.0	-20.74	Peaty clay	10,100	40	AMS	Beta-152327

Measured age before 1950 setting the half time equals to 5568 years. AMS stands for Accelerator Mass Spectrometry.

According to the radio carbon dating, the age of the soil at the depth of 25.0 m is between 5,000-10,000 years BP. These measured ages correspond to 2.5-5.0 mm/y of the apparent depositional rate. It seems that true depositional rate in this area is supposed to be about 5.0-15.0 mm/y (true depositional rate is assumed to be 2-3 times of the apparent depositional rate which is 2.5-5.0 mm/y), which is relatively fast as a depositional rate compared with printed data (e.g. Skempton, 1970; Locat and Lefebvre, 1985; Tsuchida, 1999). True depositional rate supposed to be around 1.0-10.0mm/y for alluvial soil. I interpret that samples with older ages are reworked. If this is correct, average true depositional rate regard as 5.0 mm/y. Although the age of the bottom of B1-71 at the depth of 39m cannot measured because of the lack of the organic material in the core, it is assumed to be 8,000 years B.P. at the bottom of the B1-71 in this study. Note that the assumed age is corresponding to 5,170 years B.P. at the depth of 25.0m shown in Table 4.7.

The wide range of the measured age of sample cores is supposed to be because of the differences of the organic materials. For example wood sample might be at the center of the big tree or might be near the skin of the small wood. In that case the range of the age obtained by the measurement is not always the same as the depositional age.

4.3.7 Change of depositional environment and estimated properties

According to the geological analysis, the change of the depositional environment is explained as follows (Note that averaged age is use in this section):

(1) 8,200-6,700 years B.P. (at the depth of 39m-32m, T.P.-34.74m-T.P.-27.74m):

Conglomerate supposed to be the mouse of the river. In this time sea-level already started to be rising up. Then the deposits changed from conglomerate to sand. As the result the fine fraction increased

(2) 6,700-3,100 years B.P. (at the depth of 32m-15.5m, T.P.-27.74m-T.P.-11.24m):

The depth of the location became deeper. The rate of the water flow became very slow or almost nothing because the deposits turned to be silt and clay. These observations of boring data can be explained by the growth of the sand spit forwards. By the time of 6,700 years B.P. the forwards sand spit seemed to generate a lagoon.

By this time the location might be changed to be brackish lagoon rather than a mouse of the river according to the laminae of the soft X-ray photo. The contents of sulfur measured by XRF analysis and pH-E/C measurements show the same tendency. The value of *PI* was increased as the change of the depositional environment.

(4) 3,100-1,000 years B.P. (at the depth of 15.5m-4.4m, T.P.-11.24m-T.P.-0.24m):

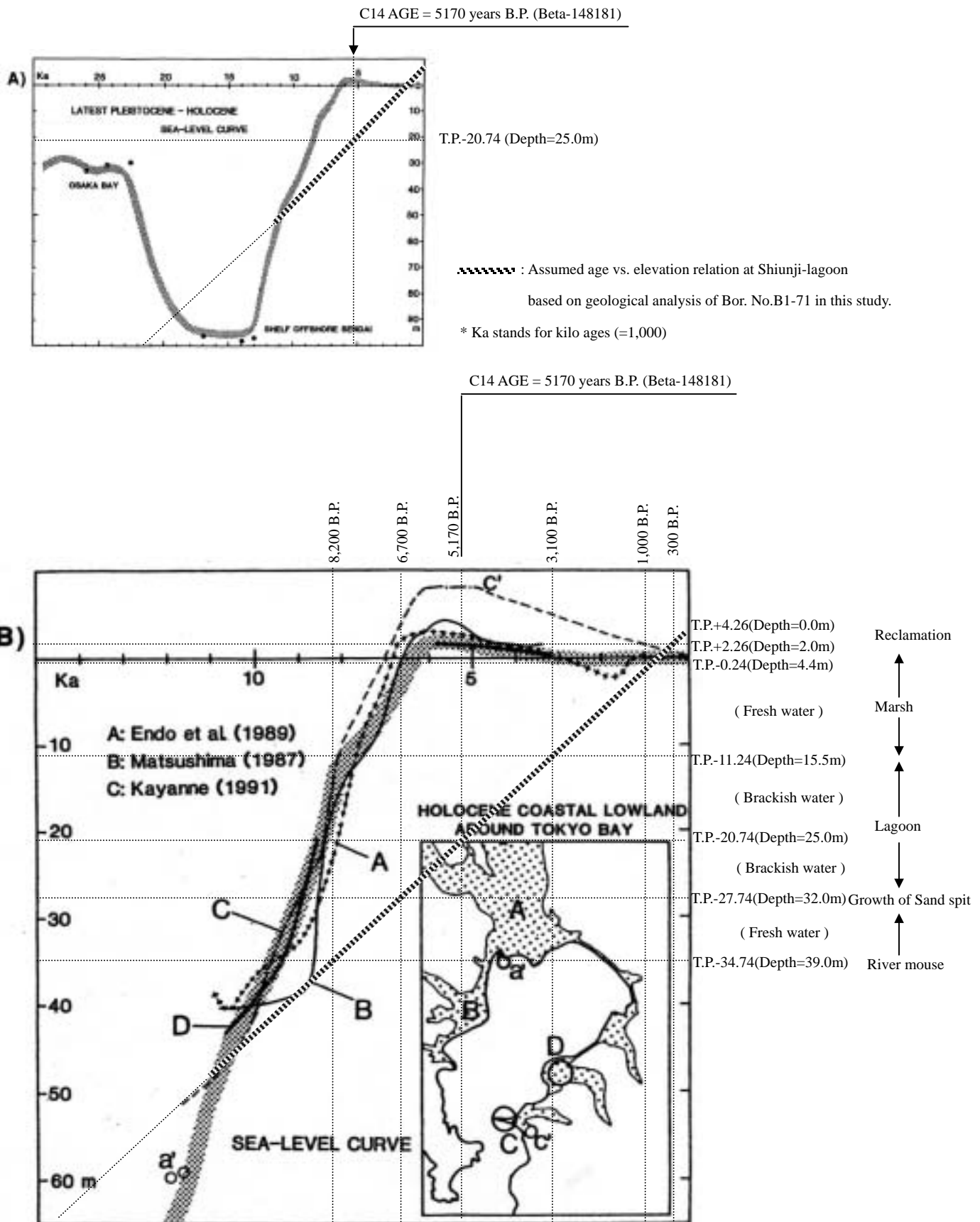
The sea-level movement stopped or decreased the rising rate. The particle size of the deposit gradually became larger from the clay to sand. It seems the depth of the water became decreased according to the existence of the roots, stalks and leaves of the plant increased. The brackish lagoon turned to be a fresh water marsh.

(5) 1,000-300 years B.P. (at the depth of 4.4m-2.0m, T.P.-0.24m-T.P.+2.26m):

The depth of marsh became shallower enough for plants to increase. The deposits contain organic material more and more. The effect of the saline water coming from the sea decreased and because of the contents of the sulfur decreased. The pH-E/C measurement shows the same tendency as well.

(6) 300 years B.P. (at the depth shallower than 2.0m, T.P.+2.26m-):

The marsh has been reclaimed by 1733.

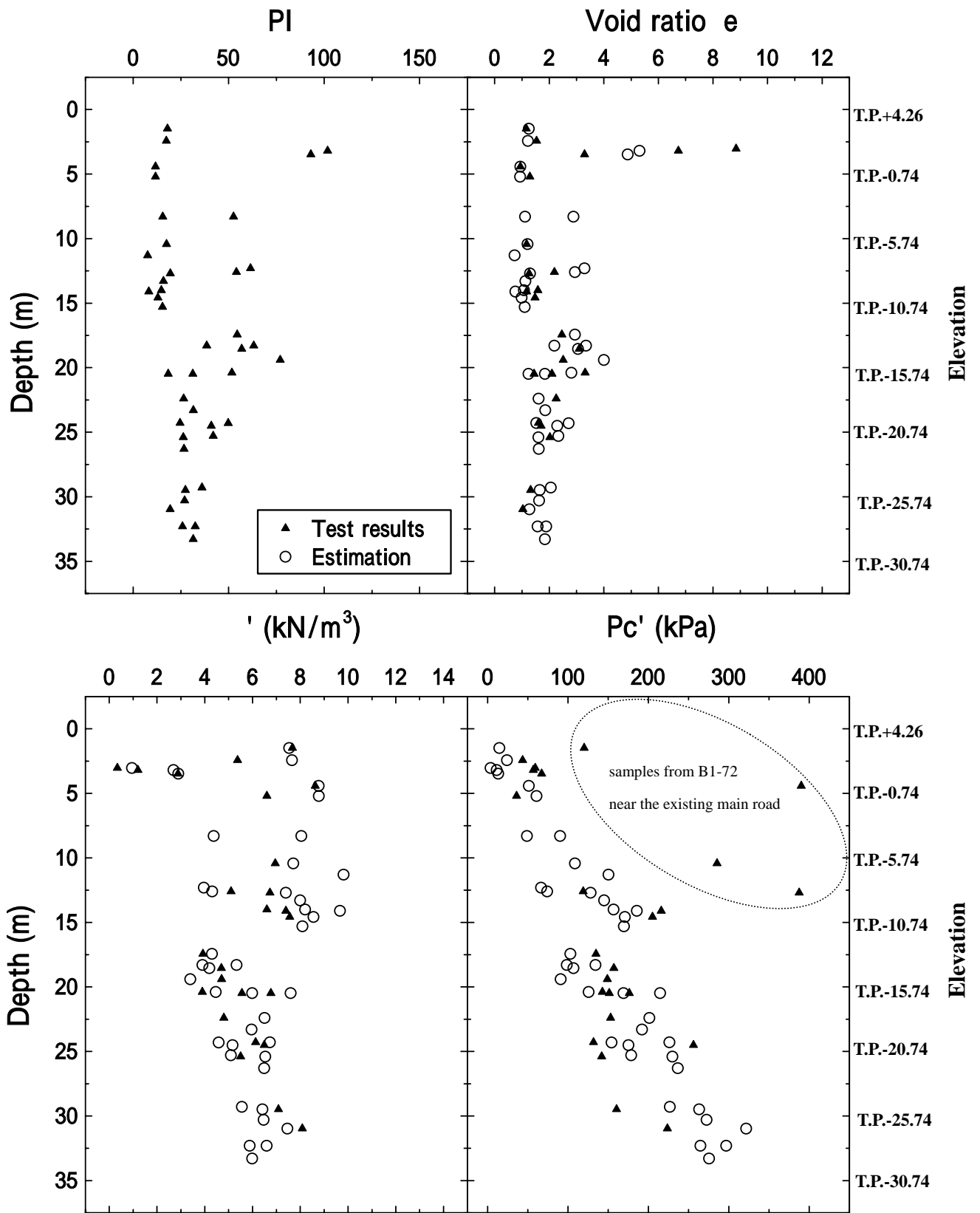


Figs.4.14 Typical alluvial sea-level change (Assumed age vs. elevation relation line are added to the diagrams after Saito, 1995)

The depositional environment is changed from the river mouth to fresh water marsh via brackish water lagoon because of the growth of the sand spit forwards 6,700 years B.P.. This interpretation cannot go into details but outline coincides other studies (e.g. Kitamura and Ogawa, 1998; Kamoi et al., 2000) Figs.4.14 shows the diagram of the typical alluvial sea-level change in Japan. Sea level is characterized by slow, steady rise from the glacial maximum until about 14.5 ka, rapid rise of about 40 mm/yr from 14.5 to 13.5 ka and at about 10 ka, slow rise during the Younger Dryas between MWP 1a and 1b, slow rise to the present level or slightly above it by about 6 ka, and possibly a slight fall since 6 ka.

The change of the depositional environment mentioned above gave the effect to the distribution of PI . The mechanical properties of Shiunji lagoon is estimated based on PI and age following the estimation chart proposed in this study. Figs.4.15 show the comparison of the estimated properties and test results. The estimated properties and test results coincide well with each other except p_c' of the samples from B1-72. According to the soil investigation report of Japan Highway Public Corporation in Niigata, there is a existing main road near the B1-72. The report mentions that the load during the construction of this road and traffic load causes the large pre-consolidation pressure p_c' for these samples compare with the other samples.

Note that the value of σ_v' , σ_h' and σ_c' are decreased down to 10% in order to obtain the coincident of p_c' (see chapter 3). The results of the calculation are listed in Appendix.3.



Figs.4.15 Estimated properties and test results of Shiunji lagoon

4.4 Conclusions

The conclusions of this chapter are as follows:

- (1) Two examples of the field observation on the void ratio in the world (Meade, 1963; Velde, 1996) are in the range of calculated depthwise distributions, which PI is in between ten to hundred. More application of the theory to the prediction of the soil parameters for natural clays and the research on the stress dependency of the parameters remain as a matter to be discussed further.
- (2) An interpretation of the data taken at the east of the San Joaquin Valley, California, USA (Meade, 1963) is carried out by means of the theory obtained in this study together with geological analysis. According to the interpretation, the depositional environment changed sometime in the period of sedimentation from marine to fresh water. Consequently the plasticity of sediments changed from high to low. Thus the reason why the distribution of void ratio increases with increasing depth of burial is becomes clear in San Joaquin Valley.
- (3) Geological analysis of the boring core samples of Shiunji lagoon (Niigata, Japan) is carried out. The possible history of the depositional environment at the location is explained based on the geological analysis. The mechanical soil properties are estimated based on PI and Age of the soil, which reflect the change of the depositional environment. The estimated properties are coincident to the test result well.
- (4) Geological approach such as the theory of the depthwise soil parameters distribution, chemical analysis and microfossil analysis make sense because those methods enable us to interpret the sequences of sediments in the filed which are the results of the change of the depositional environment.

References

- Bard, E., Hamelin, B., Arnold, M., Montaggioni, L., Cabioch, G., Faure, G. and Rougerie, F. (1996). Deglacial sea-level record from Tahiti corals and the timing of global meltwater discharge. *NATURE*, Vol. 382, pp.241-244.
- Einsele, G. (1992). *Sedimentary Basin -Evolution, Facies and Sediment Budget*. Berlin: Springer-Verlag, 628p.
- Fukusawa, H. (1997). High-resolution Reconstruction of Paleoenvironmental Information detected by using Lake Sediments. *Kankyo-joho-kagaku*, Vol.26, No.2, pp.42-53. (in Japanese)
- Grim, R.E. (1962). *Applied Clay Mineralogy*. New York: McGraw-Hill
- Horibe, S. and Tsubota, H. (1977). *Migration of materials in the sea, Science of the ocean environment* : Tokyo, Tokyo Univ. Press. pp.93-149. (in Japanese)
- Horie, T. et al. (1988). *The History shown in the 1400m boring core in Biwako*. Kyoto: Doho. (in Japanese)
- Ichihara, M., Ichihara, Y., Koyama, C., Ishimoto, M. and Hayashi, H. (1984). Discussion on the Marine Clay and Sulfide. *URBAN KUBOTA*, No.23, pp.1-31. (in Japanese)
- Imbrie, J. and Imbrie, Z. J. (1980). Modeling the Climatic Response to Orbital Variations. *SCIENCE*, Vol. 207, No. 29, pp.943-953.
- Japan Highway Public Corporation (1995). *Japan Sea Coastal Northeast Highway, Soil Investigation Report in Niigata (Nakajo Area 1st detailed investigation)*, Niigata, p115. (in Japanese)
- Kamei, T., Tokuoka, T., Sampei, Y. and Ishihara, H. (1997). Geotechnology and Sedimentary Environment of Holocene Deposits in Matsue plain. *Jour. Japan Soc. Eng. Geol.*, Vol.38, No.5, pp.280-295.(in Japanese)
- Kamoi, Y., Yasui, K., Kobayashi, I. and Watanabe, H. (2000). Surficial Geology of the Paleo-Shiotsu (Paleo-Shiunji) Lagoon, northern part of the Echigo Plain, central Japan. *Proc. Nihon Dai-Yonki Gakkai*, No.30. (in Japanese)
- Kamon, M., Ohtsubo, M. and Nakamura, T. (1995). Chemical Properties of Alluvial Soils in Japan. *Tsuchi-to-Kiso*, Vol.43, No.10, pp.17-20. (in Japanese)
- Kitamura, A. (1995). Interpretation of Boring Core -Developing of the High-Resolution Geological Analysis based on the interpretation of Boring Core-, *Hokuriku Jiban Kougaku Kenkyukai*, 15th, June. (in Japanese)
- Kitamura, A. and Ogawa, Y. (1998). Sequence Stratigraphic Analysis of “Chuseki-so” Using Drilling Data. *Tsuchi-to-Kiso*, Vol.46, No.2, pp.5-8. (in Japanese)
- Lambe, T.W. and WHITMAN, R. V. (1969). *Soil Mechanics*. New York: John Wiley & Sons.
- Locat, J. and Lefebvre, G. (1985). The compressibility and Sensitivity of an Artificially sedimented Clay Soil: The Grande-Baleine Marine Clay, Quebec, Canada. *Marine Geotechnology*, Vol.6, No.1.
- Masuda, F. (1997). Sequence stratigraphy : An introduction. *Fukadaken Library No.2*, Tokyo: Fukada Geological Institute.(in Japanese)
- Meade, R.H. (1963). Factors Influencing the Pore Volume of Fine-grained Sediments under Low-to-moderate Overburden Loads. *Sedimentology*, 2, pp.235-242.
- Mesri, G. (1973). Coefficient of Secondary Compression. *Proc. ASCE*, Vol.99, No.SM1, pp.123-137
- Nagao, K. and Yoshida, M. (1998). An Experience on Sampling Silty Soil at Lower Area behind the Dune in Northern Niigata Plain. *Tsuchi-to-Kiso*, Vol. 46, No.5, pp.34-36.
- Nakai, N., Ohta, T., Fujisawa, H. and Yoshida, M. (1982). Paleoclimatic and Sea-Level Changes deduced from Organic Carbon Isotope Ratios, C/N Ratios and Pyrite Contents of Cored Sediments from Nagoya

- Harbor, Japan. *The Quaternary Research*, Vol.21, No. 3, pp.169-177. (in Japanese)
- Ohta, Y., Umitsu, M. and Matsushima, Y. (1989). Recent Japanese Research on Relative Sea Level Changes in the Holocene and Related Problems -Review of Studies between 1980 and 1988-, *The Quaternary*, Vol.29, No.1, pp. 31-48.
- Ohtsubo, M. (1995). Formation of Iron Oxide in the Surface Zone of Marine Clay Sediment and the Geotechnical Properties of Clay. *Trans. JSIDRE.*, No.176, pp.153-158. (in Japanese)
- Posamentier, H.W. JERVEY, M.T, and VAIL P.R. (1988). Eustatic Control on Clastic Deposition I-Conceptual Framework. *Soc. Econ. Paleont. Miner. Spe. Publ.*, 42, pp.109-124.
- Posamentier, H.W. and VAIL, P.R. (1988). Eustatic Control on Clastic Deposition II-Sequence and Systems Tract Models. *Soc. Econ. Paleont. Miner. Spe. Publ.*, 42, pp.125-154.
- Richard G. Fairbanks (1989). A 17,000-year glacio-eustatic sea level record: influence of glacial melting rates on the Younger Dryas event and deep-ocean circulation. *NATURE*, Vol. 342, pp.637-642.
- Saito, Y. (1995). High-resolution sequence stratigraphy of an incised-valley fill in a wave- and fluvial-dominated setting: latest Pleistocene-Holocene examples from the Kanto Plain, central Japan. *Mem. Geol. Soc. Japan*, No.45, pp.76-100, August.
- Sato, M. and Yokoyama, T. (1992). Analysis of paleo-environment based on electric conductivity of the STICS-water –On two drilled cores at Osaka Bay, Japan. *Jour. Geol. Soc. Japan*, Vol.98, No.9, pp.825-839. (in Japanese)
- Skempton, A.W. (1953). The Colloidal Activity of Clays. *Proc. 3rd. ICSM*, Vol.1.
- Suter, J.R. (1994). *Deltaic coasts. In: Carter R. W. G. and Woodroffe, C. D. (eds.) Coastal evolution: Late Quaternary shoreline morphodynamics*, Cambridge: Cambridge University Press.
- Tsuchida, T. (1999). Strength Mobilization due to Cementation of Clay, *Report of the Port and Harbour Research Institute*, Vol.38, No.2, pp.99-129.
- Utashiro, T., Takano, T. and Hasegawa, Y. (1979). Niigata Heiya no keisei to sono Saigai wo megutte. *URBAN KUBOTA*, No.17, pp.22-55. (in Japanese)
- Velde, B. (1996). Compaction Trends of Clay-rich Deep Sea Sediments. *Marine Geology*, 133, pp.193-201.
- Yasui, S., Watanabe, K., Kamo, Y. and Kobayashi, I. (2000). Holocene foraminiferal fauna and sedimentary environment in the Shirone area, Echigo Plain, central Japan. *Sci., Rep., Niigata Univ., Ser., E(Geology)*, No.15, pp. 67-89.
- Yokoyama, T. and Sato, M.(1987). Analysis of paleo-environment based on electric conductivity of the stirred clayey sediments into water –On two drilled cores of Osaka Group in Senriyama Hills and Biwako Group at bottom of Lake Biwa, Japan. *Jour. Geol. Soc. Japan*, Vol.93, No.9, pp.667-679. (in Japanese)

Table A2 Results of the laboratory tests 2 of 4

Bor. No	Layer	Depth (m)	Uni-axial test			Tri-axial test		Consolidation test			
			q_u (kgf/cm ²)	ϵ_f (%)	E_{50} (kgf/cm ²)	c (kgf/cm ²)	ϕ (度)	C_c	P_c (kgf/cm ²)	m_v (cm ² /kgf)	c_v (cm ² /day)
B1-69	As1	2.30									
B1-69	Ap	3.30									
B1-69	As1	5.30									
B1-69	As1	7.30									
B1-69	As1	9.30									
B1-69	Ac1-2-1	12.30									
B1-69	Ac1-2-1	13.30									
B1-69	Ac1-2-2	17.30									
B1-69	Ac1-2-2	20.30									
B1-69	Ac1-2-2	24.30									
B1-69	Ac1-2-2	27.30									
B1-69	As2	29.30									
B1-69	Ac3	31.30									
B1-69	As3	35.30									
B1-69	Ag3	38.20									
B1-70	Ac1-1	2.50	0.157	6.55	6.5	0.02	15.02	1.20	0.44	1.82E-01	2.35E+02
B1-70	Ap	3.50	0.223	5.50	6.4	0.41	25.22	4.81	0.67	1.95E-01	1.06E+02
B1-70	As1	5.30									
B1-70	As1	7.30									
B1-70	Ac1-2-1	10.40	0.342	2.20	25.4	0.25	24.40	0.38	2.86	1.81E-02	2.20E+03
B1-70	Ac1-2-1	12.30									
B1-70	Ac1-2-1	14.50	1.084	7.71	61.7			0.42	2.05	2.69E-02	1.10E+03
B1-70	Ac1-2-2	16.30									
B1-70	Ac1-2-2	18.50	0.951	3.13	48.7			1.45	1.57	5.60E-02	8.20E+01
B1-70	Ac1-2-2	20.50	0.933	4.08	41.7			0.80	1.52	4.35E-02	3.15E+02
B1-70	Ac1-2-2	24.40	0.998	3.76	53.4	0.21	16.92	0.68	1.32	4.80E-02	3.25E+02
B1-70	Ac1-2-2	26.30									
B1-70	As2	29.30									
B1-70	Ac3	31.00	1.195	3.49	57.2			0.35	2.23	2.18E-02	1.32E+03
B1-70	As3	34.30									
B1-70	Ag3	37.30									
B1-70	Ag3	42.20									
B1-70	Ag3	47.20									
B1-70	As4	52.30									
B1-70	As4	57.20									
B1-70	As4	63.30									
B1-70	As4	68.20									
B1-71	Ac1-1	1.30									
B1-71	Ap	3.30									
B1-71	As1	5.30									
B1-71	As1	7.30									
B1-71	As1	10.30									
B1-71	Ac1-2-1	13.30									
B1-71	Ac1-2-2	16.30									
B1-71	Ac1-2-2	19.30									
B1-71	Ac1-2-2	22.30									
B1-71	Ac1-2-2	25.30									
B1-71	Ac3	28.30									
B1-71	Ac3	31.30									
B1-71	As3	33.30									
B1-71	Ag3	36.20									
B1-71	Ag3	38.10									
B1-72	Ac1-1	1.50	0.136	4.23	7.6	0.24	16.57	0.30	1.20	3.60E-02	2.68E+03
B1-72	Ac1-1	2.30									
B1-72	Ap	3.10	0.338	4.50	15.9	0.60	11.30	2.08	0.59	1.65E-01	2.50E+02
B1-72	Ap	4.50	1.260	6.95	21.4	0.13	27.45	0.18	3.90	6.50E-03	2.78E+03
B1-72	Ap	5.30									
B1-72	As1	8.30									
B1-72	As1	10.30									
B1-72	Ac1-2-1	12.50	0.641	5.03	24.6	0.43	17.10	0.39	3.88	1.38E-02	2.30E+03
B1-72	Ac1-2-1	14.30									
B1-72	Ac1-2-2	15.30									
B1-72	Ac1-2-2	17.50	1.030	2.40	64.6			0.80	1.35	5.00E-02	5.10E+02
B1-72	Ac1-2-2	19.30									
B1-72	Ac1-2-2	20.50	1.104	5.68	47.0			0.52	1.76	2.97E-02	6.50E+02
B1-72	Ac1-2-2	22.30									
B1-72	Ac1-2-2	24.50	0.769	6.22	23.3	0.29	15.25	0.45	2.56	2.03E-02	4.50E+02
B1-72	Ac1-2-2	25.30									
B1-72	Ac1-2-2	26.30									
B1-72	Ac1-2-2	27.30									
B1-72	As2	28.30									
B1-72	Ac3	29.50	1.023	3.65	44.3			0.48	1.60	3.48E-02	3.30E+02
B1-72	Ac3	31.30									
B1-72	As3	32.30									
B1-72	Ag3	35.30									

Table.A6 Chemical analysis of the standards proposed by JGS (2 of 2)

Table 6 1998 recommended or preferable (with asterisks) values for n samples, "Instrumental analysis series" (n 5 from SiO2 to T-Fe2O3)

	JR-3	JGb-2	JH-1	JSy-1	JMn-1
SiO2	72.76	46.47	48.18	60.02	14.11
Al2O3	11.90	23.48	5.66	23.17	4.30
Fe2O3	2.61	0.62	1.39*	-	-
FeO	1.86	5.41	8.09*	-	-
MnO	0.083	0.13	0.19	0.0024	33.09
MgO	0.050	6.18	16.73	0.016	3.12
CaO	0.093	14.10	15.02	0.25	2.91
Na2O	4.69	0.92	0.71	10.74	2.80
K2O	4.29	0.059	0.53	4.82	0.94
TiO2	0.21	0.56	0.67	0.0015*	1.06
P2O5	0.017	0.017	0.099	0.014*	0.54
H2O+	0.72*	1.46*	1.82*	-	7.90*
H2O-	0.24*	0.14	0.18*	-	-
T-Fe2O3	4.72	6.69	10.27	0.084	14.40
Ag	0.036*	-	-	-	-
As	1.1*	0.96*	1.0*	0.90*	75.4
Au (ng g ⁻¹)	-	-	-	-	0.95*
B	11.4*	4.9*	10.8*	14.5*	138*
Ba	65.8	36.5	106	15.7	17.7
Ba	7.6	-	0.43*	0.80*	7.8*
Bi	0.21*	0.022*	0.067*	0.009*	4.3*
C	230*	880*	1630*	340*	905*
Cd	0.064*	-	-	-	15.5*
Ce	327	3.0	17.6	2.6	277
Co	0.98	25.8	51.5	0.16*	1732
Cr	3.5	125	616	2.0	26.6
Cs	1.0	0.51	0.87	0.69	0.60
Cu	2.9	11.4	8.6	1.3	11132
Dy	21.5*	0.60*	2.5	0.37	28.3*
Er	14.0*	0.36*	1.2	0.30	14.6
Eu	0.53	0.59	0.86	0.16	7.6
Ga	36.6	15.9	7.9	23.5	37.1*
Gd	19.7*	0.48*	2.7*	0.27	29.8*
Hf	40.3	0.25	1.4	1.2	6.2*
Hg (ng g ⁻¹)	3.4*	1.9*	1.9*	0.5*	-
Ho	4.7*	0.15*	0.53	0.094	5.8
La	179	1.5	7.9	1.2	122
Li	120*	15.7*	12.1*	15.3*	71.7*
Lu	2.8	0.062	0.17	0.076	2.1
Mo	0.49	0.42	0.77	0.048*	318
Nb	510	1.9	4.2	0.51	27.6*
Nd	107	1.8	11.6	1.2	137
Ni	1.6*	13.6	58.2	1.1	12632
Pb	32.8	1.5	2.6	4.9	430
Pr	33.1	0.39*	2.3*	0.32	31.4*
Rt (ng g ⁻¹)	-	-	-	-	110*
Rb	453	2.9	14.4	66.3	10.9
S	39*	599*	567*	13*	940*
Sb	0.17*	0.12*	0.067*	0.15	37.5
Sc	0.50	24.7	77.6	-	13.0*
Sm	21.3	0.51	3.1	0.27	30.2
Sn	17.4	0.48*	0.92*	0.17	4.4*
Sr	10.4	438	153	19.3	792
Ta	36.8	0.29	0.23	0.013*	0.64*
Tb	4.29	0.15	0.52	0.057*	4.8
Th	112	0.19	1.4	0.23	11.7
Tl	0.93*	-	-	0.96*	-
Tm	-	0.059*	0.19*	0.053	2.1
U	21.1	0.041*	0.58	0.20	5.0
V	4.2	174	228	2.1	424
W	7.8*	1.6*	-	0.06*	45.3*
Y	166	4.5	13.7	2.6	111
Yb	20.3	0.39	1.2	0.41	13.8
Zn	209	48.5	61.8	3.2	1068
Zr	1494	11.6	48.3	70.2	344

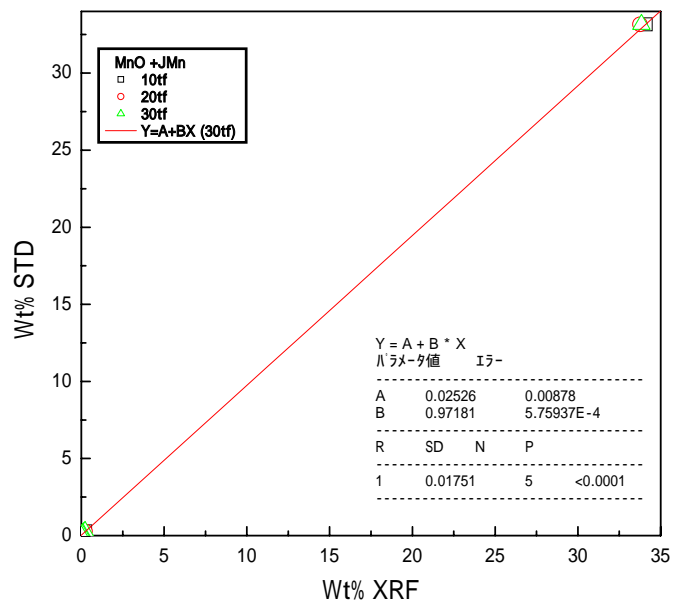
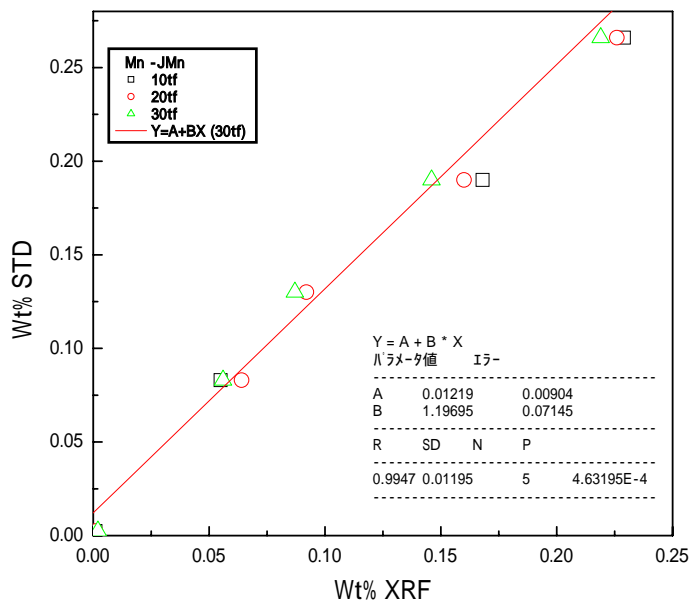
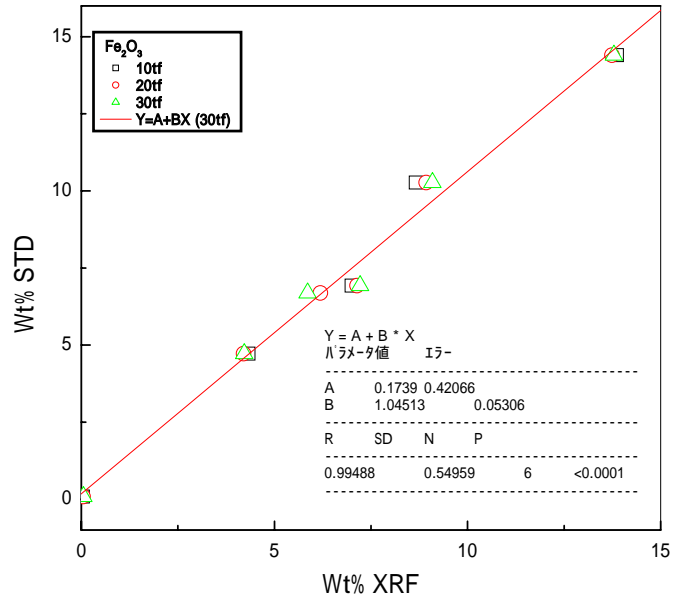
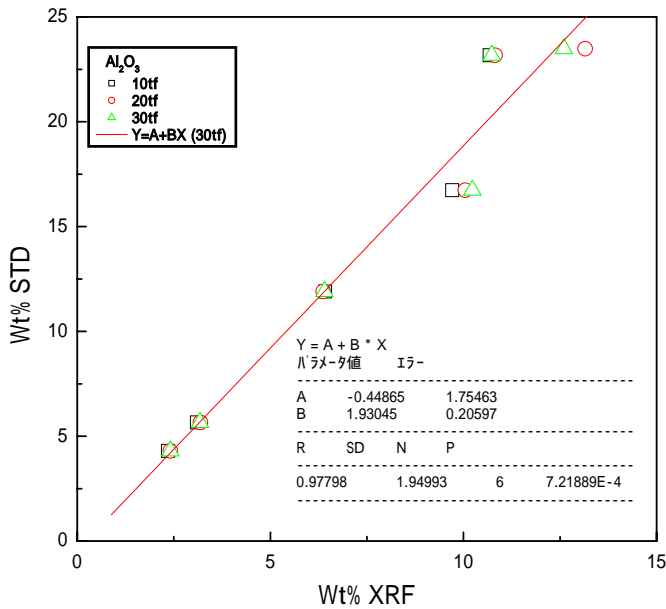
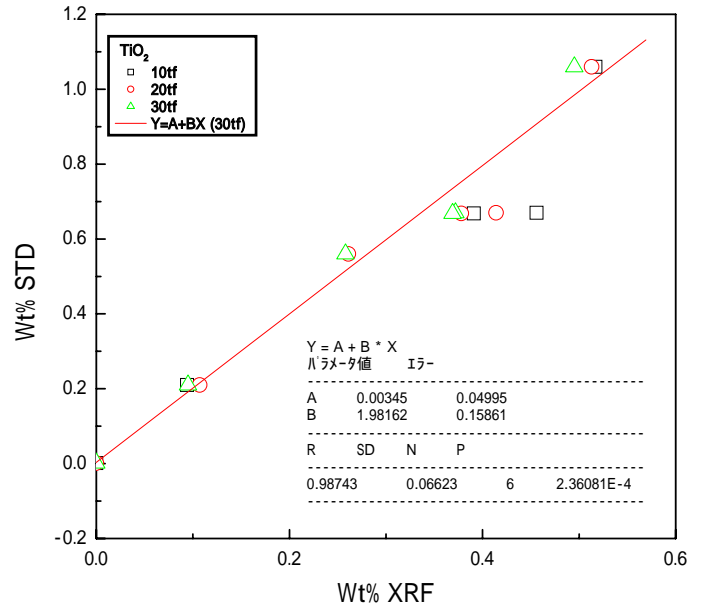
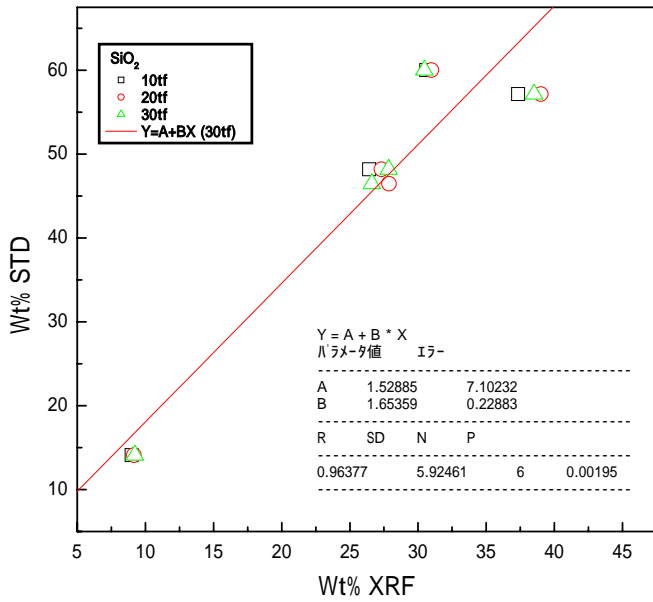


Fig.A1 Calibration curves of major elements (1 of 2) 119

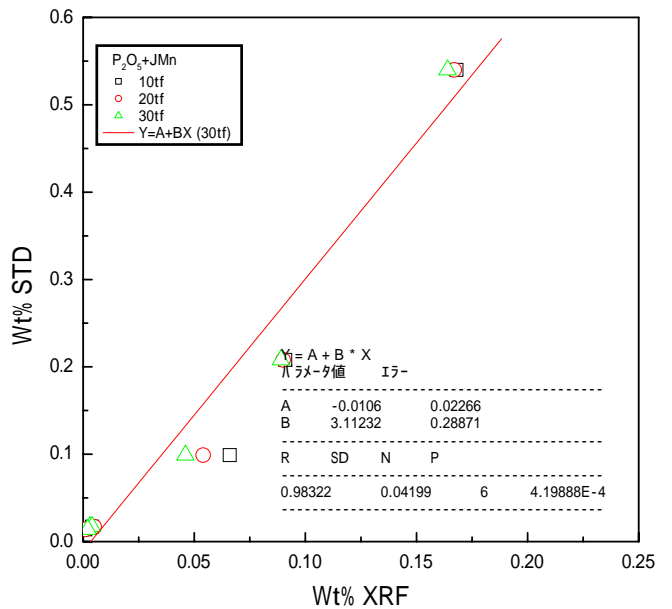
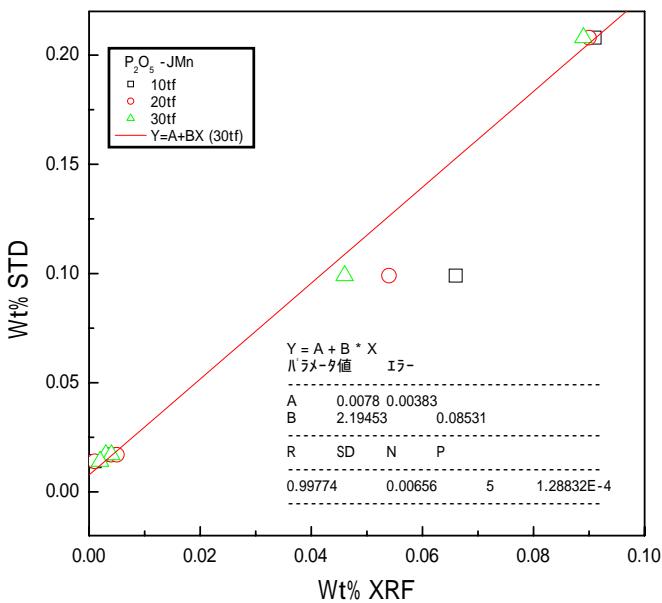
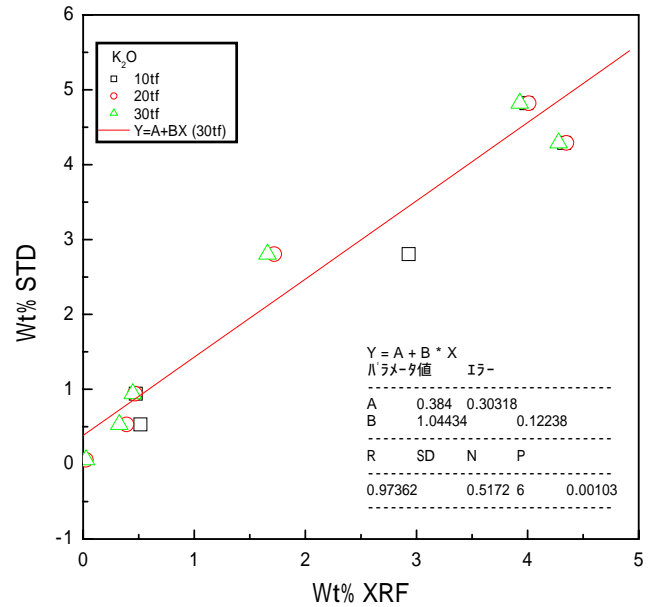
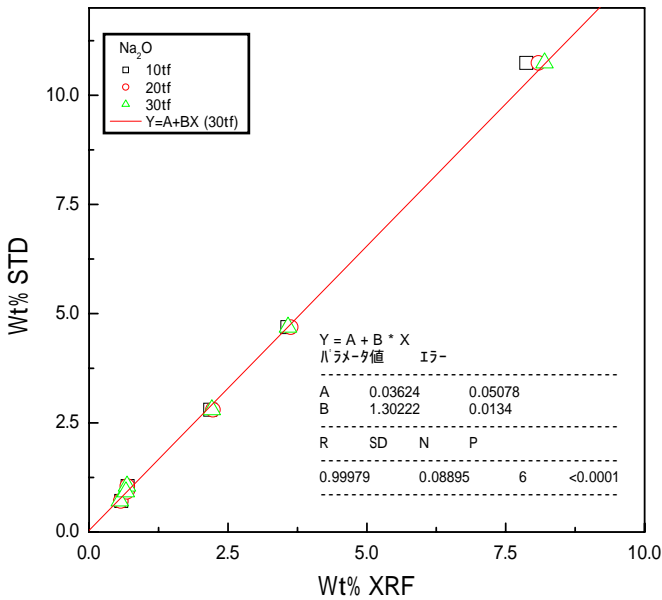
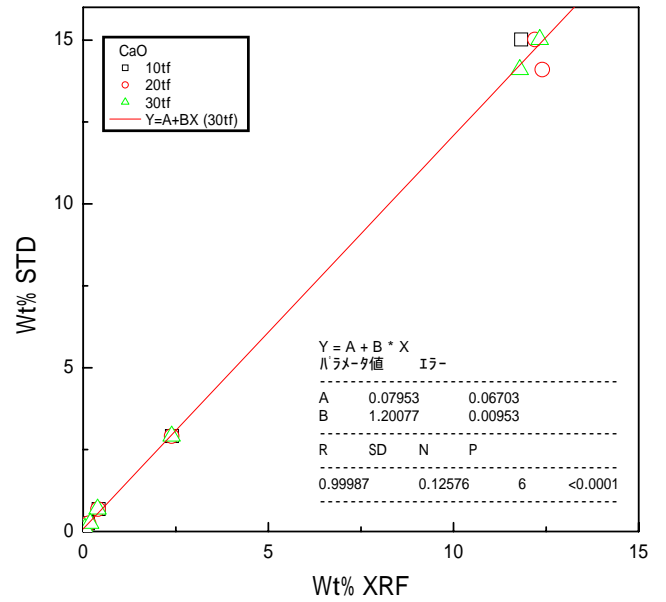
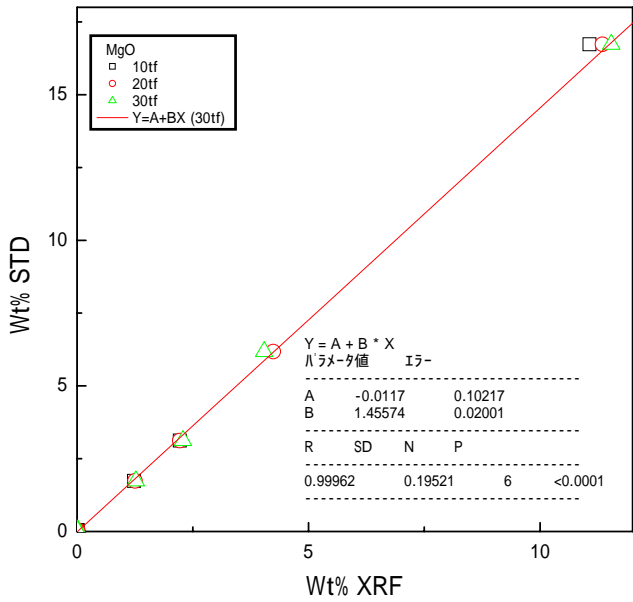


Fig.A2 Calibration curves of major elements (2 of 2) 120

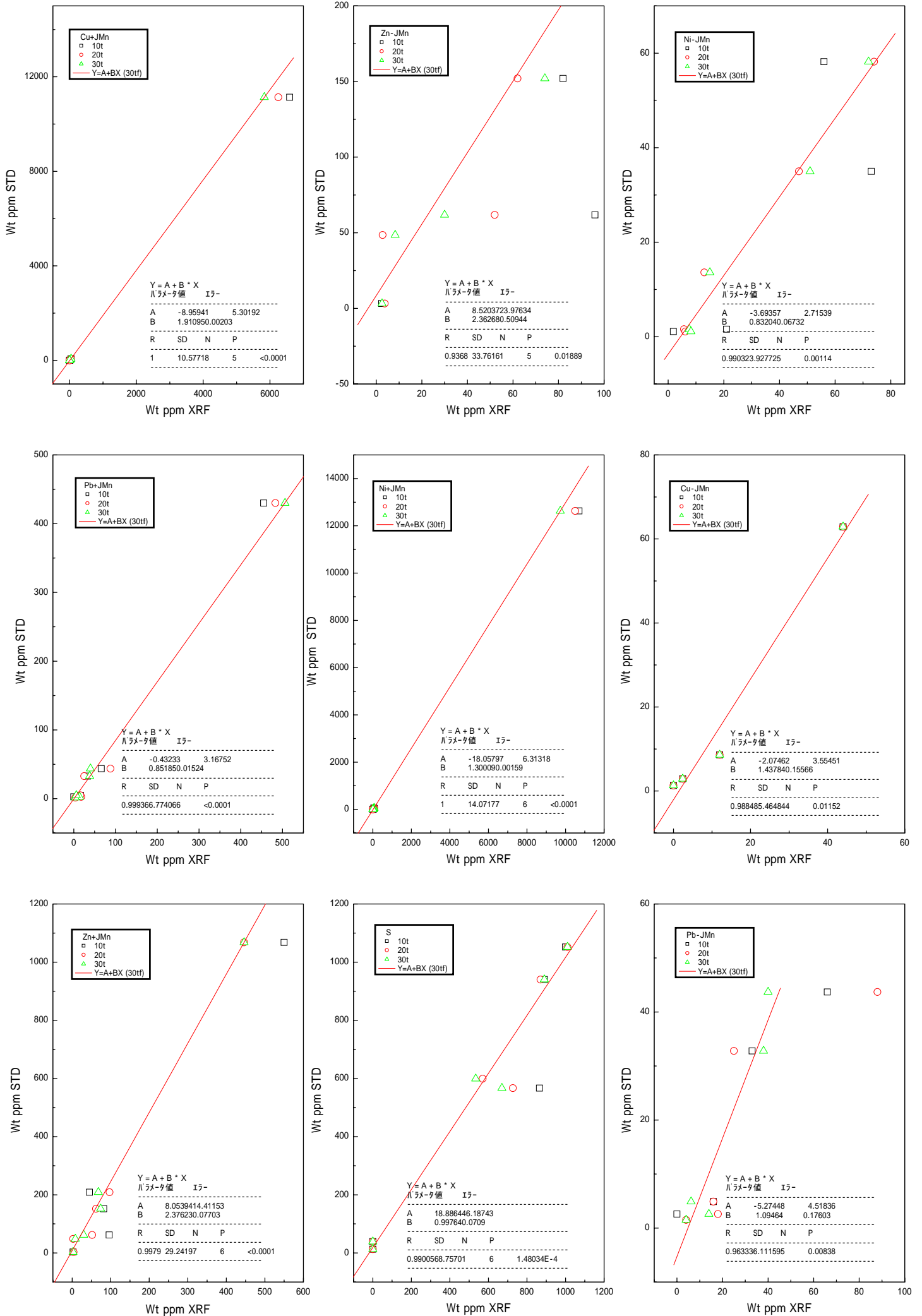


Fig.A3 Calibration curves of minor elements

Table.A7 List of calibration curves

$$\text{Wt\%} = A + \text{Wt\%(XRF)} \times B$$

Element	A	B	R(coefficient of correlation)
SiO ₂	1.52885	1.65359	0.96377
TiO ₂	0.00345	1.98162	0.98743
Al ₂ O ₃	-0.44865	1.93045	0.97798
Fe ₂ O ₃	0.17390	1.04513	0.99488
MnO (less than 0.21%)	0.01219	1.19695	0.99470
MnO (more than 0.21%)	0.02526	0.97181	1.00000
MgO	-0.01170	1.45574	0.99962
CaO	0.07953	1.20077	0.99987
Na ₂ O	0.03624	1.30222	0.99979
K ₂ O	0.38400	1.04434	0.97362
P ₂ O ₆ (less than 0.09%)	0.00780	2.19453	0.99774
P ₂ O ₆ (more than 0.09%)	-0.01060	3.11232	0.98322
Cu(less than 45ppm)	-2.07462	1.43784	0.98848
Cu(more than 45ppm)	-8.95941	1.91095	1.00000
Zn(less than 400ppm)	8.52037	2.36268	0.99368
Zn(more than 400ppm)	8.05394	2.37623	0.99790
Ni(less than 70ppm)	-3.69357	0.83204	0.99032
Ni(more than 70ppm)	-18.05797	1.30009	1.00000
Pb(less than 40ppm)	-5.27448	1.09464	0.96333
Pb(more than 40ppm)	-0.43233	0.85185	0.99936
S	18.8864	0.99764	0.99005

Appendix.3

Table.A8 The result of the estimation of B1-71 of Shiunji lagoon

Elevation T.P. (m)	Depth (m)	PI(measured)	e	'(kN/m ³)	P _o '(kPa)	OCR	P _o '(kPa)
+2.76	1.5	18	1.257	7.531	11.2	1.306	14.7
+1.86	2.4	17.4	1.221	7.653	18.3	1.320	24.2
+1.26	3.0	338.5	16.814	0.954	2.8	1.345	3.8
+1.06	3.2	101.8	5.311	2.694	8.5	1.340	11.4
+0.76	3.5	93	4.877	2.893	10.0	1.343	13.4
-0.14	4.4	11.7	0.938	8.774	38.4	1.335	51.4
-0.94	5.2	11.7	0.936	8.782	45.5	1.340	61.1
-4.04	8.3	15.5	1.113	8.047	66.4	1.357	90.2
-4.04	8.3	52.6	2.887	4.374	36.0	1.366	49.2
-6.14	10.4	17.5	1.205	7.711	79.7	1.365	108.8
-7.04	11.3	7.6	0.733	9.812	110.4	1.362	150.4
-8.04	12.3	61.4	3.289	3.964	48.3	1.380	66.6
-8.34	12.6	54.1	2.941	4.314	53.8	1.380	74.3
-8.44	12.7	19.5	1.297	7.401	93.4	1.372	128.2
-9.04	13.3	15.9	1.125	7.999	105.7	1.372	145.1
-9.74	14.0	14.8	1.073	8.203	114.2	1.373	156.8
-9.84	14.1	8.2	0.759	9.662	135.7	1.369	185.8
-10.34	14.6	13	0.987	8.557	124.3	1.374	170.7
-11.04	15.3	15.4	1.100	8.096	123.1	1.376	169.5
-13.14	17.4	54.5	2.946	4.308	74.2	1.390	103.1
-14.04	18.3	38.5	2.189	5.331	96.7	1.389	134.3
-14.04	18.3	63.1	3.351	3.907	70.8	1.393	98.6
-14.24	18.5	56.9	3.057	4.190	76.7	1.392	106.8
-15.14	19.4	77	4.004	3.397	65.2	1.396	91.0
-16.14	20.4	51.7	2.808	4.464	90.2	1.395	125.8
-16.24	20.5	31.2	1.841	5.984	121.6	1.391	169.2
-16.24	20.5	18.4	1.238	7.597	154.7	1.387	214.6
-18.14	22.4	26.4	1.613	6.506	144.6	1.393	201.4
-19.04	23.3	31.5	1.852	5.960	137.7	1.395	192.2
-20.04	24.3	24.6	1.527	6.728	162.3	1.395	226.3
-20.04	24.3	49.8	2.712	4.580	110.2	1.400	154.3
-20.24	24.5	40.9	2.293	5.163	125.3	1.399	175.3
-21.04	25.3	41.9	2.339	5.091	127.6	1.400	178.7
-21.14	25.4	26.2	1.601	6.536	164.7	1.396	230.1
-22.04	26.3	26.6	1.619	6.491	169.4	1.398	236.8
-25.04	29.3	36	2.058	5.560	161.5	1.404	226.6
-25.24	29.5	27.3	1.649	6.416	187.8	1.402	263.2
-26.04	30.3	26.9	1.630	6.463	194.3	1.402	272.5
-26.74	31.0	19.4	1.278	7.462	229.8	1.400	321.8
-28.04	32.3	32.5	1.891	5.880	188.3	1.406	264.8
-28.04	32.3	25.8	1.577	6.596	211.4	1.404	296.8
-29.04	33.3	31.4	1.839	5.988	195.9	1.406	275.6

Chapter 5

CONCLUSIONS

Conclusions

The motivation of this study was to make practical use of geology to a part of civil engineering. Geological information gives civil engineers the change of the depositional environment of soil, in other words the history of the soil. The history of the soil must be related to the nature of the soil but no concrete relationship between geological information and mechanical soil properties are proposed so far.

PI and Age of the soil are chosen as the parameters which represents the change of the depositional environment in order to propose a method to estimate mechanical soil properties in this study. The theory for the estimation of mechanical soil properties based on *PI* and Age is proposed in chapter 2.

Theoretical depthwise distributions of the soil parameters and stress history are reasoned out based on Bjerrum's hypothesis. Assumptions are made in this study as follows. 1) The theory is based on Bjerrum's hypothesis. 2) Cementation, bonding and desiccation are not taken into account. 3) Primary and delayed compression may occur at the same time. 4) Excess pore water pressure caused by sedimentation has already dissipated during the geological time. 5) The rate of the sedimentation is constant. 6) Depositional environment does not change.

The distribution of soil parameters such as age, void ratio, unit weight, initial overburden soil pressure, *OCR* and pre-consolidation pressure derived in chapter 2. Required information for the soil parameter estimation are plastic limit *PI* and Age of the lowermost of the formation. Estimation chart is proposed for the soil parameter estimation based on Age and *PI* of the soil. Theoretical distributions of soil parameters are obtained for several types of depositional rate.

The parametric studies were carried out based on the proposed theory in chapter 3. It enables us to estimate the depthwise distribution of the soil parameters. Moreover effects of the history and properties of the soil such as age, depositional rate, *PI*, γ , γ_s and the ratio

γ are investigated in this chapter. According to the parametric study the effect of PI is considerably strong to each parameter.

Age T_0 at the bottom of the formation does not effect on the depthwise distribution of age, void ratio and unit weight. T_0 gives an effect on OCR and P_c' , however, the effect is not so strong because the effect is proportional to the logarithm of the age and it is possible to obtain the age with in the error of one order. Depositional rate influences the depthwise distribution of all the parameters. The difference of the calculated value caused by the difference of the depositional rate is about 5%-10%.

The effect of the same changes of material properties γ , ρ , to the age, P_o' , OCR and P_c' are negligible. However the effect to the shape of the depthwise distribution of void ratio and unit weight is that the smaller the those parameters the smaller the depthwise changes of the void ratio and unit weight. The changes of γ (in this case ρ , are not changed) gives a strong impact on the depthwise distribution of OCR and P_c' . The bigger the value of γ , the larger the OCR and P_c' . Note that ρ does not have any relation with the distribution of the age, void ratio, unit weight and P_o' . The changes of the ratio γ/ρ gives effect only to the OCR and P_c' . The bigger the value of the ratio γ/ρ , the larger the OCR and P_c' .

The applications of the estimation method together with interpretation of the depositional environment are shown in chapter 4. Two examples of the field observation on the void ratio in the world (Meade, 1963; Velde, 1996) are in the range of calculated depthwise distributions, which PI is in between ten to hundred. More application of the theory to the prediction of the soil parameters for natural clays and the research on the stress dependency of the parameters remain as a matter to be discussed furthers.

An interpretation of the data taken at the east of the San Joaquin Valley, California, USA (Meade, 1963) is carried out by means of the theory obtained in this study together with geological analysis. According to the interpretation, the depositional environment changed sometime in the period of sedimentation from marine to fresh water. Consequently the plasticity of sediments changed from high to low. Thus the reason why the distribution of void ratio increases with increasing depth of burial is becomes clear in San Joaquin Valley.

Geological analysis of the boring core samples of Shiunji lagoon (Niigata, Japan) is carried out. The possible history of the depositional environment at the location is explained based on the geological analysis. The mechanical soil properties are estimated based on PI and Age of the soil, which reflect the change of the depositional environment. The estimated properties are coincident to the test result well.

Geological approach such as the theory of the depthwise soil parameters distribution, chemical analysis and microfossil analysis make sense because those methods enable us to interpret the sequences of sediments in the filed which are the results of the transition of the

depositional environment. The concrete relationship between depositional environment and mechanical soil properties are proposed in this study based on *PI* and Age of the soil. These properties are used as initial soil conditions of soil for Finite element elasto-plastic or elasto-viscoplastic analysis. The interpretation of depositional environment of soil helps civil engineers understanding the spatial distribution of formations and making a reliable soil profile.

Recommendations for further study

There are 3 recommendations for the further study on the relationship between depositional environment and the mechanical properties of soil regarding to the prediction of the initial conditions of soil.

1. Experimental studies on the σ_v , σ_h and σ_{θ} during the sedimentation is required to improve the prediction of the mechanical properties of soil related the initial conditions. How to reproduce the elapse of the geological time in a laboratory is a big question.
2. Field observation and geological analysis to explain the relationship between the depositional environment and *PI* are required. The effect of the particle size, clay mineral, adsorbed cation, organic materials, non-crystallized silicate and microfossils on *PI* are the questions.
3. The effects of the phenomena such as cementation which are not included in the assumptions in this study on the mechanical properties of soil are another questions. The result of this study may help us to separate the known effects from the unknown effects on the mechanical properties of soil.